



MONASH University

Novel electrolytes for emerging sodium energy storage application

Siti Aminah Mohd Noor

A thesis submitted to the Faculty of Science, Monash University, in fulfillment of
requirements for the degree of Doctor of Philosophy

July 2014

**School of Chemistry
Monash University
Melbourne, Australia**

Notice 1

Under the Copyright Act 1968, this thesis must be used only under the normal conditions of scholarly fair dealing. In particular no results or conclusions should be extracted from it, nor should it be copied or closely paraphrased in whole or in part without the written consent of the author. Proper written acknowledgement should be made for any assistance obtained from this thesis.

General Declaration
Monash University
Monash University Institute of Graduate Research

**Declaration for thesis based or partially based on conjointly published or
unpublished work**

In accordance with the Monash University Doctorate regulations 17.2 Doctor of Philosophy and master of Philosophy (MPhil) regulations, the following declarations are made:

I hereby declare that this thesis contains no material, which has been accepted for the award of any other degree or diploma at any university or equivalent institution and that, to the best of my knowledge and belief, this thesis contains no material previously published or written by another person, except where due reference is made in the text of the thesis.

This thesis includes 3 original papers published in peer-reviewed journals and 2 unpublished publications. The core theme of the thesis is ‘novel electrolytes for emerging sodium energy storage application’. The ideas, developments and writing up of all the papers in the thesis were the principal responsibility of myself, the candidate, working within the School of Chemistry under the supervision of Prof Douglas R. MacFarlane and Prof Maria Forsyth.

The inclusion of co-authors reflects the fact that the work came from active collaboration between researchers and acknowledgements input into team based research.

My contribution to the work involved the following:

CHAPTER No	PUBLICATION TITLE	STATUS	NATURE AND EXTENT OF CANDIDATE'S CONTRIBUTION
2	Ionogels based on ionic liquids as potential highly conductive solid state electrolytes	Published	Main investigator in experimentation, research planning, results interpretations, manuscript writing Contribution: 90 %
3	Properties of sodium-based ionic liquid electrolytes for sodium secondary battery application	Published	Main investigator in experimentation, research planning, results interpretations, manuscript writing Contribution: 90 %
4	Ion conduction and phase morphology in sulfonate copolymer ionomers based on ionic liquid–sodium cation mixtures	Published	Main investigator in experimentation, research planning, results interpretations, manuscript writing Contribution: 90 %
5	Decoupled ion conduction in poly(2-acrylamido-2methyl-1-propane-sulfonic acid) (PAMPS) homopolymers	Submitted	Main investigator in experimentation, research planning, results interpretations, manuscript writing Contribution: 90 %
6	Gel-ionic liquid based sodium ion conductors for sodium batteries	To be submitted	Main investigator in experimentation, research planning, results interpretations, manuscript writing Contribution: 90 %

I have ordered sections of submitted or published papers in order to generate a consistent presentation within the thesis.

Signed:
Siti Aminah Mohd Noor
School of Chemistry
Monash University

Date:

‘.....And for those who fear Allah, He (ever) prepares a way out, And He provides for him from (sources) he never could imagine. And if any one puts his trust in Allah, sufficient is ((Allah)) for him. For Allah will surely accomplish his purpose: verily, for all things has Allah appointed a due proportion.’

65:2-3

TABLE OF CONTENTS

	Page
ABSTRACT	i
ACKNOWLEDGEMENTS	iv
SYMBOLS AND ABBREVIATIONS	v
CHAPTER ONE Introduction	
1.0 Introduction	1
1.1 General development of electrolytes	2
<i>1.1.1 Liquid electrolytes</i>	2
<i>1.1.2 Solid-state electrolytes</i>	4
<i>1.1.3 Single ion conductors</i>	5
1.2 Ionic liquids	8
1.3 Polymer-IL gels	11
1.4 Sodium batteries	13
1.5 Aim of study and thesis overview	15
<i>1.5.1 Aim of study</i>	15
<i>1.5.2 Thesis overview</i>	16
1.6 Bibliography	19

**CHAPTER TWO Ionogels based on ionic liquids as potential
highly conductive solid state electrolytes**

2.1	General Overview	22
2.2	Specific Declaration	24
2.3	Publication 1, <i>Electrochimica Acta</i> ; 91 (2013) 219-226	25

**CHAPTER THREE Ionic liquids – sodium ion conductors for
sodium batteries**

3.1	General Overview	36
3.2	Specific Declaration	38
3.3	Publication 2, <i>Electrochimica Acta</i> ; 114 (2014) 766-711	39
3.4	Specific Declaration	46
3.5	Publication 3, to be submitted to <i>Electrochimica Acta</i>	47
3.6	Supporting information	67
3.7	Bibliography	71

CHAPTER FOUR Ionomers as cation only ion conductors

4.1	General Overview	73
4.2	Specific Declaration	76
4.3	Publication 4, <i>Journal of Material Chemistry A</i> ; 2 (2014) 365-374	77
4.4	Supporting Information	89
4.5	Specific Declaration	93
4.6	Publication 5, submitted to <i>Polymer</i>	94

4.7	Supporting Information	125
4.8	Bibliography	129

CHAPTER FIVE Conclusions and future work

5.1	Conclusions	130
5.2	Future work	132

ABSTRACT

The increasing energy demand along with the growing understanding of the environmental consequences of the use of fossil fuels, have created a need for the development of new and advanced sustainable energy sources. One aspect of this need that arises from the intermittency of many sources is large scale electrical energy storage. Current high energy density electrochemical energy storage technologies rely on electrolytes based on flammable solvents, which are typically volatile organic compounds (VOCs) that result in major safety problems when applied to many novel applications. Using ionic liquids as electrolytes has been explored, as they potentially offer a solution to the safety problem of organic solvents, such as negligible vapor pressure and non flammability.

On the other hand, while Li-ion batteries remain an important energy storage technology, there are concerns about the long-term availability and cost of lithium. Alternative electrochemical systems to lithium-based technologies are being investigated to ensure power storage devices are as low-cost and efficient as possible. Sodium-based technologies are promising alternative due to sodium's high abundance, low cost, low atomic mass, and relatively high (negative) electrochemical reduction potential.

This thesis concentrates on three types of sodium-based ionic liquid electrolytes of relevance to emerging sodium energy storage applications. In the first section, it describes the preparation of ionogel electrolytes. In this system, we aimed to

investigate the effect of the formation of a silica network on the ionic liquid properties. We found that the ionic conductivity of 3 wt.% silica ionogels is close to that of the pure IL and the T_g does not vary significantly as silica content increased. This shows that the formation of the silica network does not affect the dynamic properties of the IL.

In the second section of this thesis, sodium-based ionic liquid electrolytes are prepared and compared with lithium-based ionic liquid electrolytes. The sodium electrolytes possess high ionic conductivity, though marginally lower than that of equivalent lithium systems. Deposition and dissolution of sodium metal was observed through cyclic voltammetry analysis. In order to improve the mechanical properties of these liquid electrolytes, two types of gel electrolytes were investigated: (i) silica gel electrolytes and (ii) PMMA-gel electrolytes. With the former facile plating and stripping of sodium metal was observed through cyclic voltammetry. The ionic conductivity of both gel systems slightly decreased as the physical properties changed from a liquid to gel. However, the T_g was not significantly affected, hence the motional dynamics of liquid electrolytes are not notably affected in the transition to the gel state in these electrolytes. These findings show that sodium-based ionic liquid electrolytes can be a promising candidate for secondary sodium battery applications.

In the final section of this thesis polyelectrolyte systems were developed that were designed to be single ion conductors, by tethering the anion to the polymer

backbone; such systems are often referred to as ionomers. Two types of ionomers were investigated. The hypothesis guiding the design of these systems was that anionic centers on the polymer that are only weakly associated with the corresponding counterion, would allow decoupling of the cation motion from the bulk dynamics of the material. We found that the ionic conductivity strongly decoupled from the T_g of the backbone, particularly for compositions below 50% Na^+ for both systems of ionomers. Characterization showed the T_g of the ionomers did not vary significantly as the amount of Na^+ varied, while the conductivity increased with decreasing Na^+ content, indicating conductivity increasingly decoupled from T_g . On the other hand, phase separation was clearly observed by SEM and Raman spectroscopy. The introduction of plasticizer significantly increased the ionic conductivity by several orders of magnitude. The effect of different types of ammonium counter-cations on the conductivity of ionomers was also investigated. We observed a decreasing T_g with increasing bulkiness of the quaternary ammonium cation, and an increasing degree of decoupling from T_g within these systems.

ACKNOWLEDGMENTS

Alhamdulillah.. Alhamdulillah.. Alhamdulillah.. In the name of Allah, the Most Gracious, the Most Merciful. Without His blessings, I would never be able to complete my PhD.

I would like to begin with expressing my deep and sincere gratitude to my supervisors and my mentors, Prof Doug Macfarlane and Prof Maria Forsyth for their guidance, attention and support, both scientifically and morally over the past three years. There are no words that can express my gratitude. Both of you are very awesome! ☺

To my sponsors, Malaysian Ministry of Higher Education and National Defence University of Malaysia, thank you very much for realizing my dream to study abroad! The financial supports from the Australian Research Council and DRM's and MF's Australian Laureate Fellowship are greatly acknowledged.

Thank you to the members of Macfarlane and Forsyth group who has always been there whenever I needed help! Leo, many thanks for the great discussions about conductivity and CV! Special thanks to Dr. Peter, Finlay, Dr. Paul, Dr. Sun, Dr. Daniel, Dr. Gary, Dr. Martin, Dr. Patrick, Dr. Matze, Dr. Judith and Dr. Bjorn for their help in laboratory matters, instrumental supports and helping me have a clear view on my project. To other colleagues, Azila, Alison, Jelena, Hui, Ahmed, Mega, Vijay, Jiaye, Matt, Chun, Anthony, Tristan, Jenny and all other group members (you know who you are☺), many thanks for all the supports and encouragement!

Big thanks to my dear housemates at BS, Alia, Fafa, Jaja, Anis, Thiyah, Yasmin and Wana. Not to forget my usrah mates, Syaer, Dila, Aliah, Fairuz, Amal, Umairah, Fatin, Tmc and Fathen. Also to ISMA Australia, thank you very much for bringing me to this wonderful journey. To the polymer electrolyte group members back in UKM (especially Sukor and Nadhrah) and UPNM's friends (esp: Leli!), many thanks for the wonderful discussions and moral support. Thanks heap guys!

Finally, from the bottom of my heart, I would like to express my honest gratitude to my mom (Hjh Badariah), my dad (Hj Mohd Noor), my granny (Hjh Indok Selo) and my siblings, A.Jeff, A.Awie, Ibu, Enal, Anja, Cikda, Anie and Ewan. None of this would have been possible without their prayers and love. Their endless encouragement, concern and support throughout this whole period are extremely appreciated. There are no words to convey how much I love each and every one of you. Love you!

SYMBOLS AND ABBREVIATIONS

Instrumental Abbreviations:

EIS	Electrochemical Impedance Spectroscopy
SEM	Scanning Electron Microscope
Solid-state NMR	Solid-state Nuclear Magnetic Resonance
MAS	Magic Angle Spinning
ATR-FTIR	Attenuated Total Reflectance-Fourier Transform Infrared Spectroscopy
TGA	Thermogravimetric Analysis
DSC	Differential Scanning Calorimetry
CV	Cyclic Voltammetry

Acronyms and symbols:

FWHM	Full Width at Half Maximum
VTF	Vogel-Tamman-Fulcher
H ₂ O	Water
ILs	Ionic liquid(s)
M	Mole per litre
min	Minute
mL	Milliliters
MW	Molecular weight
ν	Stretching vibration
wt. %	Weight percent
Tf	Triflate
NTf ₂ ⁻	bis(trifluoromethylsulfonyl) imide
C _x mIm	1-alkyl-3-methylimidazolium (x = alkyl chain length)
C _x mpyr	1-alkyl-1-methylpyrrolidinium (x = alkyl chain length)



Chapter 1

Introduction

1.0 INTRODUCTION

Over the last few decades, the growth of research on rechargeable batteries has significantly contributed to the development of advanced energy and power sources. Rechargeable batteries have become a leading energy source in portable devices, electric vehicles and hybrid electric vehicles. There also has been mushrooming in demand for large size, installed battery packs, because most public buildings (hotels, hospitals etc) must have uninterruptable power supply. This has created interest in a range of new and advanced battery technologies.

The three fundamental components of a battery are the negative electrode (referring to the anode, where oxidation proceeds when the battery is discharged); the positive electrode (which is the cathode, where reduction proceeds as the battery is discharged); and the electrolyte (the substance containing free ions that carries the ionic current in the device). The electrolyte is a key component of a battery, since it serves both as the reservoir for ionic reactants/products and also as the medium for ion transport, and thus much research has been expended on improving the performance, safety and cost of electrolytes. Fig. 1 shows examples of charge discharge process in batteries and the construction of various lithium ion battery formats, together with their main components.

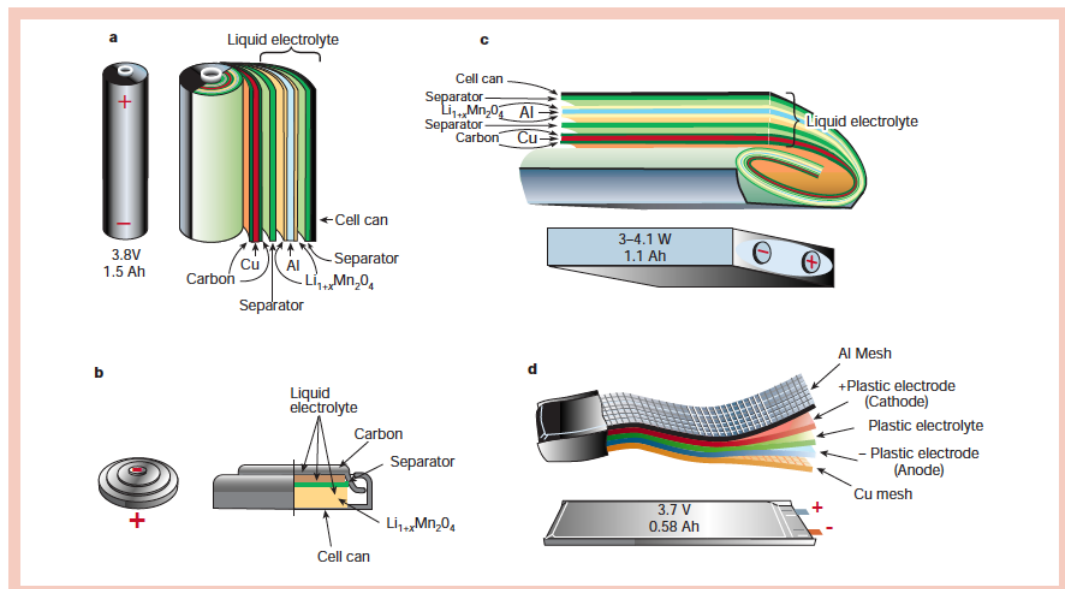
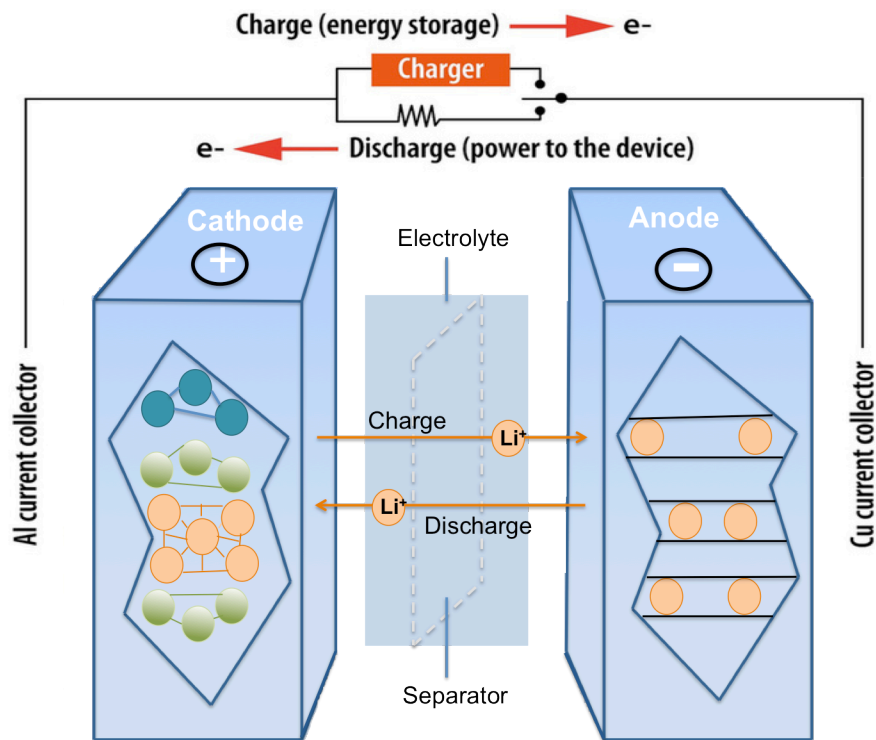


Fig. 1 Charge-discharge process in Lithium ion batteries (top) and Various Li-ion battery configurations with their components (bottom). (a) cylindrical; (b) coin; (c) prismatic; and (d) thin and flat (reproduced from Tarascon & Armand¹)

1.1 General development of electrolytes

In order to achieve high performance, a battery electrolyte must possess high ionic conductivity, be stable at both the high potential of the battery cathode and the low potential of the battery anode. Furthermore, in the case of liquid electrolytes, it has to be compatible with a physical separator (usually a porous polymeric material) that avoids physical and electronic contact between the anode and cathode, and also sufficiently wet the anode, cathode, and separator. An environmentally benign electrolyte with low vapor pressure and low cost also needed for safety purposes.

1.1.1 *Liquid electrolytes*

A variety of conventional aqueous electrolytes are used in practical commercially available devices such as the zinc/manganese dioxide primary cell, lead/acid batteries, alkaline electrolyte secondary batteries^{2, 3}. Non-aqueous, aprotic electrolytes are needed for lithium/thionyl chloride and lithium ion batteries². Commercial lithium-ion battery electrolytes are based on an organic solvent mixture, usually carbonate solvents, with dissolved LiPF_6 as the Li^+ source³. Carbonates are widely used as solvents because of their ability to dissolve high concentrations of lithium salt, up to more than 1M. This is due to their distinctive aprotic, but strongly polar properties arising from their high dielectric constants. The most common carbonate solvent used in the market is ethylene carbonate (EC) mixed with low viscosity linear alkyl carbonates co-solvents such as dimethyl carbonate^{3, 4}. These solutions provide very high ionic conductivity ($>10^{-3} \text{ S.cm}^{-1}$) at room temperature and are also compatible with the battery voltage operating

window. However, organic electrolytes are flammable and volatile, which can lead to major safety problems when applied to many applications. These conventional organic electrolytes present major problems associated with leakage of corrosive and toxic materials⁵. There has also been a number of significant fires/explosions associated with the organic electrolytes and there are growing doubts about the safety of large scale battery packs based on these electrolytes^{6, 7}. As a result of these concerns solid polymer electrolytes (SPEs) and gel electrolytes have been developed to overcome some of these problems, though where volatile components still exist in /the electrolyte the fire hazard usually remains to some extent.

1.1.2 Solid-state electrolytes

Polymer electrolytes are of immense interest due to their applicability in energy conversion and storage devices such as fuel cells and batteries. They present significant advantages over liquid electrolytes on one hand, due to the removal of volatile and liquid components, and over ceramic electrolytes on the other hand due to their potential flexibility and moldability. Polymer electrolytes have been under investigation since the late 1970s when Wright et al.⁸, discovered that polyether complexes of alkali salts were ionically conductive and later Armand et al.⁹, suggested that these could potentially be useful in solid state batteries. Over the past three decades there has been intense research in improving the ionic conductivity in SPEs¹⁰. Amorphous polyethylene oxide (PEO) based systems have generally shown the highest conductivity, with further significant improvement in properties and conductivity obtained by including nanofillers¹¹⁻¹⁵. However, their performance is

limited by the fact that the cation transport number (eg. Li^+) is typically significantly less than 0.5 and the ionic conductivity at ambient temperature is too low to be used in practical devices.

A gel is a material that possesses both liquid and solid type properties. Gels are viscoelastic solid-like materials comprised of a cross-linked elastic network and a solvent, which is the major component¹⁶. In recent years, gel electrolytes have been widely investigated in order to develop safe, high performance batteries. A number of gels containing salts with mixed alkyl carbonates as plasticizer produced usefully high ionic conductivity¹⁷⁻²⁰. However, such gel electrolytes containing low molecular weight organic plasticizers have a risk of leakage and drying out in practical battery systems²¹. Flammability also remains an issue in these cases. Recent studies have described versatile gelled ionic liquid (IL) electrolytes as an excellent substitute for liquid electrolytes in electrochemical devices due to their most appealing feature of non-flammability and no measureable vapor pressure²²⁻²⁵.

1.1.3 Single ion conductors

In devices utilizing a cation charge carrier, anion mobility is undesirable, as the device would then suffer from undesirable concentration polarization, in which anion build up occurs at the electrode/electrolyte interface during cell charging and discharging^{10, 26}. This concentration polarization lowers the cell potential available and is potentially resistive, hence diminishing battery rate performance. One method of achieving only cation conductivity in a polymer system is to tether the

anion to the polymer backbone, as in polyelectrolyte (also known as ionomer) systems^{10, 27, 28}.

In general, polyelectrolytes are defined as materials that have polymeric backbones with covalently bonded ionic groups attached to them (either cationic or anionic). The functionality of the system depends on the ionic group attached to the polymer backbone²⁹. Common functional groups are SO_3^- , COO^- , and NH_3^+ . A morphological feature of some polyelectrolytes such as NAFION, a perfluorosulfonate polymer, involves aggregations of ionic side-chains providing a micro-phase separated structure involving a hydrophobic matrix and hydrophilic ionic cluster regions²⁹. Fig. 2 illustrates the structures of a simple polymer, a simple electrolyte with anionic side chains and a microphase separated system with anionic side chain.

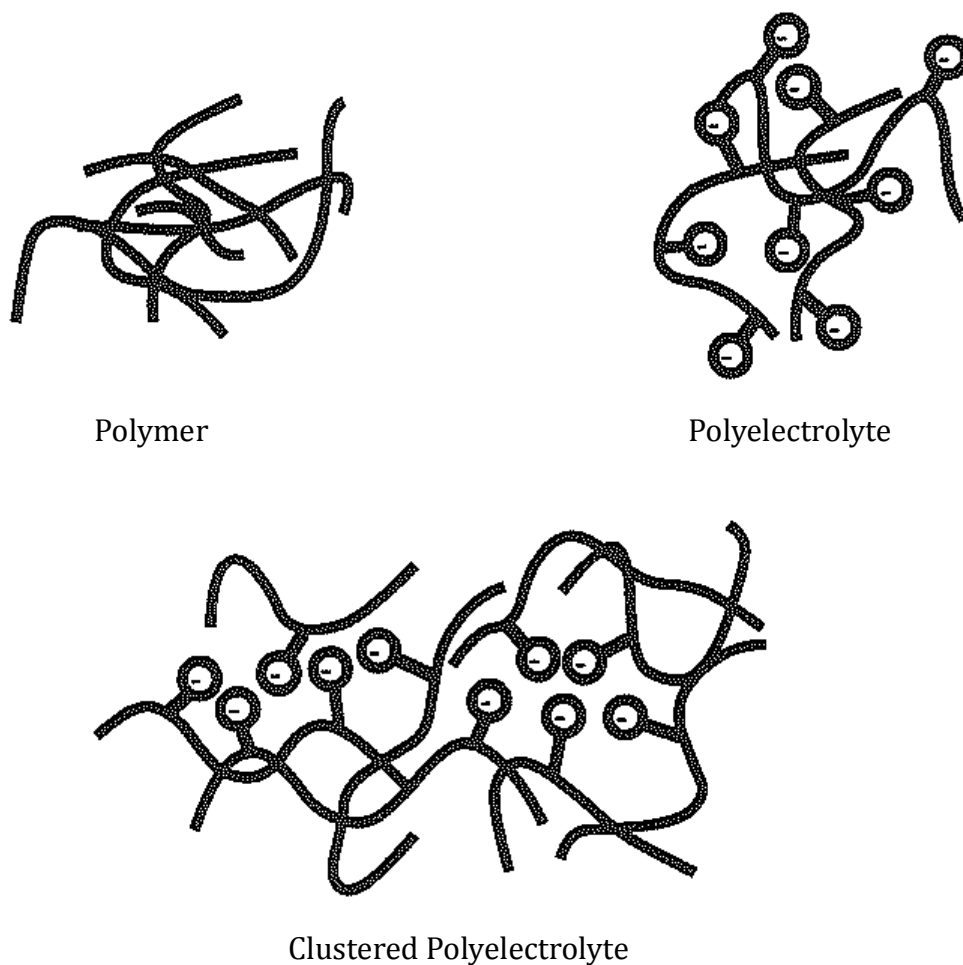


Fig. 2 Schematic representation of a simple polymer, polyelectrolyte with anion side chains and microphase separated system with anion side chain. Reproduced from Gray²⁹.

Numerous single ion conductor ionomer systems have been developed over the years; for example: those based on poly(2-acrylamido-2-methyl-1-propane-sulfonic acid) (PAMPS)^{30, 31} and copolymers of sulfonate polyester, sulfonated ethylene/styrene and sulfonated styrene-ethylene/butylene-styrene³²⁻³⁵. In general, however, the anion on the polymer backbone is somewhat basic, from which the

cation does not readily dissociate, resulting in low ionic conductivity. A number of methods have been employed in an attempt to increase the ionic conductivity; for example the AMPS monomer has been copolymerized with N,N-dimethylacrylamide (DMAA) to separate the ionic moieties along the backbone and thereby avoid multiple anion association to the cation³⁶. The addition of an organic solvent or ionic liquid has been shown to assist lithium ion dissociation from the backbone leading to high ionic conductivities and good performance in Li-ion batteries³⁷⁻⁴⁰.

Recently, Colby et al. have investigated cation dynamics in polyester based ionomers and sulfonated polystyrene, with a variety of cations ranging from the inorganic Na^+ , Li^+ and Cs^+ , to organic cations which are typically used to prepare ionic liquid salts⁴¹. It was very interesting to observe that the glass transition temperatures of these ionomers were significantly reduced when the organic cations were used as the ionomer charge carriers, with the ionic conductivity increasing by as much as 10^4 times when an ionic liquid-like cation of tetrabutylammonium ion was used instead of a sodium cation²⁷. This was attributed primarily to a lowering in the glass transition temperature, T_g , due to the weaker electrostatic interactions between the cation and the backbone tethered sulfonate anion.

1.2 Ionic liquids

The selection of suitable non-flammable electrolytes is an important issue for realizing a safe battery system without compromising the performance of the

electrolytes in practical devices. Ionic liquids (ILs) possess the beneficial properties that can be used to realize a safe and high-performance battery. ILs can be defined as low melting liquids, which are comprised wholly of anions and cations; typically they are liquid below 100°C^{42, 43}. ILs can have a series of distinctive properties such as negligible vapor pressure, non flammability, high thermal stability, high ionic conductivity, wide operating temperature range and wide electrochemical stability window (though it is important to note that not all ILs possess all of these properties)⁴²⁻⁴⁵. These properties lead to an obvious and immediate advantage over traditional solvents. In addition, IL properties can be tailored through the combination of cations and anions, modifying characteristics such as acidity/basicity, hydrophobicity/hydrophilicity, density, viscosity and dissolvability to many organic and inorganic materials to suit specific requirements⁴⁶⁻⁴⁸. As a result of these distinctive characteristics, ILs are recognized as “designer solvents”^{42, 46}. Ionic liquids have been investigated for many applications including electroplating, batteries, electrochemical capacitors and photo electrochemical cells⁴⁷⁻⁴⁹.

On the basis of their composition, ILs can be categorized into different classes that basically include aprotic, protic and zwitterionic types, with each one suitable for a specific application⁴⁷. For example, aprotic ILs are suitable for lithium batteries and supercapacitors, protic ILs suitable for fuel cells while zwitterionic ILs are suitable for ILs-based membranes. Moreover, variation of ion structure can lead to various specific applications, which range from energy storage and conversion to metal

deposition, also as reaction media in chemistry, biochemistry and even biomechanics^{43, 47}. The most important and widely studied cations in these salts include dialkylimidazolium, pyrrolidinium, and pyridinium derivatives, with bulky and soft anions such as $[\text{PF}_6]^-$, $[\text{BF}_4]^-$, $[\text{CF}_3\text{SO}_3]^-$, and $[(\text{CF}_3\text{SO}_2)_2\text{N}]^-$ as shown in Fig. 3.

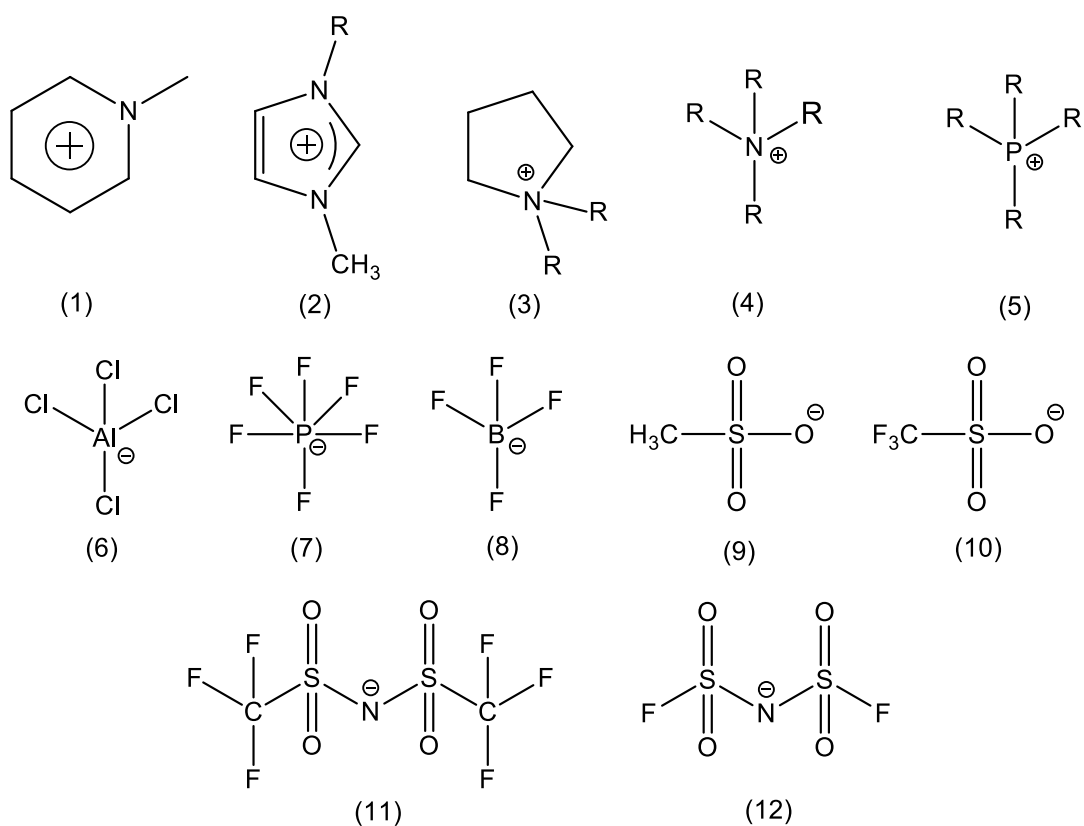


Fig. 3 Commonly used cations and anions in ILs. (1) alkylpyridinium, (2) dialkylimidazolium, (3) dialkylpyrrolidinium, (4) tetralkylammonium, (5) tetralkylphosphonium, (6) tetrachloroaluminate, (7) hexafluorophosphate, (8) tetrafluoroborate, (9) mesylate, (10) triflate, (11) bis(trifluoromethylsulfonyl)imide, (12) bis(fluorosulfonyl)imide.

1.3 Polymer-IL gels

Ionic liquid based polymer gels are also known as “ionogels”, where an IL phase has interpenetrated through a solid phase, giving rise to a material with solid-like properties⁵⁰. The preparation of ionogels falls into three broad categories, which are based upon the nature of the solid-like network used: (i) organic (low-molecular weight gelators or polymers); (ii) inorganic (metal oxide, carbon nanotubes or the networks derived from a sol-gel process); and (iii) hybrid organic-inorganic (typically polymers reinforced with inorganic fillers)⁵⁰. The immobilization of ionic liquids within organic or inorganic matrices enables their unique properties in the solid state, preventing drawbacks related to shaping and risk of leakage²². ILs can play a role as plasticizer in polymer matrices and will help to increase the conductivity of the system⁵¹. Furthermore, use of a highly cross-linked polymer can benefit mechanical stability without a significant decrease in conductivity⁵²⁻⁵⁴.

In many cases, the ionogel is simply formed by swelling the polymer in the IL or by adding the polymer in a co-solvent to the IL and then removing the solvent^{55, 56}. Another route to the formation of ionogels is the polymerisation of a monomer within the IL^{51, 52, 57, 58}. However, using this method requires careful control of the monomer concentrations to prevent miscibility issues. The miscibility between IL and the polymer is the most important factor to be considered during gelation in order to achieve sufficient interpenetration of the two phases⁵⁹. An additional consideration when using polymers as the gelling agent is that a loss of mechanical strength can occur should the ratio of IL to polymer be too high⁵¹. Therefore, the

amount of IL needs to be controlled, because an excessive amount of IL would reduce the mechanical properties of the gels.

Kumar & Hashmi⁶⁰ reported a gel polymer electrolyte based on an IL and polymer doped with a sodium salt. The gel electrolytes possessed excellent dimensional stability in the form of a freestanding thick film. The highest ionic conductivity obtained for this system was $5.74 \times 10^{-3} \text{ S.cm}^{-1}$ at room temperature (27°C). In addition, Yoshimoto et al.⁶¹, studied the influence of ILs on the ionic conductivity in gel electrolytes. Their system consisted of three substances, a polymer, an IL and a magnesium salt. This system produced self-standing transparent films with sufficient mechanical strength. They showed that the ionic conductivity increases with increasing content of the IL. The highest ionic conductivity achieved was at $3.5 \times 10^{-3} \text{ S.cm}^{-1}$ at 60°C for the system containing 80% IL. They also suggested that the magnesium ion (Mg^{2+}) could be mobile in the gel system.

Susan et al.⁵¹, have reported examples of ionogels formed by in-situ radical polymerization of monomers in ILs. They prepared ionogels by in-situ radical polymerization of vinyl monomers in 1-ethyl-3-methylimidazolium bis(trifluoromethylsulfonyl)amide ($\text{C}_2\text{mImNTf}_2$). A series of vinyl monomers were used to form the ionogels such as methyl methacrylate (MMA), vinyl acetate, acrylonitrile, styrene, 2-hydroxyethyl methacrylate, methyl acrylate and acrylamide. Among those monomers, only MMA and methyl acrylate were compatible with $\text{C}_2\text{mImNTf}_2$. Polymerization of MMA in $\text{C}_2\text{mImNTf}_2$ produced flexible, transparent and self-standing films and the glass transition (T_g) of the ionogels decreased with increasing mole fraction of $\text{C}_2\text{mImNTf}_2$. The ionic conductivity of this system is close to $10^{-2} \text{ S.cm}^{-1}$ at room temperature. In the

system containing a mixture of IL and salt, it is important to determine which ions are actually conducting to ensure that target ion (ie Li for lithium battery applications) is mobile

1.4 Sodium batteries

Most of the recent research on rechargeable batteries is based on lithium and zinc systems^{2, 3, 62}. Lithium ion batteries are widely used for almost all portable electronic devices because lithium has a combination of useful properties such as small ionic size (which allows fast diffusion in solids), very negative redox potential (and therefore high cell voltage), and light weight (which enables high specific energy devices). However, lithium based batteries present a number of major safety limitations, due to the use of the volatile organic electrolyte, which can lead to a fire/explosion hazard^{63, 64}. Moreover, while Li-ion batteries remain an important energy storage technology, there are concerns about the longer-term availability and cost of lithium⁶⁵. This is because lithium reserves are unevenly distributed in the world and located in remote and politically sensitive areas^{66, 67}. Thus, the extended usage of lithium in larger scale applications may significantly increase the price of lithium compounds. This issue will become more important if the demands for this technology stretch into larger scale transport and stationary power storage applications.

With sodium's greater abundance, low cost, low atomic mass (compared with other metal such as zinc), as well as its relatively high electrochemical reduction potential ($E^{\circ}(\text{Na}^+/\text{Na}) = -2.71\text{V}$ versus standard hydrogen electrode; only 300 mV above

lithium)^{2, 60, 68, 69}, it is considered to be a promising candidate for energy storage applications as an alternative to lithium. The use of sodium in batteries has been reported almost 50 years ago and is being commercialized in technologies such as sodium sulfur⁷⁰ and Na-NiCl₂⁷¹ systems, which use β -alumina as a solid electrolyte.

Na-S and Na-NiCl₂ batteries provide reasonable power and energy densities, temperature stability, and low cost due to the high abundance of the raw materials and suitability for high volume mass production. Furthermore, Na-S technology exhibits cycling flexibility and low maintenance requirements. However, in both systems, in order to obtain sufficient sodium conduction, a high operating temperature, approximately 573 K, is required which reduces the energy density of the battery system due to the need to incorporate heaters and thermal insulation. At the operating temperatures, in the case of Na-S system, molten sulphur, sodium and the polysulphide compounds are highly corrosive, hence, resistant containers are needed. The use of mostly solid cathode materials makes Na-NiCl₂ batteries intrinsically safer and less corrosive than Na-S batteries. Nonetheless, there is still the need of further improvement in power and reliability and especially in decreasing the operating temperature.

Due to the unique properties of ILs mentioned above, work on sodium-IL batteries is emerging. Nohira and co-workers^{72, 73} have reported intermediate-temperature ionic liquid systems of NaNTf₂-KNTf₂ and NaNTf₂-CsNTf₂, for use as electrolytes in sodium secondary batteries. These systems were found to perform well at

operating temperatures between 333 and 393 K and also possess wide electrochemical windows, up to 5.2 V at 363 K. This operating temperature range gives these systems a significant advantage compared to Na/S and Na/NiCl₂ batteries, which must be operated at around 573 K. Nevertheless, it is desirable for portable energy sources to have high performance at room temperature. Work by Buchner et al.³³, on the 1-butyl-3-methylimidazolium IL doped with NaBF₄, shows that the added sodium salt has only a minor influence on the transport properties of the IL. On the other hand, Egashira et al.⁶⁸, suggested NaBF₄ is not very soluble in diethylmethoxyethylammonium tetrafluoroborate, and proposed to use a polyether of poly(ethylene glycol) dimethyl ether (PEGDME) as a coordinating agent.

1.5 Aims of this study and thesis overview

1.5.1 Aims of the research

The main aim of this project is to produce high performance, safe and low-cost of solid-state electrolytes for electrochemical devices, with a main focus being electrolytes for Na based batteries. Owing to the unique properties of an ILs we first examined Na containing IL electrolytes, comparing their properties to analogous Li-IL electrolytes. We then investigated different approaches to gelling these IL electrolytes. Finally we prepared and tested a number of ionomer systems containing sodium ions as solid-state electrolytes.

1.5.2 Thesis overview

This thesis is presented in a ‘thesis by publication’ format. It consists of 5 journal articles (3 published and 2 submitted), together with background and a literature review of the research area. Each chapter contains a general overview of the articles along with their supporting information.

Chapter 1. Introduction

This chapter provides an overview of the general development of electrolytes, background and literature review of ionic liquids and the trends towards sodium-based batteries.

Chapter 2. *Ionogels based on ionic liquids as potential highly conductive solid-state electrolytes*

In this chapter, the sol-gel approach to gelation of an ionic liquid was investigated. The effect of silica content in the ionogels was characterized and analyzed in terms of chemical interactions, thermal stability and ionic conductivity. This section was published in *Electrochimica Acta*

Chapter 3. *Sodium ion conductors for sodium batteries*

In this chapter, the potential of sodium-based RTIL electrolytes as a promising candidate for sodium batteries was investigated. Two types of electrolytes were prepared and characterized:

- A comparison of sodium and lithium ionic liquid electrolytes based on the RTIL, 1-butyl-1-methylpyrrolidinium bis(trifluoromethylsulfonyl) amide ($C_4\text{mpyrNTf}_2$) were reported. This section was published in *Electrochimica Acta* as a paper entitled “*Properties of sodium-based ionic liquid electrolytes for sodium secondary battery applications*”.
- The effect of gelation of the liquid electrolytes above were investigated and studied in terms of the ionic conductivity, thermal properties, chemical interactions from infrared spectroscopy and cyclic voltammetry. This part to be submitted to *Electrochimica Acta* as a paper entitled “*Gel-ionic liquid based sodium ion conductors for sodium batteries*”.

Chapter 4. Ionomers as cation only ion conductors

In this chapter, we studied ionomer systems that have the potential to act as “single ion/mixed cation” conductors.

- A series of sulfonate based copolymer ionomers based on a combination of ionic liquid and sodium cations were prepared and characterized. The decoupling of ionic conductivity from the T_g of the backbone were revealed. A paper was published in *Journal of Materials Chemistry A* entitled “*Ion conduction and phase*

morphology in sulfonate copolymer ionomers based on ionic liquid-sodium cation mixtures”.

- A family of novel sulfonate based homopolymers were prepared by partially replacing sodium cations with different types of ionic liquid type ammonium cations. The degree of decoupling from local segmental motions of the ionomers was found to increase with increasing bulkiness of the quaternary ammonium cation. This work has been submitted to *Polymer Journal* as a paper entitled “*Decoupled ion conduction in poly(2-acrylamido-2-methyl-1-propane-sulfonic acid) (PAMPS) homopolymers*”.

Chapter 5. General conclusions and future work

1.6 Bibliography

1. Tarascon, J. M.; Armand, M. *Nature* **2001**, *414*, 359-367.
2. Dell, R. M. *Solid State Ionics* **2000**, *134*, 139-158.
3. Palacín, M. R. *Chem. Soc. Rev.* **2009**, *38*, 2565-2575.
4. Xu, K. *Chem. Rev. (Washington, DC, U. S.)* **2004**, *104*, 4303-4417.
5. Latif, F.; Aziz, M.; Katun, N.; Ali, A. M. M.; Yahya, M. Z. *J. Power Sources* **2006**, *159*, 1401-1404.
6. Nelson, R. *EE: Evaluation Engineering* **2013**, *52*, 14-15.
7. Williard, N.; He, W.; Hendricks, C.; Pecht, M. *Energies* **2013**, *6*, 4682-4695.
8. Fenton, D. E.; Parker, J. M.; Wright, P. V. *Polymer* **1973**, *14*, 589.
9. Lascaud, S.; Perrier, M.; Armand, M.; Prud'homme, J.; Kapfer, B.; Vallée, A.; Gauthier, M. *Electrochim. Acta* **1998**, *43*, 1407-1414.
10. Gray, F. M., *Solid polymer electrolytes : fundamentals and technological applications*. New York, NY : VCH: New York, NY, 1991.
11. Chung, S. H.; Wang, Y.; Persi, L.; Croce, F.; Greenbaum, S. G.; Scrosati, B.; Plichta, E. *J. Power Sources* **2001**, *97-98*, 644-648.
12. Scrosati, B.; Croce, F.; Panero, S. *J. Power Sources* **2001**, *100*, 93-100.
13. Marcinek, M.; Bac, A.; Lipka, P.; Zalewska, A.; Zukowska, G.; Borkowska, R.; Wieczorek, W. *J. Phys. Chem. B* **2000**, *104*, 11088-11093.
14. Wieczorek, W.; Raducha, D.; Zalewska, A.; Stevens, J. R. *J. Phys. Chem. B* **1998**, *102*, 8725-8731.
15. Mohapatra, S. R.; Thakur, A. K.; Choudhary, R. N. P. *Ionics* **2008**, *14*, 255-262.
16. Sangeetha, N. M.; Maitra, U. *Chem. Soc. Rev.* **2005**, *34*, 821-836.
17. Chen, F.; Ma, X.; Qu, X.; Yan, H. *J. Appl. Polym. Sci.* **2009**, *114*, 2632-2638.
18. Rajendran, S.; Sivakumar, P.; Babu, R. S. *Bull. Mater. Sci.* **2006**, *29*, 673-678.
19. Lee, K. M.; Suryanarayanan, V.; Ho, K. C. *J. Photochem. Photobiol. A.* **2009**, *207*, 224-230.
20. Ileperuma, O. A. *Materials Technology* **2013**, *28*, 65-70.
21. Morita, M.; Shirai, T.; Yoshimoto, N.; Ishikawa, M. *J. Power Sources* **2005**, *139*, 351-355.
22. Vioux, A.; Viau, L.; Volland, S.; Le Bideau, J. *C. R. Chim.* **2010**, *13*, 242-255.
23. Gayet, F.; Viau, L.; Leroux, F.; Mabilille, F.; Monge, S.; Robin, J. J.; Vioux, A. *Chem. Mater.* **2009**, *21*, 5575-5577.
24. Göbel, R.; Hesemann, P.; Weber, J.; Möller, E.; Friedrich, A.; Beuermann, S.; Taubert, A. *Phys. Chem. Chem. Phys.* **2009**, *11*, 3653-3662.
25. Le Bideau, J.; Gaveau, P.; Bellayer, S.; Néouze, M. A.; Vioux, A. *Phys. Chem. Chem. Phys.* **2007**, *9*, 5419-5422.
26. Wang, W.; Liu, W.; Tudryn, G. J.; Colby, R. H.; Winey, K. I. *Macromolecules* **2010**, *43*, 4223-4229.

27. Tudryn, G. J.; Liu, W.; Wang, S. W.; Colby, R. H. *Macromolecules* **2011**, *44*, 3572-3582.
28. Roach, D. J.; Dou, S.; Colby, R. H.; Mueller, K. T. *J. Chem. Phys.* **2013**, *138*.
29. Gray, F. M., *Polymer electrolytes*. Cambridge : Royal Society of Chemistry: Cambridge, 1997.
30. Tiyaipiboonchaiya, C.; Pringle, J. M.; MacFarlane, D. R.; Forsyth, M.; Sun, J. *Macromol. Chem. Phys.* **2003**, *204*, 2147-2154.
31. Ünal, H. I.; Yilmaz, H. *J. Appl. Polym. Sci.* **2002**, *86*, 1106-1112.
32. Annala, M.; Lipponen, S.; Kallio, T.; Seppälä, J. *J. Appl. Polym. Sci.* **2012**, *124*, 1511-1519.
33. Hu, H.; Liu, W.; Yang, L.; Xiao, M.; Wang, S.; Han, D.; Meng, Y. *Int. J. Hydrogen Energy* **2012**, *37*, 4553-4562.
34. Santiago, A. A.; Vargas, J.; Cruz-Gómez, J.; Tlenkopatchev, M. A.; Gaviño, R.; López-González, M.; Riande, E. *Polymer (United Kingdom)* **2011**, *52*, 4208-4220.
35. Tudryn, G. J.; O'Reilly, M. V.; Dou, S.; King, D. R.; Winey, K. I.; Runt, J.; Colby, R. H. *Macromolecules* **2012**, *45*, 3962-3973.
36. Tiyaipiboonchaiya, C.; MacFarlane, D. R.; Sun, J.; Forsyth, M. *Macromol. Chem. Phys.* **2002**, *203*, 1906-1911.
37. Byrne, N.; Howlett, P. C.; MacFarlane, D. R.; Forsyth, M. *Adv. Mater. (Weinheim, Ger.)* **2005**, *17*, 2497-2501.
38. Travas-Sejdic, J.; Steiner, R.; Desilvestro, J.; Pickering, P. *Electrochim. Acta* **2001**, *46*, 1461-1466.
39. Park, M. J.; Kim, S. Y. *J. Polym. Sci., Part B: Polym. Phys.* **2013**, *51*, 481-493.
40. Bekiarian, P. G.; Doyle, M.; Farnham, W. B.; Feiring, A. E.; Morken, P. A.; Roelofs, M. G.; Marshall, W. J. *J. Fluorine Chem.* **2004**, *125*, 1187-1204.
41. Wang, W.; Tudryn, G. J.; Colby, R. H.; Winey, K. I. *J. Am. Chem. Soc.* **2011**, *133*, 10826-10831.
42. Earle, M. J.; Seddon, K. R. *Pure Appl. Chem.* **2000**, *72*, 1391-1398.
43. Forsyth, S. A.; Pringle, J. M.; MacFarlane, D. R. *Aust. J. Chem.* **2004**, *57*, 113-119.
44. Forsyth, S. A.; Batten, S. R.; Dai, Q.; MacFarlane, D. R. *Aust. J. Chem.* **2004**, *57*, 121-124.
45. Appetecchi, G. B.; Montanino, M.; Balducci, A.; Lux, S. F.; Winterb, M.; Passerini, S. *J. Power Sources* **2009**, *192*, 599-605.
46. Chowdhury, S. A.; Scott, J. L.; MacFarlane, D. R. *Pure Appl. Chem.* **2008**, *80*, 1325-1335.
47. Armand, M.; Endres, F.; MacFarlane, D. R.; Ohno, H.; Scrosati, B. *Nat. Mater.* **2009**, *8*, 621-629.
48. Macfarlane, D. R.; Tachikawa, N.; Forsyth, M.; Pringle, J. M.; Howlett, P. C.; Elliott, G. D.; Davis, J. H.; Watanabe, M.; Simon, P.; Angell, C. A. *Energy. Environ. Sci.* **2014**, *7*, 232-250.
49. Every, H.; Bishop, A. G.; Forsyth, M.; MacFarlane, D. R. *Electrochim. Acta* **2000**, *45*, 1279-1284.

50. Le Bideau, J.; Viau, L.; Vioux, A. *Chem. Soc. Rev.* **2011**, *40*, 907-925.
51. Susan, M. A. B. H.; Kaneko, T.; Noda, A.; Watanabe, M. *J. Am. Chem. Soc.* **2005**, *127*, 4976-4983.
52. Klingshirn, M. A.; Spear, S. K.; Subramanian, R.; Holbrey, J. D.; Huddleston, J. G.; Rogers, R. D. *Chem. Mater.* **2004**, *16*, 3091-3097.
53. Rupp, B.; Schmuck, M.; Balducci, A.; Winter, M.; Kern, W. *Eur. Polym. J.* **2008**, *44*, 2986-2990.
54. Sterner, E. S.; Rosol, Z. P.; Gross, E. M.; Gross, S. M. *J. Appl. Polym. Sci.* **2009**, *114*, 2963-2970.
55. Uk Hong, S.; Park, D.; Ko, Y.; Baek, I. *Chem. Commun. (Cambridge, U. K.)* **2009**, 7227-7229.
56. Yoon, J.; Kang, D. K.; Won, J.; Park, J. Y.; Kang, Y. S. *J. Power Sources* **2012**, *201*, 395-401.
57. Stanzione, J. F.; Jensen, R. E.; Costanzo, P. J.; Palmese, G. R. *ACS Appl. Mater. Interfaces* **2012**, *4*, 6142-6150.
58. Frank-Finney, R. J.; Bradley, L. C.; Gupta, M. *Macromolecules* **2013**, *46*, 6852-6857.
59. Winterton, N. *J. Mater. Chem.* **2006**, *16*, 4281-4293.
60. Kumar, D.; Hashmi, S. A. *Solid State Ionics* **2010**, *181*, 416-423.
61. Yoshimoto, N.; Shirai, T.; Morita, M. *Electrochim. Acta* **2005**, *50*, 3866 - 3871.
62. Kar, M.; Winther-Jensen, B.; Forsyth, M.; MacFarlane, D. R. *Phys. Chem. Chem. Phys.* **2013**, *15*, 7191-7197.
63. Choi, J. A.; Shim, E. G.; Scrosati, B.; Kim, D. W. *Bull. Korean Chem. Soc.* **2010**, *31*, 3190-3194.
64. Lane, G. H.; Bayley, P. M.; Clare, B. R.; Best, A. S.; MacFarlane, D. R.; Forsyth, M.; Hollenkamp, A. F. *J. Phys. Chem. C* **2010**, *114*, 21775-21785.
65. Ellis, B. L.; Nazar, L. F. *Curr. Opin. Solid State Mater. Sci.* **2012**, *16*, 168-177.
66. Berens, A. R.; Hodge, I. M. *Macromolecules* **1982**, *15*, 756-761.
67. Dou, S.; Zhang, S.; Klein, R. J.; Runt, J.; Colby, R. H. *Chem. Mater.* **2006**, *18*, 4288-4295.
68. Egashira, M.; Asai, T.; Yoshimoto, N.; Morita, M. *Electrochim. Acta* **2011**, *58*, 95-98.
69. Kiran Kumar, K.; Ravi, M.; Pavani, Y.; Bhavani, S.; Sharma, A. K.; Narasimha Rao, V. V. R. *Physica B: Condensed Matter* **2011**, *406*, 1706-1712.
70. Sudworth, J. L. *J. Power Sources* **1984**, *11*, 143-154.
71. Coetzer, J. *J. Power Sources* **1986**, *18*, 377-380.
72. Fukunaga, A.; Nohira, T.; Kozawa, Y.; Hagiwara, R.; Sakai, S.; Nitta, K.; Inazawa, S. *J. Power Sources* **2012**, *209*, 52-56.
73. Yamamoto, T.; Nohira, T.; Hagiwara, R.; Fukunaga, A.; Sakai, S.; Nitta, K.; Inazawa, S. *J. Power Sources* **2012**, *217*, 479-484.



Chapter 2

Ionogels based on ionic liquids as
potential highly conductive solid state
electrolytes

2.1 General Overview

Interest in high-performance solid - state electrolytes is currently developing since they have evident advantages over fluid materials in application in electrochemical devices¹⁻⁴ as discussed in section 1.1.2. Solid polymer electrolytes are particularly attractive because they can be flexible and shaped into different desired geometries. Along with the unique combination of IL properties (see section 1.2), the immobilization of ILs within a polymer network makes it possible to take advantage of these unique properties in a solid state. The superiority of these electrolytes over conventional plasticized polymer electrolytes lies in the non-volatility of the ILs and their thermal stability^{1, 2, 5, 6}.

Various methods to confine and immobilize ILs in a polymer network have been reported, including by polymerization of monomers in ionic liquids, solvent casting or swelling of polymers⁶⁻⁸. Typical high volume fractions of the IL in a polymer membrane disfavor the mechanical properties and leave the possibility of IL leakage from the polymer membrane⁹. The sol-gel approach is currently attracting growing interest in order to achieve the mechanical properties desired of an IL gel electrolyte¹⁰⁻¹². Typically however, it is difficult to achieve high ionic liquid contents.

In this chapter, immobilization of ILs at high loading in a silica network was investigated by a one-pot sol gel synthesis using tetraethoxysilane (TEOS) in an

ionic liquid, 1-butyl-3-methylimidazolium tetrafluoroborate C_4mImBF_4 . The silica network thus formed produced novel ionogels, as described in Publication 1 in this chapter¹³. The effect of silica content in the IL was characterized and analyzed using impedance spectroscopy, differential scanning calorimetry, attenuated total reflectance-Fourier transform infrared (ATR-FTIR), solid-state nuclear magnetic resonance (NMR) and thermogravimetric analysis (TGA). The details of this study have been published in *Electrochimica Acta* in a paper entitled “Ionogels based on ionic liquid as potential highly conductive solid state electrolytes”¹³.

2.2 Specific Declaration

PART B: Suggested Declaration for Thesis Chapter

Monash University

Declaration for Thesis Chapter 2

Declaration by candidate

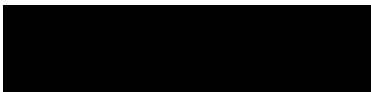
In the case of Chapter 2, the nature and extent of my contribution to the work was the following:

Nature of contribution	Extent of contribution (%)
Initiation, key ideas, performed the experiments, synthesis, data analysis and interpretation, manuscript development and writing up	90

The following co-authors contributed to the work. If co-authors are students at Monash University, the extent of their contribution in percentage terms must be stated:

Name	Nature of contribution	Extent of contribution (%) for student co-authors only
Douglas MacFarlane	Key ideas, proof reading and final drafting	-
Maria Forsyth	Key ideas, proof reading and final drafting	-
Paul Bayley	Assisted in solid-state NMR analysis	-

The undersigned hereby certify that the above declaration correctly reflects the nature and extent of the candidate's and co-authors' contributions to this work*.

Candidate's Signature		Date 17/7/2014
Main Supervisor's Signature		Date 17/7/2014

*Note: Where the responsible author is not the candidate's main supervisor, the main supervisor should consult with the responsible author to agree on the respective contributions of the authors.

2.3 Publication 1

Ionogels based on ionic liquids as potential highly conductive solid state electrolytes

S.A.M.Noor,^{a,b} P.M. Bayley,^c M. Forsyth,^c D.R. MacFarlane^{a*}

^a *School of Chemistry, Monash University, Clayton Campus, Victoria, Australia*

^b *Chemistry Department, Centre for Defence Foundation Studies, National Defence University of Malaysia, 57000, Kuala Lumpur, Malaysia*

^c *ARC Centre of Excellence for Electromaterials Science (ACES) Institute for Frontier Materials Deakin University, Victoria, Australia*

* *Corresponding Author:*

Electrochimica Acta

91 (2013) 219-226

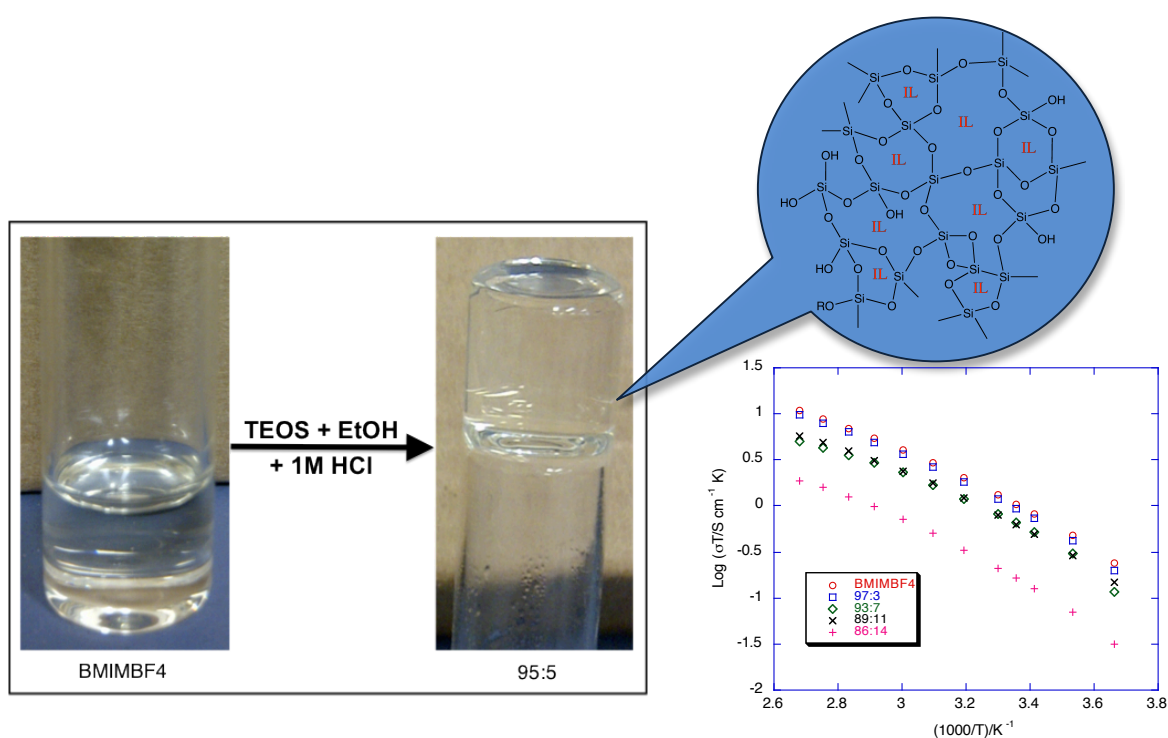
DOI: 10.1010/j.electacta.2012.11.113

Graphical Abstract

Ionogels based on ionic liquids as potential highly conductive solid state electrolytes

Siti Aminah Mohd Noor, Paul M Bailey, Maria Forsyth, Douglas R MacFarlane*

A novel ionogels via straightforward one-pot synthesis of silica in ionic liquid for a
potential highly conductive solid state electrolytes





Ionogels based on ionic liquids as potential highly conductive solid state electrolytes

S.A.M. Noor^{a,b}, P.M. Bayley^c, M. Forsyth^c, D.R. MacFarlane^{a,*}

^a School of Chemistry, Monash University, Clayton Campus, Victoria, Australia

^b Chemistry Department, Centre for Defence Foundation Studies, National Defence University of Malaysia, 57000 Kuala Lumpur, Malaysia

^c ARC Centre of Excellence for Electromaterials Science (ACES), Institute for Frontier Materials Deakin University, Victoria, Australia

ARTICLE INFO

Article history:

Received 11 September 2012

Received in revised form

25 November 2012

Accepted 26 November 2012

Available online 19 December 2012

Keywords:

Butylmethylimidazolium tetrafluoroborate

[BMIm][BF₄]

Sol–gel process

Ionogels

Solid state electrolytes

ABSTRACT

The preparation and properties of ionogels as potential highly conductive solid state electrolytes has been investigated. The ionogels have been prepared by a one-pot sol–gel synthesis using tetraethoxysilane (TEOS) in an ionic liquid, 1-butyl-3-methyl imidazolium tetrafluoroborate [BMIm][BF₄]. The effect of silica content in the ionogels was characterized and analyzed in terms of chemical interactions, thermal stability and ionic conductivity. Immobilization of the IL in the silica network was observed even at high loading of IL (97 wt.%). Hydrogen bond networks between BF₄[−] and the hydroxyl group in the silica was suggested as the mechanism of this immobilization, which was characterized by FTIR and solid-state NMR. TGA analysis shows that the prepared ionogels were stable up to around 450 °C, where a final one-step degradation occurs. The ionic conductivity was found to decrease as the amount of silica increased. However, with high loading of IL (97 wt.%) the ionic conductivity was close to that of the pure IL. From the results obtained, these ionogels can be considered potential candidates for electrochemical devices where high ionic conductivity in solid state materials is desirable.

© 2012 Elsevier Ltd. All rights reserved.

1. Introduction

Current high power electrochemical energy storage technologies rely on electrolytes based on flammable solvents, which are typically volatile organic compounds (VOCs) that result in major safety problems when applied to many novel applications. The selection of suitable non-flammable electrolytes is an important issue for realizing safe electrochemical devices without compromising their performance and practicality. The present strong focus on ionic liquids (ILs) is inspired by their distinctive combination of properties. ILs can be defined as low melting salts; typically they are liquid below 100 °C [1]. Certain families of ILs have a series of useful properties such as negligible vapor pressure, non flammability, high thermal stability, high ionic conductivity, wide operating temperature range and wide electrochemical stability window. These properties lead to an obvious and immediate advantage over traditional solvents [2–5].

In addition to the flammability problem, conventional organic liquid electrolytes also present a major problem of leakage of corrosive and toxic materials. Therefore, solid polymer electrolytes (SPEs) have been developed to overcome these problems. However, SPEs possess relatively low conductivity at ambient temperature, too low to be used in many practical devices [6]. Thus both

properties of liquid and solid electrolyte are needed to realize safety and high performance of batteries and research has turned to gelled liquids to achieve this. The gel state can be defined in three propositions as described by Flory [7], which are (a) two or more components in the system; (b) solid-like mechanical properties and (c) the liquid–solid system is stable on the time scale of analysis. In recent years, gel electrolytes have been widely investigated in order to develop safe and high performance batteries. A large number of gels containing salts dissolved in a polymer with mixed alkyl carbonates as plasticizers produce high ionic conductivity. However, the presence of low molecular weight plasticizer such as ethylene carbonate (EC) and propylene carbonate (PC) has a drawback in that these components highly active with respect to lithium electrodes [8]. An alternative to carbonate plasticizers is to use an IL where their negligible volatility and non-flammability lead to safer materials and thus improved life and safety features. These are significant advantages when ILs are used as electrolytes in batteries. Recent studies have described versatile gel IL electrolytes as an excellent substitute for liquid electrolytes in electrochemical devices due to their appealing feature of freestanding film and high thermal stability properties. This feature contributes to easy handling in cell design, modularity and reliability in electrochemical devices [9]. Thus, the immobilization of an IL within a polymer membrane makes it possible to take advantage of their unique properties in the solid state [10].

Various methods to confine and immobilize ILs in a polymer network have been reported, including by polymerization of

* Corresponding author. Tel.: [redacted]; fax: +61 3 9905 4597.
E-mail address: [redacted] (D.R. MacFarlane).

monomers in ionic liquids, solvent casting or swelling of polymers [11–13]. Typical high volume fractions of the IL in a polymer membrane disfavor the mechanical properties of electrolyte and leave the possibility of IL leakage from the polymer membrane [14]. The sol–gel approach is currently attracting growing interest in order to achieve the mechanical properties of an IL gel in an electrolyte. Typically however, it is difficult to achieve high ionic liquid contents. For example in the gels described by Gayet et al. [10], the highest achieved was 90 wt.% with presence of modified PMMA as mechanical support for the ionogel [6,14–17].

In the present study, we report one-pot synthesis of a silica network in an ionic liquid leading to novel ionogels. The effect of silica content in the IL is discussed. The prepared ionogels are characterized using complex impedance spectroscopy, differential scanning calorimetry (DSC), solid-state NMR, attenuated total reflectance-Fourier transform infrared (ATR-FTIR) and thermogravimetric analysis (TGA).

2. Experimental

2.1. Materials

1-Butyl-3-methyl imidazolium tetrafluoroborate [BMIm][BF₄] with high purity, tetraethylorthosilicate, TEOS (99%, for synthesis grade) and organic synthesis grade of ethanol procured from Merck were used as received. 1 M HCl was prepared from 32% concentrated HCl (UniVAR).

2.2. Preparation of ionogels

A mixture of BMImBF₄, TEOS and ethanol was stirred for 2 h at 40 °C. Then the homogeneous solution was cooled to room temperature and 1 M HCl was added drop wise under vigorous stirring for another one minute. The final mole ratio TEOS:EtOH:H₂O:HCl is 1.0:1.6:5.2:0.2. The gels were left to age in a closed vial for at least 24 h; gelation of the ionogel usually occurs within 5 h. Aging was continued for another ten days in an open vial at room temperature; Residual volatile components were completely removed by drying at 40 °C for another two days in a vacuum oven. The ionogels obtained were totally transparent, indicating good homogeneity. The content of TEOS was varied from 10 to 40 wt.%. The final composition of the ionogel was determined from the mass loss during the aging process, assuming that there was no evaporation of IL during the aging process. The measured weight loss was within weighing error that expected on the basis of the loss of ethanol and water from the mixture, indicating that the TEOS is fully hydrolyzed. The final composition of the ionogels produced was thus found to be (IL:SiO₂) 97:3, 93:7, 89:11 and 84:16.

2.3. Characterization

2.3.1. Impedance spectroscopy

In order to determine the ionic conductivity of the ionogels, alternating current (AC) impedance measurements were carried out using high frequency response analyzer (HFRA; Solartron 1296) over frequency range of 0.01 Hz to 10 MHz with 30 mV perturbation amplitude. Ten points per decade were measured. The analysis was conducted in the temperature range from 273 to 373 K.

2.3.2. Differential scanning calorimetry (DSC)

To provide information about the temperatures of the different phase transitions, DSC measurements have been carried out on the prepared samples. DSC was performed with a DSC Q100 series instrument (TA Instruments) and the data was evaluated using Universal Analysis 2000 software. Approximately 8–10 mg of ionogel samples were tested in the temperature range of 123–373 K at a

scanning rate of 10 K min^{−1}. The glass transition temperature was determined at the midpoint of the heat-capacity change.

2.3.3. Solid-state nuclear magnetic resonance (NMR)

All NMR measurements were performed on a Bruker Avance III operating at 11.7 T with a 2.5 mm ¹⁹F/¹H/X MAS probe using zirconia rotors spinning at 5 kHz. Single pulse experiments on ²⁹Si were measured with a 4.5 μs RF pulse, corresponding to a flip angle of about 60°, with 496 scans (lower concentration samples were acquired with 2048 scans) and a recycle delay of 120 s. Cross-polarization experiments on ²⁹Si were acquired with a ramped contact pulse of 10 ms duration and 50 kHz ¹H decoupling (spinal.64 decoupling scheme) and a recycle delay of 5 s with 8192 scans collected. All ¹H experiments were acquired with a single $\pi/2$ pulse of 2.45 μs, 16 scans and a 5 s recycle delay. Experiments performed on ¹⁹F were acquired with a single $\pi/2$ pulse of 2.5 μs, 32 scans and a 5 s recycle delay. ¹¹B experiments were performed using a $\pi/2$ – τ – π – τ – π pulse sequence (with τ = 500 μs) to effectively suppress the background signal from the probe stator. Chemical shift referencing of ²⁹Si, ¹H, ¹⁹F and ¹¹B was performed using: tetrakis(trimethylsilyl)silane, saturated sodium 2,2-dimethyl-2-silapentane-5-sulfonate in D₂O, poly(tetrafluoroethylene) and 0.1 M boric acid in H₂O, respectively.

2.3.4. Attenuated total reflectance-Fourier transform infrared spectroscopy (ATR-FTIR)

ATR-FTIR was carried out to investigate the interactions that occur in the ionogels using a Bruker Equinox 55 coupled with Golden Gate single bounce diamond micro-attenuated total reflectance crystal and liquid nitrogen cooled Mercury/Cadmium Telluride detector. Measurements were made in the range 4000–600 cm^{−1} with a resolution of 4 cm^{−1}. Data was analyzed using an OPUS 6.0 Analyzer. Baseline correction has been done to all ionogels sample.

2.3.5. Thermogravimetric analysis (TGA)

Thermal behavior of the ionogels was characterized using a Mettler-Toledo TGA/DSC 1 in a 70 μL alumina crucible under nitrogen flow with a heating rate of 10 K min^{−1} from 313 to 873 K. Approximately 3–5 mg of the ionogels were tested. The obtained data was analyzed using STARE DBV10.00 software.

3. Results and discussion

3.1. Ionic conductivity

The ionic conductivity measurements were carried out with the aim of observing the effect of silica addition on the electrical properties of the ionogel electrolyte systems. Ionic conductivity was measured at five different loadings of silica from 0 to 16 wt.%. The ionic conductivity of pure [BMIm][BF₄] without silica at room temperature (298 K) was 3.5×10^{-3} S cm^{−1}. This ionic conductivity decreased as the amount of silica increased, as shown in Table 1. The primary reason for this is the decrease in concentration of the ions, however, as the amount of silica increases the ionogel also becomes hard and brittle, along with shrinkage of the sample, as can be observed from Fig. 1b, due to evaporation volatile components such as ethanol. This is consistent with reduction of ionic liquid content and lower pore connectivity in the ionogel as wt.% of silica increases, which may further lower the ionic conductivity. Interestingly, with addition of 3 wt.% of silica, the ionic conductivity (3.1×10^{-3} S cm^{−1}) is close to that of the pure IL. This behavior also can be seen in the system of *f*-PMMA-silica-[BMIm][NTf₂] as reported by Gayet et al. [10]. Thus it appears that the IL is confined in the silica network but the network does not itself have a

Table 1
Ionic conductivity, T_g and VTF parameters of BMIMBF₄ and various weight ratios of IL:silica.

Sample	σ (RT)/K $\pm 2\%$	T_g (DSC)/K ± 1	T_0 /K	R	E_a at 333 K/(kJ/mol) ± 1	B /K	$\log(\sigma_0)/S\text{ cm}^{-1}\text{ K}$
BMIMBF ₄	3.5 e–3	189	164 \pm 2	0.999	26	376 \pm 9	2.83 \pm 0.03
97:3	3.1 e–3	189	170 \pm 3	0.999	27	352 \pm 14	2.73 \pm 0.05
93:7	2.2 e–3	190	166 \pm 11	0.999	25	331 \pm 48	2.32 \pm 0.16
89:11	1.9 e–3	191	170 \pm 4	0.999	22	336 \pm 19	2.43 \pm 0.07
86:14	5.5 e–4	191	176 \pm 4	0.999	27	337 \pm 20	2.01 \pm 0.07

significant effect on the ionic conductivity of the ionogel. No leakage of the IL can be observed even after several months, which further corroborates that IL is well confined in silica matrix.

In order to analyze the mechanism of ionic conduction, the ionic conductivity dependence on temperature was studied in the temperature range of 273–373 K. Fig. 2a shows the Arrhenius plot of temperature dependent conductivity ($\log \sigma T$) versus the inverse absolute temperature for the ionogels with various weight ratios of IL:silica. From the Arrhenius plot, it can be seen that the ionic conductivity shows curvature indicating that Vogel–Tamman–Fulcher (VTF) behavior is involved. VTF behavior suggests that migration of the ions in the ionogel matrix is similar to ionic conduction in a viscous liquid. In the VTF equation (Eq. (1)), there are three parameters involved; σ_0 is a pre-exponential factor, B is pseudo-activation energy while T_0 is a temperature at which the conductivity disappears. In the free volume model of transport in liquids and polymers, this is the temperature at which free volume becomes zero [18].

$$\sigma T = \sigma_0 \exp \left[\frac{-B}{T - T_0} \right] \quad (1)$$

In order to obtain these parameters, the plot was fitted with the VTF equation and the values of these parameters are summarized

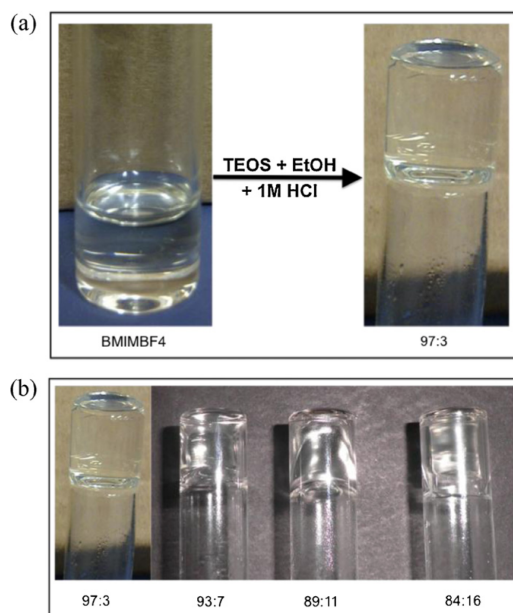


Fig. 1. Formation of ionogel (a) and physical appearance of ionogels with different weight ratios of IL:silica (b).

in Table 1. Generally, the value of T_0 obtained for these materials is near the T_g value measured from DSC analysis, as expected. The pre-exponential values of the ionogels decreased as the amount of silica increased indicating a reduction in the number of mobile species, accounting for a large part of the decrease in the ionic conductivity. However, the values of B and E_a almost remain constant suggesting that the structural dynamics and energetics of the conduction process in the gels is not significantly affected by the increasing amount of silica [19]. This idea is supported by the value of T_g from DSC analysis as discussed later. It can also be seen from the Arrhenius plot that the conductivity does not show any abrupt change with temperature, indicating that IL does not leak from the silica network.

3.2. Differential scanning calorimetry (DSC)

DSC thermograms during the heating scan from -150 to 100 °C of BMIMBF₄ and ionogels with different weight ratios of IL:silica are shown in Fig. 3. The glass transition temperature (T_g) of bulk BMIMBF₄ was measured at 189 K. From the thermogram, the value of T_g increases only slightly (likely within experimental error) with silica content, from 189 to 191 K. This situation is a stark contrast to the change in its physical properties observed, from soft gel to hard and brittle gel. This suggests that the presence of silica does not strongly affect the motional dynamics of the IL ions (as also indicated by the values of B and E_a almost remaining constant as silica content increased). This is a highly desirable decoupling of the mechanical properties from the ion transport properties that can produce an ideal combination of properties in a gel electrolyte. It also further confirmed that the silica matrix acts only as a support for the ionogels.

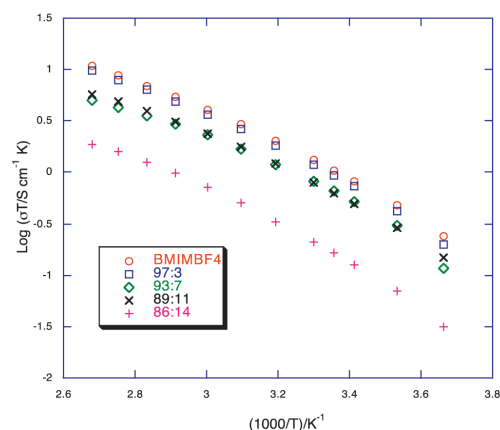


Fig. 2. Arrhenius plot of BMIMBF₄ and various weight ratios of IL:silica.

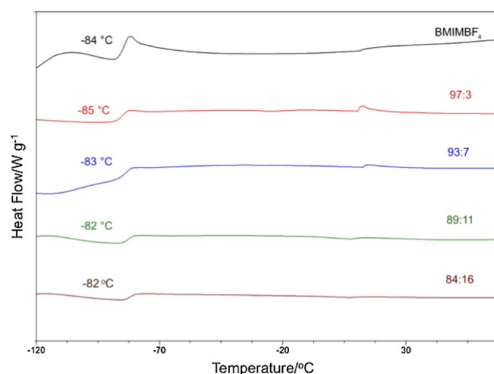


Fig. 3. DSC thermogram of BMIMBF₄ and various weight ratios of IL:silica.

3.3. Solid-state NMR

Polymerization of silicon alkoxides occurs through condensation reactions by elimination of water or alcohol. The gelation of the sol is initiated by this polycondensation process. However, this condensation process may not be complete during the gelation time, as discussed previously, with some amount of water and alkoxy groups remaining in the gel after this first stage [20]. The further elimination of water and alcohol during drying after gelation continues the reaction toward more complete condensation, as discussed within the context of the NMR spectra below. In order to determine the extent of condensation and the nature of the silica

polymers produced in the ionogel, solid-state ²⁹Si NMR analysis has been undertaken for each ionogel composition. The types of silicon bonding present (denoted by the Qⁿ nomenclature shown in the figure) after the hydrolysis and condensation processes are depicted in Fig. 4. The single pulse ²⁹Si NMR spectra for ionogels with different amount of silica are shown in Fig. 5. The spectra were fit with a 50:50 mixed Gaussian/Lorentzian line shape to reveal two distinct peaks at about -97 and -110 ppm, which represent silicon atoms of Q³ and Q⁴, respectively [21]. The black line indicates the spectrum from the measurement, while the red and blue spectra are the two distinct peaks that have been revealed by fitting with 50:50 mixed Gaussian/Lorentzian line shape, the green is the summation of these two peaks. The overall chemical unit can be considered to be Si(OSi)_n(OY)_{4-n} where Y can be R or H. From the spectra, it can be seen that the majority of the silicon environments are Q⁴ with a smaller fraction of Q³ also present in all ionogels. This suggests that the ionogels are highly condensed with an increasing amount of silica present (i.e. more Q⁴) as more TEOS is loaded into the IL. The reaction conditions used are such that we expect the majority of TEOS to be fully hydrolyzed Si(OH)₄ after the first hydrolysis step [22]. Previous work [22] has shown that when TEOS is used as a precursor in the sol gel process, the tendency for TEOS to fully hydrolyze is higher than if tetramethylorthosilicate (TMOS) is used as a precursor. As a result, the condensation between Si—OH groups to form Si—O—Si and H₂O is expected to be greater than the condensation between Si—OH and Si—OR that will form Si—O—Si and alcohol. Furthermore, Karout and Pierre [21] found a higher fraction of Q³ compared to Q⁴ when methyltrimethoxysilane (MTMS) and TMOS were used as a precursor, likely due to the fact that during the initial hydrolysis process, not all of the TMOS is hydrolysed (in contrast to the TEOS case where the initial hydrolysis step has been shown to readily occur). Therefore, when TEOS is used it is expected that a greater amount of Q⁴ is produced than Q³.

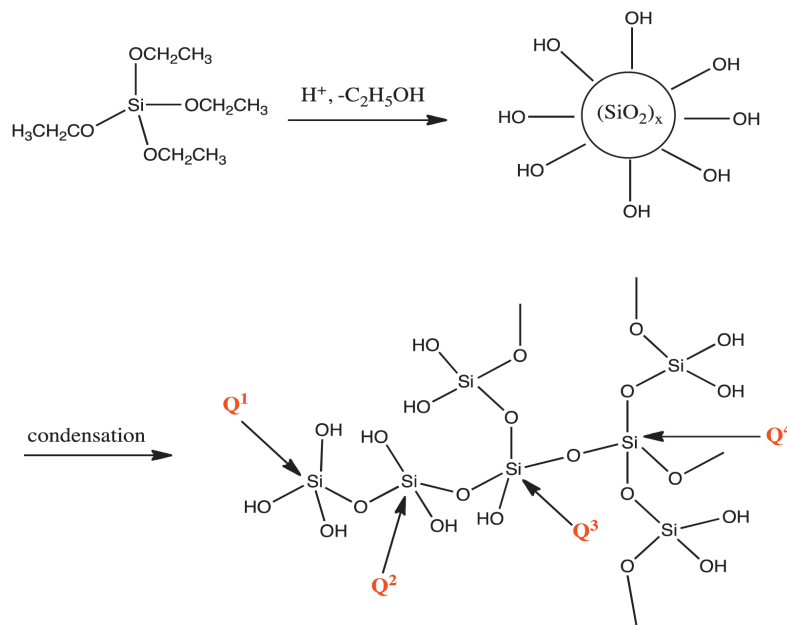


Fig. 4. Schematic of sol-gel process and Qⁿ terms used for silicon bound in SiO₄ tetrahedra of various structural types.

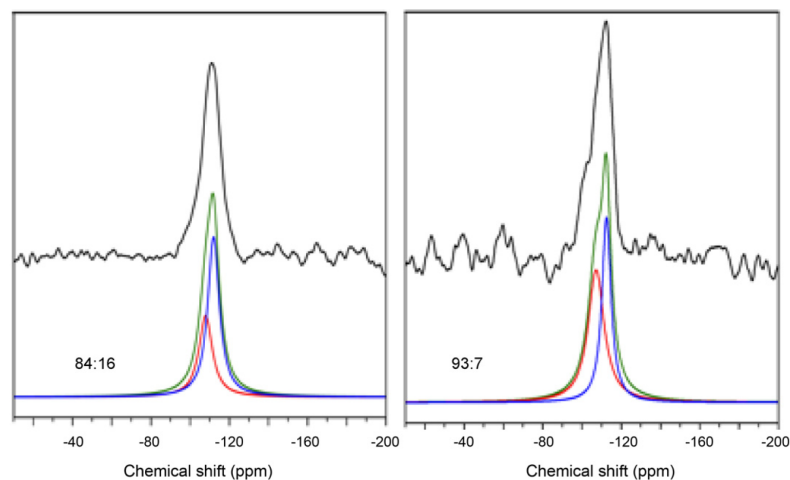


Fig. 5. ^{29}Si NMR spectra for ionogels with different weight ratios of IL:silica. The black line indicates the spectrum from the measurement, while the red and blue spectra are the two distinct peaks that have been revealed by fitting with 50:50 mixed Gaussian/Lorentzian line shape, the green is the summation of these two peaks. (For interpretation of the references to color in this figure legend, the reader is referred to the web version of the article.)

In addition, the higher percentage of Q^4 in the 84:16 ionogel compared to the other ionogel systems with higher IL contents, resulted in the physical properties of this system becoming hard and brittle, as discussed earlier. In order to further investigate the presence of species other than Q^4 , ^1H - ^{29}Si CP NMR can also be used. This provides higher resolution and better signal to noise spectra in considerably shorter times, although the peak integrations are no longer quantitative. These spectra are shown in Fig. 6 and confirm the presence of Q^3 and Q^4 in the ionogels.

^1H , ^{11}B and ^{19}F NMR were also obtained to investigate the effect of the formation of silica via sol-gel process on the ionic liquid species. All the fundamental peaks corresponding to ^1H [BMIM] cation room temperature for all ionogels are present in Fig. 7. These results are basically in agreement with other NMR characterization of pure BMIMBF $_4$ [23]. However, there is an additional peak

observed at around 3.2 ppm for the 93:7 ionogel and 2.8 ppm for the 89:11 and 84:16 ionogels, which belongs to SiOH. The chemical shift of SiOH groups can be found in the range of 1.7–3 ppm [24]. This peak was shielded to high field and the intensity decreased

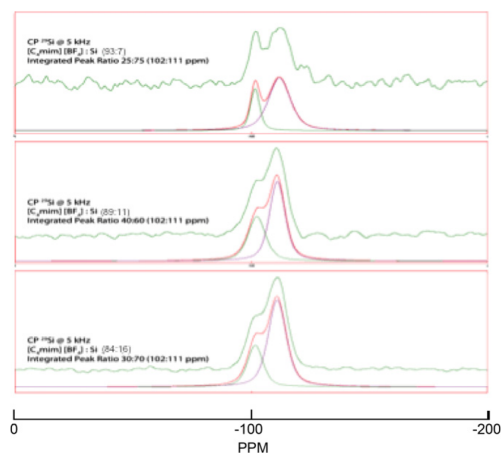


Fig. 6. ^{29}Si CP NMR spectra of ionogels with various amount of silica.

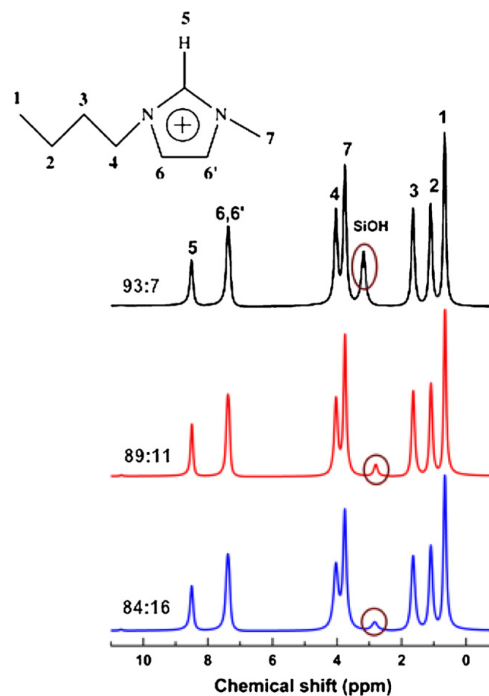


Fig. 7. ^1H NMR spectra for all ionogel systems.

as the amount of silica increased, indicating that most of the TEOS has been hydrolyzed and further condensed to form Q^4 chains. This result is in agreement with the ^{29}Si NMR results, where the percentage of Q^4 is higher in 84:16 system compared to the materials with higher ionic liquid contents. Fig. 8a and b represents ^{11}B and ^{19}F NMR spectra, respectively. The ^{11}B spectra are identical between all the samples and suggest that the average boron environment is unchanged whilst the ^{19}F resonance shifts very slightly and may indicate some interaction between the fluorine and TEOS that is suggested to promote the hydrolysis reaction in these materials. This will be further discussed in FTIR analysis later.

3.4. Attenuated total reflectance-Fourier transform infra-red (ATR-FTIR)

Fig. 9 represents the FTIR spectra of pure IL and ionogels with different loading of silica. For the pure IL, the C–H stretching modes can be observed at 2877, 2964, 3121 and 3161 cm^{-1} , the C–N stretching mode of the imidazole ring at 1573, 1466 and 1169 cm^{-1} , while the asymmetric bending of C–N at 651 and 653 cm^{-1} . Four identical vibration modes of BF_4^- can be seen in two regions, being one triple antisymmetric and one single symmetric B–F stretching. The triply degenerate vibration mode is IR active while the non-degenerate mode is Raman active [25].

Fig. 10 shows the comparative infrared spectra of BMIMBF₄ and ionogels with various weight ratios of IL:silica. The region of the triply degenerate antisymmetric B–F stretching is shown in Fig. 10a. From the spectra these triplet bands can be found at 1045, 1033 and 1016 cm^{-1} . The intensity of the band at 1016 cm^{-1} decreased with increasing amount of silica. Meanwhile, another band at 1033 and 1049 cm^{-1} almost disappeared as the wt.% of silica increased because both bands almost combine. In addition, the single sharp band of symmetric B–F stretching can be observed at 753 cm^{-1} , as shown in Fig. 10b. This band becomes broader and its intensity decreases as the amount of silica increases. These observations indicate that the BF_4^- anion helps the condensation process of the alkoxy silanes to form a silica network in the ionogels. According to Okabe et al. [26], the BF_4^- ion can play a role as a powerful promoter for hydrolytic condensation of alkoxy silanes and provide a site-selective growth of the silica network. Moreover, the bands around 3500 cm^{-1} provide further information about the role of $[\text{BF}_4]^-$ in the gels. According to Yang et al. [27] hydrogen-bonded chains of silanols in silica particles can be observed as a broad peak at 3478 cm^{-1} . In the ionogel system, the hydrogen-bonded silanol chains were detected at 3635 and 3572 cm^{-1} as depicted in Fig. 10c

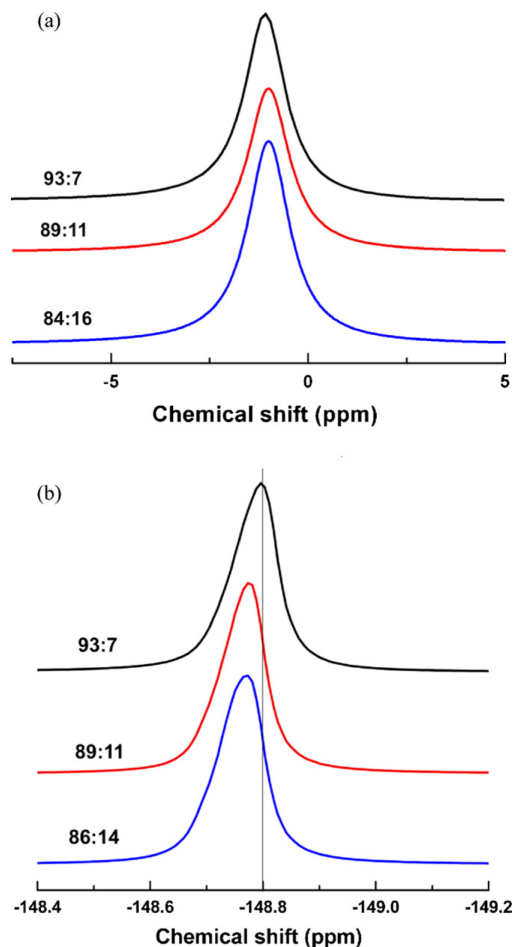


Fig. 8. ^{11}B (a) and ^{19}F (b) NMR spectra of various weight ratios of IL:silica.

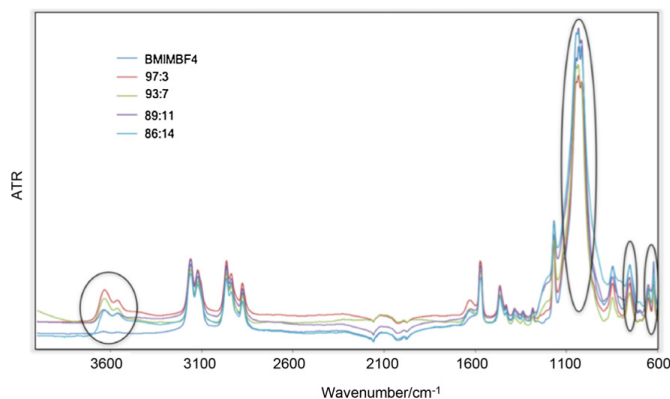


Fig. 9. FTIR spectra of BMIMBF₄ and ormosil ionogels with different weight ratios of IL:silica.

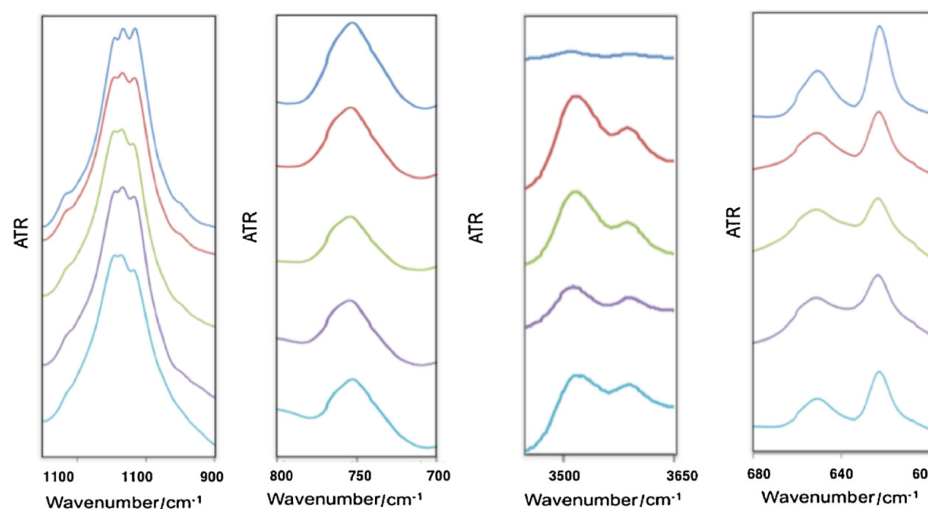


Fig. 10. FTIR spectra of the ionogels: (a) B–F asymmetric stretching, (b) B–F symmetric stretching, (c) Si–OH stretching and (d) asymmetric bending of C–N.

(the pure IL has no bands in this region). This observation shows that a broad band of hydrogen-bonded silanol chains was split into two bands and shifted to higher wavenumbers, indicating a strong interaction between the BF_4^- anion and the hydroxyl group of silanol. This interaction is due to the strong electronegativity of the F atom.

Furthermore, the intensity of the two sharp C–N asymmetric bending bands (Fig. 10d) was also decreased as higher amount of silica formed in the ionogels. This suggests that these vibration modes were slightly affected by formation of the network in the ionogels. Conversely, there was no shift in any of the other IL vibration modes indicating no drastic change in chemical environment of the IL species caused by formation of silica network in the ionogels.

3.5. Thermogravimetric analysis (TGA)

Thermal analysis has been performed to determine the decomposition temperature of the prepared ionogels as well as the

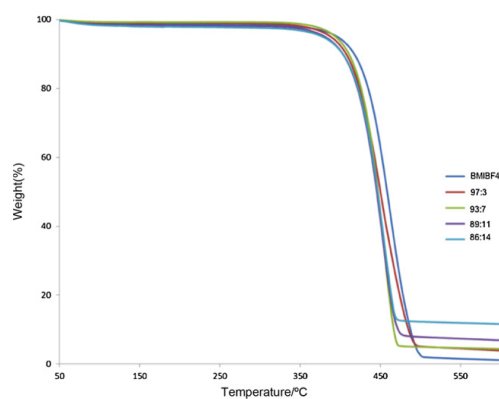


Fig. 11. TGA curves of ionogels with various weight ratios of IL:silica.

Table 2

Degradation temperature of IL and ionogels with various weight ratios of IL:silica.

Sample	T_d
BMIMBF ₄	461
97:3	453
93:7	453
89:11	451
86:14	451

thermal stability. Fig. 11 represents the TGA curves for pure IL and the prepared ionogels. There is a small (<1%) initial mass loss between 50 °C and 150 °C. As the wt.% of silica increases, this initial weight loss also increases. This initial mass loss corresponds to further condensation of remaining silanols, as suggested by Mizumo et al. [28] and also any water absorbed by the small pieces of sample during handling for the TGA experiment. BMIMBF₄ and the prepared ionogels were found to be stable up to a final one-step degradation at 450 °C as presented in Table 2, indicating high thermal stability over a wide range of temperatures. This finding suggests that the good thermal properties of the IL are not affected by formation of the ionogel. Similar behavior has been observed in polymer/ionic liquid systems where the thermal behavior of the IL remained at high temperatures [13].

4. Conclusions

Ionogels with various wt.% of silica has been successfully prepared by a one-pot sol–gel synthesis. The prepared ionogels were investigated by impedance spectroscopy, DSC, solid-state NMR, FTIR and TGA. The compatibility of the IL in the silica network is thought to be the result of hydrogen bonding between BF_4^- and hydroxyl groups in the silica. This interaction makes a high loading of IL (97 wt.%) possible without separation and allows the ionic conductivity of these ionogels to be close to the pure IL. Moreover, the prepared ionogels were found to be stable up to 450 °C. Due to these findings, ionogel can be considered as potential candidates as solid state electrolytes in electrochemical devices.

Acknowledgements

The authors are grateful to the Australian Research Council for funding under the Federation Fellowship (DRM) and Laureate Fellowship (MF) schemes. We also acknowledge the ARC for support of the NMR facility through the grant LE110100141.

References

- [1] M.J. Earle, K.R. Seddon, Ionic liquids. Green solvents for the future, *Pure and Applied Chemistry* 72 (2000) 1391.
- [2] S.A. Forsyth, S.R. Batten, Q. Dai, D.R. MacFarlane, Ionic liquids based on imidazolium and pyrrolidinium salts of the tricyanomethanide anion, *Australian Journal of Chemistry* 57 (2004) 121.
- [3] G.B. Appetecchi, M. Montanino, A. Balducci, S.F. Lux, M. Winterb, S. Passerini, Lithium insertion in graphite from ternary ionic liquid–lithium salt electrolytes: I. Electrochemical characterization of the electrolytes, *Journal of Power Sources* 192 (2009) 599.
- [4] J.A. Choi, E.G. Shim, B. Scrosati, D.W. Kim, Mixed electrolytes of organic solvents and ionic liquid for rechargeable lithium-ion batteries, *Bulletin of the Korean Chemical Society* 31 (2010) 3190.
- [5] S.R. Sivakkumar, D.R. MacFarlane, M. Forsyth, D.W. Kim, Ionic liquid-based rechargeable lithium metal–polymer cells assembled with polyaniline/carbon nanotube composite cathode, *Journal of the Electrochemical Society* 154 (2007) A834.
- [6] Y. Kobayashi, Y. Mita, S. Seki, Y. Ohno, H. Miyashiro, N. Terada, Comparative study of lithium secondary batteries using nonvolatile safety electrolytes, *Journal of the Electrochemical Society* 154 (2007) A677.
- [7] P.J. Flory, Introductory lecture, *Faraday Discussions of the Chemical Society* 57 (1974) 7.
- [8] V.N. Afanas'ev, A.G. Grechin, Chemical modification of electrolytes for lithium batteries, *Russian Chemical Review* 71 (2002) 775.
- [9] N. Yoshimoto, T. Shirai, M. Morita, A novel polymeric gel electrolyte systems containing magnesium salt with ionic liquid, *Electrochimica Acta* 50 (2005) 3866.
- [10] F. Gayet, L. Viau, F. Leroux, S. Monge, J.J. Robin, A. Vioux, Polymer nanocomposite ionogels, high-performance electrolyte membranes, *Journal of Materials Chemistry* 20 (2010) 9456.
- [11] D. Kumar, S.A. Hashmi, Ionic liquid based sodium ion conducting gel polymer electrolytes, *Solid State Ionics* 181 (2010) 416.
- [12] B. Singh, S.S. Sekhon, Polymer electrolytes based on room temperature ionic liquid: 2,3-dimethyl-1-octylimidazolium triflate, *Journal of Physical Chemistry B* 109 (2005) 16539.
- [13] M.A.B.H. Susan, T. Kaneko, A. Noda, M. Watanabe, Ion gels prepared by in situ radical polymerization of vinyl monomers in an ionic liquid and their characterization as polymer electrolytes, *Journal of the American Chemical Society* 127 (2005) 4976.
- [14] A. Vioux, L. Viau, S. Volland, J. Le Bideau, Use of ionic liquids in sol–gel; ionogels and applications, *Comptes Rendus des Chimica* 13 (2010) 242.
- [15] M.A. Néouze, J. Le Bideau, P. Gaveau, S. Bellayer, A. Vioux, Ionogels, new materials arising from the confinement of ionic liquids within silica-derived networks, *Chemistry of Materials* 18 (2006) 3931.
- [16] R. Göbel, P. Hesemann, J. Weber, E. Möller, A. Friedrich, S. Beuermann, A. Taubert, Surprisingly high, bulk liquid-like mobility of silica-confined ionic liquids, *Physical Chemistry Chemical Physics* 11 (2009) 3653.
- [17] J. Le Bideau, P. Gaveau, S. Bellayer, M.A. Néouze, A. Vioux, Effect of confinement on ionic liquids dynamics in monolithic silica ionogels: ^1H NMR study, *Physical Chemistry Chemical Physics* 9 (2007) 5419.
- [18] S.I. Smedley, *The Interpretation of Ionic Conductivity in Liquids*, Plenum Press, New York/Washington, New Zealand, 1980.
- [19] G. Frand, C. Rousselot, O. Bohnke, New Solid Electrolytes for Electrochromic Smart Windows, *Int Soc for Optical Engineering*, Toulouse, France, 1992, 157 pp.
- [20] A.D. Irwin, J.S. Holmgren, J. Jonas, Solid-state ^{29}Si NMR study of polycondensation during heat treatment of sol–gel-derived silicas, *Materials Letters* 6 (1987) 25.
- [21] A. Karout, A.C. Pierre, Silica gelation catalysis by ionic liquids, *Catalysis Communications* 10 (2009) 359.
- [22] C.A. Fyfe, P.P. Aroca, Quantitative kinetic analysis by high-resolution ^{29}Si NMR spectroscopy of the initial stages in the sol–gel formation of silica gel from tetraethoxysilane, *Chemistry of Materials* 7 (1995) 1800.
- [23] J. Gao, J. Liu, B. Li, W. Liu, Y. Xie, Y. Xin, Y. Yin, X. Jie, J. Gu, Z. Zou, A quick and green approach to prepare [Rmim]OH and its application in hydrophilic ionic liquid synthesis, *New Journal of Chemistry* 35 (2011) 1661.
- [24] N.J. Clayden, S. Esposito, P. Pernice, A. Aronne, Solid state ^1H NMR study, humidity sensitivity and protonic conduction of gel derived phosphosilicate glasses, *Journal of Materials Chemistry* 12 (2002) 3746.
- [25] T. Buffeteau, J. Grondin, Y. Danten, J.C. Lassègues, Imidazolium-based ionic liquids: quantitative aspects in the far-infrared region, *Journal of Physical Chemistry B* 114 (2010) 7587.
- [26] A. Okabe, T. Fukushima, K. Ariga, M. Niki, T. Aida, Tetrafluoroborate salts as site-selective promoters for sol–gel synthesis of mesoporous silica, *Journal of the American Chemical Society* 126 (2004) 9013.
- [27] H. Yang, C. Yu, Q. Song, Y. Xia, F. Li, Z. Chen, X. Li, T. Yi, C. Huang, High-temperature and long-term stable solid-state electrolyte for dye-sensitized solar cells by self-assembly, *Chemistry of Materials* 18 (2006) 5173.
- [28] T. Mizumo, T. Watanabe, N. Matsumi, H. Ohno, Preparation of ion conductive inorganic–organic composite systems by in situ sol–gel reaction of polymerizable ionic liquids, *Polymers for Advanced Technologies* 19 (2008) 1445.

2.5 Bibliography

1. Gayet, F.; Viau, L.; Leroux, F.; Monge, S.; Robin, J. J.; Vioux, A. *J. Mater. Chem.* **2010**, *20*, 9456-9462.
2. Gayet, F.; Viau, L.; Leroux, F.; Mabilie, F.; Monge, S.; Robin, J. J.; Vioux, A. *Chem. Mater.* **2009**, *21*, 5575-5577.
3. Le Bideau, J.; Viau, L.; Vioux, A. *Chem. Soc. Rev.* **2011**, *40*, 907-925.
4. Lakshminarayana, G.; Tripathi, V. S.; Tiwari, I.; Nogami, M. *Ionics* **2010**, *16*, 385-395.
5. Le Bideau, J.; Gaveau, P.; Bellayer, S.; Néouze, M. A.; Vioux, A. *Phys. Chem. Chem. Phys.* **2007**, *9*, 5419-5422.
6. Kumar, D.; Hashmi, S. A. *Solid State Ionics* **2010**, *181*, 416-423.
7. Singh, B.; Sekhon, S. S. *J. Phys. Chem. B* **2005**, *109*, 16539-16543.
8. Susan, M. A. B. H.; Kaneko, T.; Noda, A.; Watanabe, M. *J. Am. Chem. Soc.* **2005**, *127*, 4976-4983.
9. Vioux, A.; Viau, L.; Volland, S.; Le Bideau, J. *C. R. Chim.* **2010**, *13*, 242-255.
10. Shi, F.; Zhang, Q.; Li, D.; Deng, Y. *Chemistry - A European Journal* **2005**, *11*, 5279-5288.
11. Okabe, A.; Fukushima, T.; Ariga, K.; Niki, M.; Aida, T. *J. Am. Chem. Soc.* **2004**, *126*, 9013-9016.
12. Néouze, M. A.; Le Bideau, J.; Gaveau, P.; Bellayer, S.; Vioux, A. *Chem. Mater.* **2006**, *18*, 3931-3936.
13. Noor, S. A. M.; Bayley, P. M.; Forsyth, M.; MacFarlane, D. R. *Electrochim. Acta* **2013**, *91*, 219-226.



Chapter 3

Ionic liquids - sodium ion conductors

for sodium batteries

3.1 General Overview

Lithium ion batteries have dominated the portable electronic industry and other electrical devices as high energy density storage devices¹⁻⁴. The motivation for using lithium in battery technology initially stems from the fact that Li is the lightest and most electropositive metal, as discussed in section 1.4. The demand for lithium ion batteries is rapidly increasing, however, concerns regarding sustainability of lithium supplies, and thereby its costs, as well as safety issues relating to flammable organic electrolytes have risen⁵⁻⁷. This has prompted researchers to consider other anodic metals such as sodium⁸⁻¹⁰, magnesium^{11, 12} and zinc¹³ as alternatives since they are significantly more abundant.

The present study developed and investigated IL based electrolytes for use in sodium batteries. A comparison of sodium and lithium ionic liquid electrolytes based on, 1-butyl-1-methylpyrrolidinium bis(trifluoromethylsulfonyl)amide ($C_4\text{mpyrNTf}_2$), doped with sodium bis(trifluoromethylsulfonyl)amide (NaNTf_2) and lithium bis(trifluoromethylsulfonyl)amide (LiNTf_2) is the subject of this chapter¹⁴. The properties of the electrolyte solutions (including viscosity, density, thermal stability (DSC), ionic conductivity and electrochemical stability) are presented and discussed in Publication 2. This paper, entitled “Properties of sodium-based ionic liquid electrolytes for sodium secondary battery applications” has been published in *Electrochimica Acta*.¹⁴

In this paper, it was found that the ionic conductivity of sodium ion containing ionic liquid electrolytes reached as high as 8 mS.cm^{-1} . From the electrochemical stability analysis by cyclic voltammetry, the deposition of sodium metal was observed to begin at -0.2 V (vs. Na^+/Na) and the resultant deposits were able to be re-oxidized back into the electrolyte at high efficiency.

These findings prompted us to further develop gelled sodium electrolyte systems based on ionic liquids, in order to realize a safe, high performance battery electrolyte with desirable mechanical properties. In this work, we prepared gel electrolytes by using either (i) nano-particle fumed silica, or (ii) radical polymerization of MMA in the electrolytes. Facile sodium cathodic and anodic currents are observed around 0 V vs Na/Na^+ at 298 K with these gels. The ionic conductivity of the gel electrolytes and chemical interaction between silica and ionic liquid were also investigated. This study is presented in this thesis as a manuscript *to be submitted to Electrochimica Acta*, entitled “Gel-ionic liquid based sodium ion conductors for sodium batteries” and here denoted as Publication 3.

3.2 Specific Declaration

PART B: Suggested Declaration for Thesis Chapter

Monash University

Declaration for Thesis Chapter 3.3

Declaration by candidate

In the case of Chapter 3.3, the nature and extent of my contribution to the work was the following:

Nature of contribution	Extent of contribution (%)
Initiation, key ideas, performed the experiments, synthesis, data analysis and interpretation, manuscript development and writing up	90

The following co-authors contributed to the work. If co-authors are students at Monash University, the extent of their contribution in percentage terms must be stated:

Name	Nature of contribution	Extent of contribution (%) for student co-authors only
Douglas MacFarlane	Key ideas, proof reading and final drafting	-
Maria Forsyth	Key ideas, proof reading and final drafting	-
Patrick Howlett	Cyclic Voltammetry discussion	-

The undersigned hereby certify that the above declaration correctly reflects the nature and extent of the candidate's and co-authors' contributions to this work*.

**Candidate's
Signature**

	Date 11/7/2014
--	--------------------------

**Main
Supervisor's
Signature**

	Date 11/7/2014
---	--------------------------

*Note: Where the responsible author is not the candidate's main supervisor, the main supervisor should consult with the responsible author to agree on the respective contributions of the authors.

3.3 Publication 2

Properties of sodium-based ionic liquid electrolytes for sodium secondary battery applications

S.A.M.Noor,^{a,b} Patrick Howlett,^{c,d} D.R. MacFarlane,^a M. Forsyth,^{c,d*}

^a *School of Chemistry, Monash University, Clayton Campus, Victoria, Australia*

^b *Chemistry Department, Centre for Defence Foundation Studies, National Defence University of Malaysia, 57000, Kuala Lumpur, Malaysia*

^c *ARC Centre of Excellence for Electromaterials Science (ACES), Australia*

^d *Institute for Frontier Materials, Deakin University, Victoria, Australia*

* *Corresponding Author:*

[REDACTED]

[REDACTED]

Electrochimica Acta

114 (2013) 766-771

DOI: 10.1016/j.electacta.2013.09.115



Properties of sodium-based ionic liquid electrolytes for sodium secondary battery applications



Siti Aminah Mohd Noor^{a,b}, Patrick C. Howlett^{c,d}, Douglas R. MacFarlane^{a,c}, Maria Forsyth^{c,d,*}

^a School of Chemistry, Monash University, Clayton Campus, Victoria, Australia

^b Chemistry Department, Centre for Defence Foundation Studies, National Defence University of Malaysia, 57000 Kuala Lumpur, Malaysia

^c ARC Centre of Excellence for Electromaterials Science (ACES), Australia

^d Institute for Frontier Materials Deakin University, Victoria, Australia

ARTICLE INFO

Article history:

Received 30 May 2013

Received in revised form

19 September 2013

Accepted 19 September 2013

Available online 12 October 2013

Keywords:

Sodium batteries

Ionic liquid

Sodium conductor

ABSTRACT

The enormous demands on available global lithium resources have raised concerns about the sustainability of the supply of lithium. Sodium secondary batteries have emerged as promising alternatives to lithium batteries. We describe here sodium bis(trifluoromethylsulfonyl) amide (NaNTf₂) electrolyte systems based on 1-butyl-1-methylpyrrolidinium bis(trifluoromethylsulfonyl) amide (C₄mpyrNTf₂) ionic liquids. The electrochemical stability of the system was examined; a pair of facile cathodic and anodic processes around 0 V vs. Na/Na⁺ were observed in cyclic voltammetry measurements and interpreted as deposition and dissolution of sodium metal. Density, viscosity and conductivity of the electrolytes were studied. It was found that the ionic conductivity of electrolytes reached as high as 8 mS/cm, decreasing slowly as the salt content increased due to increasing of viscosity and density of the electrolyte. Therefore, sodium electrolytes based on C₄mpyrNTf₂ appear to be promising for secondary sodium battery applications.

© 2013 Elsevier Ltd. All rights reserved.

1. Introduction

The increase in energy demand, along with growing understanding of the environmental consequences of the use of fossil fuels, have led to energy storage for sustainable energy applications becoming a growing global need. Lithium ion batteries are widely used for almost all portable electronic devices because lithium has a combination of useful properties such as small ionic size (which allows fast diffusion in solids), very negative redox potential (and therefore high cell voltage), and light weight (which enables high specific energy devices) [1,2]. Current lithium battery technology has several limitations including volatile and potentially flammable electrolytes and unstable metal/electrolyte interfaces [3,4]. In recent years, the use of ionic liquids as electrolytes in electrochemical devices has been explored as they potentially offer a solution to these safety issues. This is because of their unique combination of properties, which can include negligible vapour pressure, non-flammability, high thermal stability, high ionic conductivity, wide operating temperature range and wide electrochemical stability window. These properties provide clear

advantages over traditional organic solvents [3]. Numerous publications have reported the use of Li⁺ salts in ILs as electrolytes, and the electrochemical performance of these electrolytes has been examined in the context of lithium batteries [1,4–6].

However, while Li-ion batteries remain an important energy storage technology, there are concerns about the longer-term availability and cost of lithium. This issue will become more important if the demands for this technology stretch into larger scale transport and stationary power storage applications. To overcome this problem, sodium secondary battery technologies are attracting attention. The advantages of sodium for secondary batteries include: lower cost, ready availability, lower toxicity, low atomic mass and high electrochemical reduction potential [2,7–10]. Previously, Na/S [11] and Na/NiCl₂ [12] based ZEBRA batteries have been studied and are now commercially available. In both systems, β-alumina is used as the solid electrolyte, and a high operating temperature, approximately 573 K, is required which reduces the energy density of the battery system due to the need to incorporate heaters and thermal insulation [13].

Early studies in ILs explored various buffered imidazolium and quaternary ammonium chloroaluminate ILs as potential electrolytes, demonstrating sodium deposition and dissolution with good efficiency and deposit morphology [14–18]. Additives such as hydrogen chloride and thionyl chloride were shown to enhance performance, which was suggested to occur due to preferential

* Corresponding author at: Institute for Frontier Materials Deakin University, Victoria, Australia. Tel.: [redacted]
E-mail address: [redacted] (M. Forsyth).

coordination of the chloride anion, promoting sodium dissociation and enhanced conductivity.

A study on the effect of sodium and lithium triflate in polyacrylonitrile (PAN) has been reported by Osman et al. [19]. They found that the sodium electrolyte system possessed higher ionic conductivity at room temperature than the corresponding lithium-based electrolyte. In addition, sodium electrolytes based on an IL, diethyl methoxyethyl ammonium tetrafluoroborate, in the presence of a polyether of poly(ethylene glycol) dimethyl ether (PEGDME) as a coordinating agent have also been investigated by Egashira et al. [8]. The ionic conductivity of some of these systems at room temperature was 10^{-3} S cm $^{-1}$, which is sufficient for application in practical devices.

Nohira and co-workers [10,13,20] have reported intermediate-temperature ionic liquid systems (NaFSA-KFSA and NaTFSA-CsTFSA, where FSA is bis(fluorosulfonyl)amide and TFSA is bis(trifluoromethylsulfonyl)amide, referred to here as NTf $_2$) for use as electrolytes in sodium secondary batteries. They found that these electrolytes can be used at operating temperatures between 333 and 393 K and possess wide electrochemical windows, up to 5.2 V at 363 K. This operating temperature range gives these systems a significant advantage compared to Na/S and Na/NiCl $_2$ batteries, which must be operated at around 573 K. Nevertheless, it is desirable for portable energy sources to have high performance at room temperature.

In this present work, we have investigated the room temperature ionic liquid, 1-butyl-1-methylpyrrolidinium bis(trifluoromethylsulfonyl) amide ([C $_4$ mpyr][NTf $_2$]), doped with sodium bis(trifluoromethylsulfonyl) amide (NaNTf $_2$) as a potential electrolyte for sodium secondary batteries. The properties of the electrolyte solutions (including viscosity, density, thermal stability (DSC), ionic conductivity and electrochemical stability) have been examined. These properties are compared with the properties of analogous [C $_4$ mpyr][NTf $_2$] solutions containing lithium bis(trifluoromethylsulfonyl) amide (LiNTf $_2$), so that differences in the interaction of Na $^+$ versus Li $^+$ ions can be revealed.

2. Experimental

2.1. Materials and sample preparation

[C $_4$ mpyr][NTf $_2$] (99%) was obtained from Merck, NaNTf $_2$ (99.9%) from Solvionics and LiNTf $_2$ (98%) from Aldrich. All chemicals were used without further purification. The water content of [C $_4$ mpyr][NTf $_2$] was 125 ppm, as determined by Karl Fischer titration. Initially, sodium or lithium salts were added to the ionic liquid at various concentrations (0.1–0.5 M), and the solutions stirred at room temperature until the salt had fully dissolved. Then the electrolytes were heated in a vacuum oven at 90 °C for two days, to remove the residual water content. The typical water content achieved was 200 ppm.

2.2. Characterization

2.2.1. Cyclic voltammetry

1 mm diameter Ni and 1 mm diameter Cu electrodes were used as working electrodes. In the Li electrolytes, both electrodes behaved similarly. However, in the case of Na electrolytes a Cu working electrode produced higher currents and hence we focused on this working electrode. The counter and reference electrodes were either sodium (for sodium electrolytes) or lithium metal (for lithium electrolytes). A drop of electrolyte was placed on the sodium metal and then the working electrode was placed onto the drop, without touching the sodium metal. The scan rate was

20 mV s $^{-1}$. All procedures were performed under argon. The potentiostat used was a BioLogic SP 200, controlled with EC-LAB software. Measurements were carried out at room temperature.

2.2.2. Differential scanning calorimetry (DSC)

To provide information about the temperatures of the phase transitions, DSC measurements were carried out on the prepared samples, using a DSC Q100 series instrument (TA Instruments), and the data was evaluated with Universal Analysis 2000 software. Approximately 8–10 mg of prepared electrolyte sample was tested over a temperature range of 133–383 K at a scanning rate of 10 K min $^{-1}$. The glass transition temperature was determined from the onset of the heat-capacity change on the heating ramp.

2.2.3. Density and viscosity

Density measurements were performed using an Anton Paar DMA 5000 density metre. The density metre uses the 'oscillating U-tube principle' to determine the density of the liquid. Viscosity measurements were carried out using an Anton Paar AMVn viscosity metre, which uses a falling ball technique.

2.2.4. Ionic conductivity

Conductance was measured using a locally designed dip cell probe consisting of two platinum wires sheathed in glass. The cell constant was determined with a solution of 0.01 M KCl at 25 °C. To determine the ionic conductivity of the prepared electrolytes, impedance spectra were measured using a high frequency response analyzer (HFRA; Solartron 1296) over a frequency range of 0.1 Hz–10 MHz with a 30 mV amplitude. Ten points per decade were measured. The analysis was conducted at temperatures from 273 to 373 K in 10 °C intervals. The temperature was controlled to within 1 °C using a Eurotherm 2204e temperature controller interfaced to the Solartron and a cartridge heater set in a brass block with a cavity for the cell. The conductance was determined from the first real axis touchdown point in the Nyquist plot of the impedance data.

3. Results and discussion

3.1. Voltammetric results

Cyclic voltammograms of the 0.4 M sodium and lithium electrolytes, recorded at room temperature, are shown in Fig. 1. A pair of cathodic and anodic features is observed on the copper working electrode in each case. The cathodic currents correspond to the deposition of sodium or lithium metal, while the anodic currents are the dissolution of the deposited metals. The deposition of sodium begins at relatively low overpotential, around -0.2 V vs. Na/Na $^+$, and lithium around -0.3 V vs. Li/Li $^+$. Both the Li and Na voltammetry indicated good reversibility for the deposition/dissolution process, as previously reported for the Li system. The coulombic efficiencies determined from CVs are typically low due to difficulty in isolating only the Na deposition process on the cathodic scan and the unfavourable deposit morphologies that are often formed during the CV experiment. In this case both Li and Na systems show an apparent 30% efficiency. However, the lithium process is known to be greater than 80% in this IL [21] and so we are now developing galvanostatic methods to more accurately determine the coulombic efficiency of the Na deposition/dissolution process as well as incorporating this electrolyte into a sodium battery.

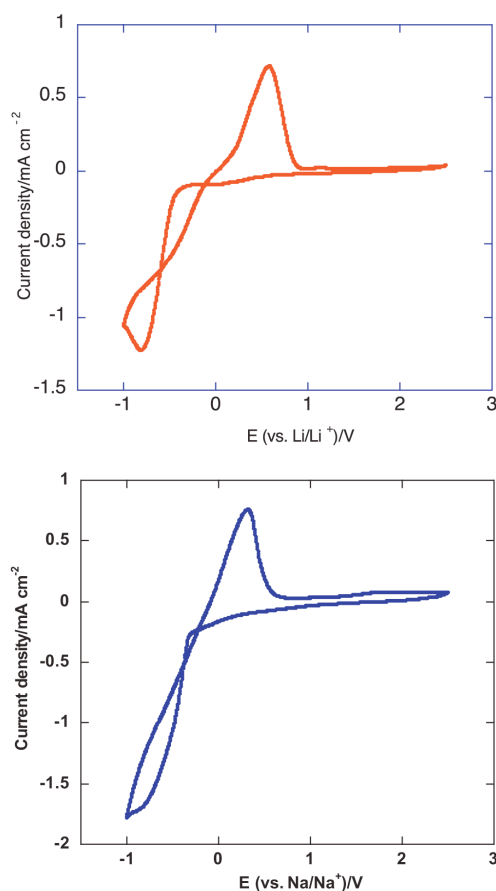


Fig. 1. Cyclic voltammograms for $C_4\text{mpyrNTf}_2$ -based electrolytes containing: (top) 0.4 M LiNTf_2 and (bottom) 0.4 M NaNTf_2 ; 20 mV s^{-1} .

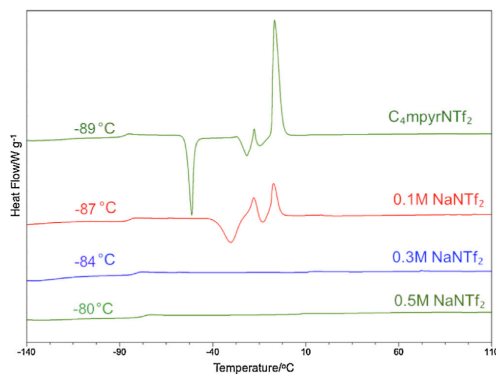


Fig. 2. DSC thermograms of $C_4\text{mpyrNTf}_2$ with various concentrations of NaNTf_2 . The T_g for each system, as determined from the onset on the heating ramp, is also given in this figure.

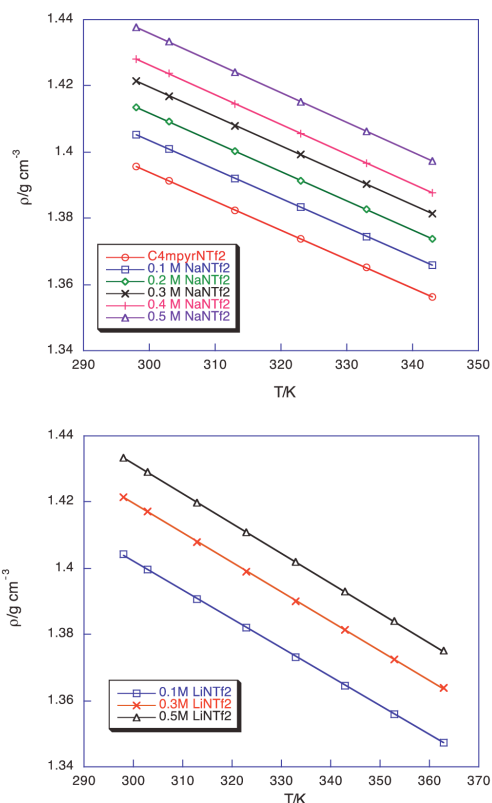


Fig. 3. Density of $C_4\text{mpyrNTf}_2$ -based electrolytes with different concentrations of: (Top) NaNTf_2 and (bottom) LiNTf_2 .

3.2. Differential scanning calorimetry (DSC)

Fig. 2 shows thermograms of $C_4\text{mpyrNTf}_2$ and of the sodium-containing electrolytes. The T_g , T_{cry} and T_m of $C_4\text{mpyrNTf}_2$ can be clearly seen. With addition of 0.1 M NaNTf_2 , the area of the T_{cry} and T_m peaks decreased significantly, and T_{cry} shifted to higher temperature. When the concentration of the sodium salt was increased to 0.3 and 0.5 M, the crystallization and melting peaks completely disappeared. This implies that crystallization has been disrupted by interactions between the sodium ions and the ionic liquid (most likely with the NTf_2 anion from the IL). T_g also increased with increasing concentration of NaNTf_2 , which is further evidence of interaction.

3.3. Density

The densities of both sodium- and lithium-containing electrolytes increased as the concentration of added salt increased. As seen in Fig. 3, the density of both electrolytes varied linearly with temperature. The data was fitted to Eq. (1) with correlation coefficients greater than 0.999, confirming the linear temperature dependence within the temperature range studied. The fitting parameters are shown in Table 1. The density of the sodium-containing electrolytes is slightly higher than that of the

Table 1
Linear fit parameters for temperature-dependent density of C₄mpyrNTf₂-based sodium-containing electrolytes.

Sample	a (g cm ⁻³)	b (g cm ⁻³ K ⁻¹)	R^2
C ₄ mpyrNTf ₂	1.6567	8.7574E-4	0.999
0.1 M NaNTf ₂	1.6672	8.7905E-4	0.999
0.2 M NaNTf ₂	1.6765	8.8225E-4	1.000
0.3 M NaNTf ₂	1.6865	8.8955E-4	0.999
0.4 M NaNTf ₂	1.6956	8.9751E-4	0.999
0.5 M NaNTf ₂	1.7052	8.9768E-4	1.000

lithium-containing electrolytes; this is as expected, because of the greater mass of the sodium cation compared to lithium.

$$\rho = a + bT \quad (1)$$

3.4. Viscosity and ionic conductivity

Fig. 4 shows Arrhenius plots of the viscosity of the sodium- and lithium- containing electrolytes. The increase in viscosity on alkali salt addition is probably due to the metal ion interaction with the NTf₂⁻ anion, forming ion pairs/clusters which are bigger and heavier in the Na⁺ case [1,21]. The temperature dependence is well

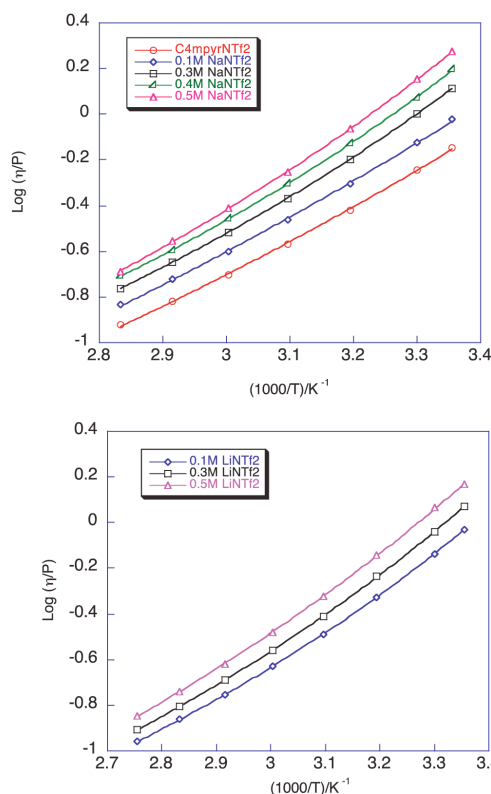


Fig. 4. Arrhenius plots of viscosity of electrolytes with different concentrations of C₄mpyrNTf₂-based electrolytes; (top) NaNTf₂ and (bottom) LiNTf₂.

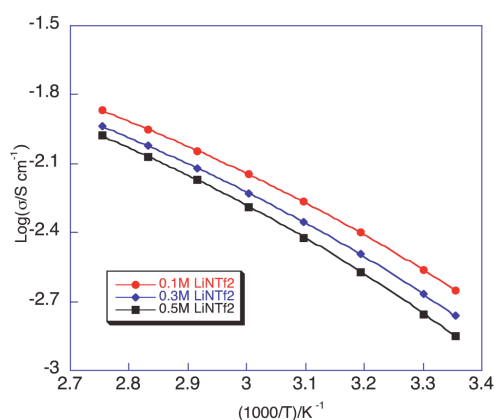
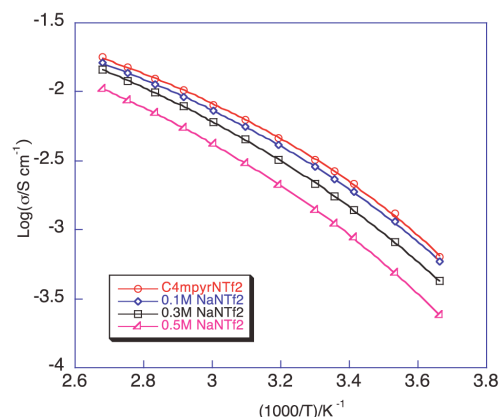


Fig. 5. Arrhenius plots of conductivity for C₄mpyrNTf₂ electrolytes with various concentrations of (top) NaNTf₂ and (bottom) LiNTf₂.

described by the Vogel–Tamman–Fulcher (VTF) equation (Eq. (2)).

$$\eta = \eta_0 \exp \left[\frac{B}{T - T_0} \right] \quad (2)$$

The parameters obtained by fitting the data to the VTF equation are given in Table 2. As the temperature increases, the viscosity decreases as expected. The pseudoactivation energy (B parameter) is related to the energy needed for ion motion in the ionic liquid and this appears to increase slightly with increasing salt content. This implies that, not only does the viscosity increase with Li/Na salt addition, but also more energy is needed for enabling ion diffusion in these more viscous, mixed systems. In addition, B values of lithium-containing electrolytes are, for the most part, slightly smaller compared to those of sodium-containing electrolytes.

Arrhenius plots of the ionic conductivity for these electrolytes are shown in Fig. 5. These are also fitted well with the VTF equation (Eq. (3)); the VTF parameters are listed in Table 3.

$$\sigma = \sigma_0 \exp \left[\frac{-B}{T - T_0} \right] \quad (3)$$

Several studies have reported that the conductivity of lithium containing ionic liquid electrolytes decrease with increasing lithium

Table 2VTF viscosity parameters for sodium-containing and lithium-containing C₄mpyrNTf₂-based electrolytes.

Sample	Log η_0 (P) NaNTf ₂	B (K) NaNTf ₂	T ₀ (K) NaNTf ₂	Log η_0 (P) LiNTf ₂	B (K) LiNTf ₂	T ₀ (K) LiNTf ₂
C ₄ mpyrNTf ₂	-2.6 ± 0.02	299 ± 5	177 ± 2	-2.6 ± 0.4	299 ± 5	177 ± 2
0.1 M	-2.7 ± 0.03	352 ± 8	168 ± 2	-2.6 ± 0.04	197 ± 2	183 ± 0.3
0.3 M	-2.6 ± 0.03	325 ± 8	183 ± 5	-2.7 ± 0.01	330 ± 4	179 ± 0.1
0.5 M	-2.8 ± 0.07	377 ± 20	176 ± 4	-2.9 ± 0.12	294 ± 37	169 ± 7

Table 3

VTF parameters for ionic conductivity.

Sample	Log σ_0 (S cm ⁻¹) NaNTf ₂	B (K) NaNTf ₂	T ₀ (K) NaNTf ₂	Log σ_0 (S cm ⁻¹) LiNTf ₂	B (K) LiNTf ₂	T ₀ (K) LiNTf ₂
C ₄ mpyrNTf ₂	-0.6 ± 0.05	-212 ± 11	191 ± 3	-0.6 ± 0.05	-212 ± 11	191 ± 3
0.1 M	-0.5 ± 0.03	-243 ± 7	183 ± 2	-0.5 ± 0.02	-247 ± 5	184 ± 1
0.3 M	-0.3 ± 0.02	-296 ± 5	176 ± 1	-0.55 ± 0.05	-240 ± 15	189 ± 4
0.5 M	-0.4 ± 0.02	-307 ± 6	177 ± 1	-0.53 ± 0.06	-250 ± 6	190 ± 5

salt concentration, as a result of the formation of ion pairs and/or ion clusters [1,4–6]. Ion pairs are neutral in charge, and hence cannot contribute to conduction, whilst the ion triplets and aggregates will also decrease the effective number of charge carriers. This is supported by an MD simulation study of Borodin et al. [21] of lithium ions in C₄mpyrNTf₂. They found that some fraction of Li⁺ cations form aggregates, where Li⁺ is bridged by Li⁺...O=S=O...Li⁺ ionic bonds. These aggregates are stable at 333 K and 303 K on a 10 ns time scale. They asserted that the Li⁺ involved in the Li⁺...O=S=O...Li⁺ clusters diffuse together with the clusters, at a significantly slower rate than Li⁺ that is not coordinated into such clusters, and hence cluster formation reduces the conductivity. This has very recently also been shown in an imidazolium NTf₂ based ionic liquid where Monti et al. [22] compared the ion speciation upon addition of LiNTf₂ and NaNTf₂ using Raman spectroscopy and DFT calculations. They showed that in the case of NaNTf₂, the sodium ion interacts with three anions to form [Na(NTf₂)₃]²⁻, in contrast to the [Li(NTf₂)₂]⁻ found for the Li based systems. They also suggest that more effective dynamic cross links are present in the case of sodium electrolytes; these observations are consistent with the higher B parameters determined for both families of electrolyte as the concentration of salt increases and also the generally higher values for the Na based systems. The concentration dependences of both conductivity and viscosity are shown in Fig. 6.

3.5. Walden plot

A classification diagram based on the Walden Rule allows a simple assessment of the ionicity of ionic liquids [23,24], as shown in Fig. 7. The Walden rule equation (Eq. (4)) relates the molar conductivity (Λ) of an electrolyte solution to its fluidity ($1/\eta$) and a temperature dependent constant, C [24].

$$\Lambda\eta = C \quad (4)$$

As a point of reference, dilute aqueous KCl solutions are often used, as these are considered to represent an ideal case in which the anions and cations are well dissociated from one another and move independently in the electric field. The Walden plot ($\log \Lambda$ vs. $\log 1/\eta$) of the sodium-containing electrolytes is depicted in Fig. 7. In each case, including that for the relatively viscous, poorly conductive 0.5 M NaNTf₂ example, the data fall only slightly below the ideal line. This result suggests that these ionic liquid electrolytes can be classified as having relatively high ionicity, in which anions and cations move mostly independently of one another [24,25]. However, with increasing temperature the data clearly trend away from the ideal line, as is often observed in electrolytes over an extended temperature range [26]. In these cases the fractional Walden rule $\Lambda\eta^\gamma = C$ is considered to provide a good description of the data, with the exponent γ (representing the slope of the line on the

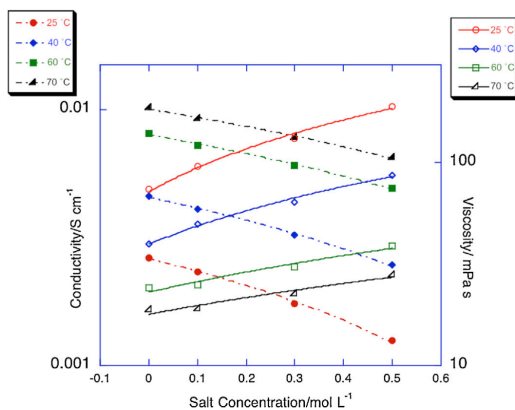


Fig. 6. Ionic conductivity and dynamic viscosity of sodium electrolytes as a function of sodium salt concentration at various temperatures.

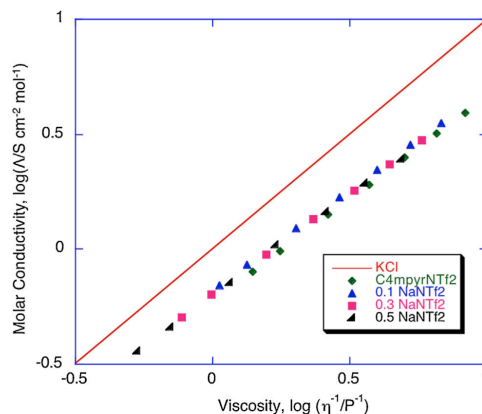


Fig. 7. Walden plots for C₄mpyrNTf₂-based electrolytes of pure IL and sodium-containing compositions.

Walden plot) typically being 0.8 ± 0.1 . In the present case we find $\gamma = 0.87 \pm 0.02$ for these $\text{NaNTf}_2\text{-C}_4\text{mpyrNTf}_2$ systems, similar to the 0.91 value observed by Schreiner for $\text{C}_2\text{mimNTf}_2$ [22]. Temperature dependent increase in ion-pairing [26,27], as suggested by Yoshizawa et al. [24] is also possible in these systems, but is not distinguishable from this more generic effect at this stage.

4. Conclusions

The electrochemical properties, thermal properties, densities, viscosities and conductivities of sodium ion containing $\text{C}_4\text{mpyrNTf}_2$ electrolytes were measured. As the concentration of added sodium salt increased, T_g of the electrolytes rose, while T_{cr} and T_m were no longer apparent. The viscosities and conductivities were well described by VTF equations. The sodium ion concentration dependence trends towards lower conductivities and higher viscosities. All systems were well described by the fractional Walden Rule with $\gamma = 0.87 \pm 0.02$. The deposition of sodium metal begins at -0.2 V (vs. Na^+/Na) and the resultant deposits were able to be oxidized back into the electrolyte at high efficiency. We conclude that sodium-containing electrolytes based on $\text{C}_4\text{mpyrNTf}_2$ are promising as electrolytes for secondary sodium batteries, since they may overcome the cost and sustainability problems associated with conventional electrolytes, while still exhibiting good conductivities and stabilities.

Acknowledgements

The authors are grateful to the Australian Research Council for funding under the Discovery Project and Laureate Fellowship (MF and DRM) schemes.

References

- [1] A. Andriola, K. Singh, J. Lewis, L. Yu, Conductivity, viscosity, and dissolution enthalpy of LiNTf_2 in ionic liquid BmimTf_2 , *J. Phys. Chem. B* 114 (2010) 11709–11714.
- [2] B.L. Ellis, L.F. Nazar, Sodium and sodium-ion energy storage batteries, *Curr. Opin. Solid State Mater. Sci.* 16 (2012) 168–177.
- [3] J.A. Choi, E.G. Shim, B. Scrosati, D.W. Kim, Mixed electrolytes of organic solvents and ionic liquid for rechargeable lithium-ion batteries, *Bull. Korean Chem. Soc.* 31 (2010) 3190–3194.
- [4] G.H. Lane, P.M. Bayley, B.R. Clare, A.S. Best, D.R. MacFarlane, M. Forsyth, A.F. Hollenkamp, Ionic liquid electrolyte for lithium metal batteries: physical, electrochemical, and interfacial studies of N-Methyl-N-Butylmorpholinium Bis(Fluorosulfonyl)Imide, *J. Phys. Chem. C* 114 (2010) 21775–21785.
- [5] J.S. Lee, N.D. Quan, J.M. Hwang, J.Y. Bae, H. Kim, B.W. Cho, H.S. Kim, H. Lee, Ionic liquids containing an ester group as potential electrolytes, *Electrochem. Commun.* 8 (2006) 460–464.
- [6] D.Q. Nguyen, J.H. Oh, C.S. Kim, S.W. Kim, H. Kim, H. Lee, H.S. Kim, Synthesis and characterization of quaternary ammonium-based ionic liquids containing Al Alkyl carbonate group, *Bull. Korean Chem. Soc.* 28 (2007) 2299–2302.
- [7] R.M. Dell, Batteries – fifty years of materials development, *Solid State Ionics* 134 (2000) 139–158.
- [8] M. Egashira, T. Asai, N. Yoshimoto, M. Morita, Ionic conductivity of ternary electrolyte containing sodium salt and ionic liquid, *Electrochim. Acta* 58 (2011) 95–98.
- [9] D. Kumar, S.A. Hashmi, Ion transport and ion-filler-polymer interaction in Poly(Methyl Methacrylate)-based, sodium ion conducting, gel polymer electrolytes dispersed with silica nanoparticles, *J. Power Sources* 195 (2010) 5101–5108.
- [10] T. Nohira, T. Ishibashi, R. Hagiwara, Properties of an intermediate temperature ionic liquid NaTfSA-CSTfSA and charge-discharge properties of NaCrO_2 positive electrode at 423 K for a sodium secondary battery, *J. Power Sources* 205 (2012) 506–509.
- [11] J.L. Sudworth, The sodium/sulphur battery, *J. Power Sources* 11 (1984) 143–154.
- [12] J. Coetzer, A new high energy density battery system, *J. Power Sources* 18 (1986) 377–380.
- [13] A. Fukunaga, T. Nohira, Y. Kozawa, R. Hagiwara, S. Sakai, K. Nitta, S. Inazawa, Intermediate-temperature ionic liquid NaTfSA-KTfSA and its application to sodium secondary batteries, *J. Power Sources* 209 (2012) 52–56.
- [14] C.-L. Yu, J. Winnick, P. Kohl, Novel electrolyte for the sodium/iron chloride battery, *J. Electrochem. Soc.* 138 (1991) 339–340.
- [15] C. Scordilis-Kelley, J. Fuller, R. Carlin, J. Wilkes, Alkali metal reduction potentials measured in chloroaluminate ambient-temperature molten salts, *J. Electrochem. Soc.* 139 (1992) 694–699.
- [16] J. Fuller, R. Osteryoung, R. Carlin, Rechargeable lithium and sodium anodes in chloroaluminate molten salts containing thionyl chloride, *J. Electrochem. Soc.* 142 (1995) 3632–3636.
- [17] K. Kim, C. Lang, R. Moulton, P.A. Kohl, Electrochemical investigation of quaternary ammonium/aluminum chloride ionic liquids, *J. Electrochem. Soc.* 151 (2004) A1168–A1172.
- [18] C.M. Lang, K. Kim, P.A. Kohl, Catalytic additives for the reversible reduction of sodium in chloroaluminate ionic liquids, *Electrochim. Acta* 51 (2006) 3884–3889.
- [19] Z. Osman, K.B.M. Isa, L. Othman, N. Kamarulzaman, Paris, (2011). DOI: 10.4028/www.scientific.net/DDF.312-315.116.
- [20] T. Yamamoto, T. Nohira, R. Hagiwara, A. Fukunaga, S. Sakai, K. Nitta, S. Inazawa, Charge-discharge behavior of tin negative electrode for a sodium secondary battery using intermediate temperature ionic liquid sodium Bis(Fluorosulfonyl) amide-potassium Bis(Fluorosulfonyl)amide, *J. Power Sources* 217 (2012) 479–484.
- [21] O. Borodin, G.D. Smith, W. Henderson, Li + cation environment, transport, and mechanical properties of the Litfsi doped N-methyl-N-Alkylpyrrolidinium +TfSi – ionic liquids, *J. Phys. Chem. B* 110 (2006) 16879–16886.
- [22] D. Monti, E. Jönsson, M.R. Palacín, P. Johansson, Ionic liquid based electrolytes for sodium-ion batteries: Na^+ solvation and ionic conductivity, *J. Power Sources* 245 (2000) 630–636.
- [23] W. Xu, L.M. Wang, R.A. Nieman, C.A. Angell, Ionic liquids of chelated orthoborates as model ionic glassformers, *J. Phys. Chem. B* 107 (2003) 11749–11756.
- [24] M. Yoshizawa, W. Xu, C.A. Angell, Ionic Liquids by proton transfer: vapor pressure, conductivity, and the relevance of GEP_{IPA} from aqueous solutions, *J. Am. Chem. Soc.* 125 (2003) 15411–15419.
- [25] Y. Pan, L.E. Boyd, J.F. Kruplak, W.E. Cleland Jr., J.S. Wilkes, C.L. Hussey, Physical and transport properties of Bis(trifluoromethylsulfonyl)imide-based room-temperature ionic liquids: application to the diffusion of $\text{Tris}(2, 2'\text{-bipyridyl})\text{ruthenium(II)}$, *J. Electrochem. Soc.* 158 (2011) F1–F9.
- [26] R.R.A. Robinson, R.R.H. Stokes, *Electrolyte Solutions*, Courier Dover Publications, London, 1970.
- [27] C. Schreiner, S. Zugmann, R. Hartl, H.J. Gores, Fractional walden rule for ionic liquids: examples from recent measurements and a critique of the so-called ideal KCl line for the walden plot, *J. Chem. Eng. Data* 55 (2010) 1784–1788.

3.4 Specific Declaration

PART B: Suggested Declaration for Thesis Chapter

Monash University

Declaration for Thesis Chapter 3.5

Declaration by candidate

In the case of Chapter 3.5, the nature and extent of my contribution to the work was the following:

Nature of contribution	Extent of contribution (%)
Initiation, key ideas, performed the experiments, synthesis, data analysis and interpretation, manuscript development and writing up	90

The following co-authors contributed to the work. If co-authors are students at Monash University, the extent of their contribution in percentage terms must be stated:

Name	Nature of contribution	Extent of contribution (%) for student co-authors only
Douglas MacFarlane	Key ideas, proof reading and final drafting	-
Maria Forsyth	Key ideas, proof reading and final drafting	-
Hyungkook Yoon	Cyclic Voltammetry measurement	-

The undersigned hereby certify that the above declaration correctly reflects the nature and extent of the candidate's and co-authors' contributions to this work*.

**Candidate's
Signature**

	Date 11/7/2014
--	--------------------------

**Main
Supervisor's
Signature**

	Date 11/7/2014
---	--------------------------

*Note: Where the responsible author is not the candidate's main supervisor, the main supervisor should consult with the responsible author to agree on the respective contributions of the authors.

3.5 Publication 3

Gel-ionic liquid based sodium ion conductors for sodium batteries

Siti Aminah Mohd Noor^{a,b}, Hyungook Yoon^{c,d}, Maria Forsyth^{c,d} and Douglas R MacFarlane^{a,c}

^a School of Chemistry, Monash University, Clayton Campus, 3800 Victoria, Australia

^b Chemistry Department, Centre for Defence Foundation Studies, National Defence University of Malaysia, 57000, Kuala Lumpur, Malaysia

^c ARC Centre of Excellence for Electromaterials Science (ACES), Australia

^d Institute for Frontier Materials Deakin University, 3125, Victoria, Australia

**Email:*

[REDACTED]

[REDACTED]

To be submitted to *Electrochimica Acta*

July 2014

Gel-ionic liquid based sodium ion conductors for sodium batteries

Siti Aminah Mohd Noor^{a,b}, Hyungook Yoon^{c,d}, Maria Forsyth^{c,d} and Douglas R MacFarlane^{a,c}

^a *School of Chemistry, Monash University, Clayton Campus, 3800 Victoria, Australia*

^b *Chemistry Department, Centre for Defence Foundation Studies, National Defence University of Malaysia, 57000, Kuala Lumpur, Malaysia*

^c *ARC Centre of Excellence for Electromaterials Science (ACES), Australia*

^d *Institute for Frontier Materials Deakin University, 3125, Victoria, Australia*

*Email: 

ABSTRACT

Owing to the unique properties of certain Ionic liquids (ILs) as safe and green solvents, as well as the potential of sodium ions as an alternative to lithium ions as charge carriers, we investigate gel sodium electrolytes as safe, low cost and high performance materials with sufficient mechanical properties for application in sodium battery technologies. In the present study, we investigate the effect of formation of two types of gel electrolytes on the properties of IL electrolytes known to support Na/Na⁺ electrochemistry. We observed plating and stripping of Na metal through the cyclic voltammetry and the ionic conductivity only slightly decreased as we changed the physical properties from liquid to gel. Therefore, the formation

of a gel does not appear to significantly affect the ion dynamics in comparison to the liquid state of the electrolyte, as further evidenced by DSC and FTIR analysis.

INTRODUCTION

The development of a non-flammable electrolytes based on ionic liquids has been extensively studied¹⁻⁵ to eliminate the problem of flammability and high vapor pressure of typical organic solvents such as propylene carbonate and ethylene carbonate. Ionic liquids become an attractive electrolyte candidate to overcome these safety issues and also to widen the operating temperature, owing to their unique properties of non-flammability, low measurable vapor pressure, wide electrochemical stability, high thermal stability as well as wide liquid temperature range⁶⁻⁹. ILs also have been reported as ‘green solvent’ since many can be recycled and the tunability of their anion and cation^{9, 10} is also attractive. On the other hand, most of the research on the development of such electrolytes is focusing on the use of lithium as charge carriers since lithium ion batteries are widely used in portable electronic devices¹¹⁻¹⁴. This is due to lithium’s combination of distinctive characteristics such as small ionic size, high electrochemical reduction potential and light weight. Looking in the high demand of lithium batteries as a main sources for portable electronic devices, and their wide potential use for electric and hybrid vehicles, concerns regarding their long term availability and cost have arisen. This is because lithium reserves are unevenly distributed in the world and located in

remote and politically sensitive areas¹⁵⁻¹⁷. Thus, the extended usage of lithium in larger scale applications may significantly increase the price of lithium compounds.

Together with sodium's high abundance, low cost, low atomic mass (comparing with other metal such as zinc and magnesium), as well as its relatively high electrochemical reduction potential ($E^0_{(\text{Na}^+/\text{Na})} = -2.71\text{V}$ versus standard hydrogen electrode; only 0.3V above lithium)^{14, 18-20}, sodium can be a promising candidate for energy storage applications as an alternative to lithium. The use of sodium in batteries has been reported almost 50 years ago and has been commercialized in technologies such as sodium sulfur²¹ and Na-NiCl₂²² systems which using β -alumina as a solid electrolyte. However, the operating temperature is very high ($\sim 573\text{ K}$). Fukunaga^{23, 24} has demonstrated sodium secondary batteries using bis(fluorosulfonyl)amide anion (FSA)⁻ ionic liquid and this systems showed a good performance at 363 K.

Previously, we reported sodium bis(trifluoromethylsulfonyl) amide (NaNTf₂) electrolyte systems based on room temperature ionic liquids of 1-butyl-1-methylpyrrolidinium bis(trifluoromethylsulfonyl)amide (C₄mpyrNTf₂)²⁵. It was found that the ionic conductivity of this electrolyte reached as high as 8 mS/cm for 0.1M NaNTf₂, which is marginally lower compared to the lithium electrolyte system. From the electrochemical stability analysis in cyclic voltammetry, facile cathodic and anodic features can be observed which correspond to deposition and dissolution of sodium metal. In such studies on Na secondary batteries, most

researchers are currently focusing on liquid electrolytes. To the best of our knowledge, no work has been reported on gel sodium electrolytes. In this study, we prepared gel ionic liquids based on our previous liquid system ($C_4\text{mpyrNTf}_2$ RTIL and NaNTf_2 salt) by using nano particle fumed silica and radical polymerization of MMA in the electrolytes. We study the effect of formation of the gel electrolytes on the ionic conductivity using impedance spectroscopy, thermal properties by differential scanning calorimetry, chemical interaction from infrared spectroscopy and cyclic voltammetry.

EXPERIMENTAL

Materials and sample preparation

$C_4\text{mpyrNTf}_2$ (99%) was obtained from Merck, NaNTf_2 (99.9%) from Solvionics, Silica fumed powder with average particle size of $0.007\ \mu\text{m}$ from Sigma Aldrich, dichloromethane (DCM) from Merck, methyl methacrylate monomer from Aldrich and benzyl peroxide (BPO) initiator from AJAX Chemicals were used. The water content of $C_4\text{mpyrNTf}_2$ was 125 ppm, as determined by Karl Fischer titration. The fumed silica powder was dried in a vacuum oven at 473 K overnight while the DCM was dried with molecular sieves and the water content was determined to be 5 ppm. All materials were transferred into a glove box after drying and the preparation of the electrolytes were done in the glove box under an argon atmosphere. Initially, sodium salt was added to the ionic liquid at various concentrations (0.1 to 0.5 M), and the solutions stirred at room temperature until the salt had fully dissolved. Then the electrolytes were heated in a vacuum oven at

90°C for two days, to remove the residual water content.

For silica-gel type electrolytes, 5 wt.% of fumed silica were dispersed into the base electrolyte solution with two drops of DCM as co-solvent and then stirred for several minutes until a homogeneous viscous solution was obtained. To form a gel electrolyte, the viscous solutions were left at room temperature to evaporate the DCM. For the PMMA-gel electrolytes, firstly, 0.5 % BPO was added into base electrolyte solution and stirred at 80 °C for several minutes. Then 8 wt.% MMA monomer and 6 mol % TEGDA were added to the solution and further stirred until a homogeneous solution was obtained. Below 8.wt% of MMA monomer, high viscous electrolytes obtained, and only above this compositions, stable gel electrolytes obtained. The solution was left in the oil bath for two hours until a PMMA-gel electrolyte formed. All samples were heated in a vacuum oven at 90 °C overnight to remove residual co-solvent and any water content prior to any characterization.

Characterization

Cyclic Voltammetry

Cyclic voltammetry was carried out using a coin cell method in a glove box with an Ar atmosphere. The counter and reference electrode was sodium metal, while the working electrode was a copper foil. The copper foil and sodium metal were washed with ethanol and hexane respectively to give a clean surface and cut into circles of 1.0 mm diameter. The gel electrolytes were placed on the surface of both

electrodes and were separated by a polypropylene separator. Then both electrodes and separator were clamped into a coin cell and the CV measured. The scan rate was 2 mVs^{-1} . The potentiostat used was a BioLogic SP 200, controlled with EC-LAB software. Measurements were carried out at room temperature.

Differential Scanning Calorimetry (DSC)

To provide information about the temperatures of the phase transitions, DSC measurements were carried out on the prepared samples, using a DSC Q100 series instrument (TA Instruments), and the data was evaluated with Universal Analysis 2000 software. Approximately 8 to 10 mg of prepared electrolyte sample was tested over a temperature range of 133 to 383 K at a scanning rate of 10 K.min^{-1} . The glass transition temperature was determined from the onset of the heat-capacity change on heating.

Ionic Conductivity

Conductance was measured using a locally designed dip cell probe consisting of two platinum wires sheathed in glass. The cell constant was determined with a solution of 0.01M KCl at 25°C . To determine the ionic conductivity of the prepared electrolytes, complex impedance measurement were made using HP428A Impedance Meter (Hewlett-Packard) over a frequency range of 20 Hz to 1 MHz. Ten points per decade were measured. The analysis was conducted at temperatures from 273 to 373 K in 10°C intervals. The temperature was controlled to within 1°C using a Eurotherm 2204e temperature controller and a cartridge heater set in a brass

block with a cavity for the cell. The conductance was determined from the first real axis touchdown point in the Nyquist plot of the impedance data.

Attenuated Total Reflectance–Fourier Transform Infrared Spectroscopy (ATR-FTIR)

ATR-FTIR was carried out to investigate the interactions that occur in the gel electrolytes using a Perkin Elmer Spectrum 100 FTIR spectrometer. Measurements were made in the range 4000 to 650 cm^{-1} with a resolution of 4 cm^{-1} . Data was analyzed using Spectrum Analyzer software.

RESULTS AND DISCUSSION

Attenuated total reflectance-Fourier transform infra-red (ATR-FTIR)

Fig. 1 presents the FTIR spectra of pure IL, the IL electrolytes and the gel electrolytes (SiO_2 and PMMA) in the range 700-1800 cm^{-1} (the full spectrum is shown in Fig. S1). For pure IL (blue spectra) the C-H stretching modes can be observed at 2877, 2964, and 3121 cm^{-1} and the C-N stretching mode of the pyrrolidinium ring at 1462 cm^{-1} ; C-S stretching at 662 cm^{-1} , S-N stretching at 682 cm^{-1} , C-F stretching at 1051 cm^{-1} , S=O symmetric stretching at 1133 and 1174 cm^{-1} , while S=O asymmetric stretching at 1328 and 1349 cm^{-1} from the counterion. The introduction of sodium salts into the IL (green spectra) does not shift or change any of the IL peaks. Monti et al²⁶ reported there is a small change in SNS stretching (730-765 cm^{-1}) peak from Raman spectra. They found that the band of SNS shifted slightly to high wave number, ~ 742 to 744 cm^{-1} . This $\nu(\text{SNS})$ vibrational mode corresponds to the expansion and contraction of the whole anion, thus becomes

useful for probing TFSI⁻ solvation and it also sensitive to the TFSI conformation. However, TFSI⁻ is a weak base, so that it induces only a very small shift and little energy is required for the conformational changes. In our case, the FTIR is run with a 4 cm⁻¹ resolution, thus it is possible that subtle changes cannot be observed in the SNS peak. Moreover, Na is much bigger than Li, therefore the interaction that might occur will be weaker. This also becomes one of the reasons why the S=O band in the IL is not affected by addition of salt.

The formation of physical gel electrolytes by incorporation of silica particles does not involve any chemical change. This can be confirmed as no additional peak or changes can be detected in the silica gel electrolyte spectra (pink spectra). According to Wu et al.²⁷, the fumed silica particles are able to interact directly through hydrogen bonding between silanol groups (Si-OH) on the surface of nano particle. The gelation process is initiated from this interaction as suggested by the SEM images reported by Raghavan et al.²⁸, Wu et al. also asserted that fumed silica gel normally presents a chain-like form, called nano particle chain aggregates (NCA), which possess polymer-like behaviors and this was confirmed by high magnification SEM by Friedlander and co-workers^{29, 30}.

Conversely, for PMMA gel electrolytes, a new peak can be observed at 1728 cm⁻¹, which represents the carbonyl groups in PMMA. There is no significant change that can be detected in the regions where the IL peaks appear, indicating the formation of gel electrolytes does not significantly affect the bonding environment of the IL

itself.

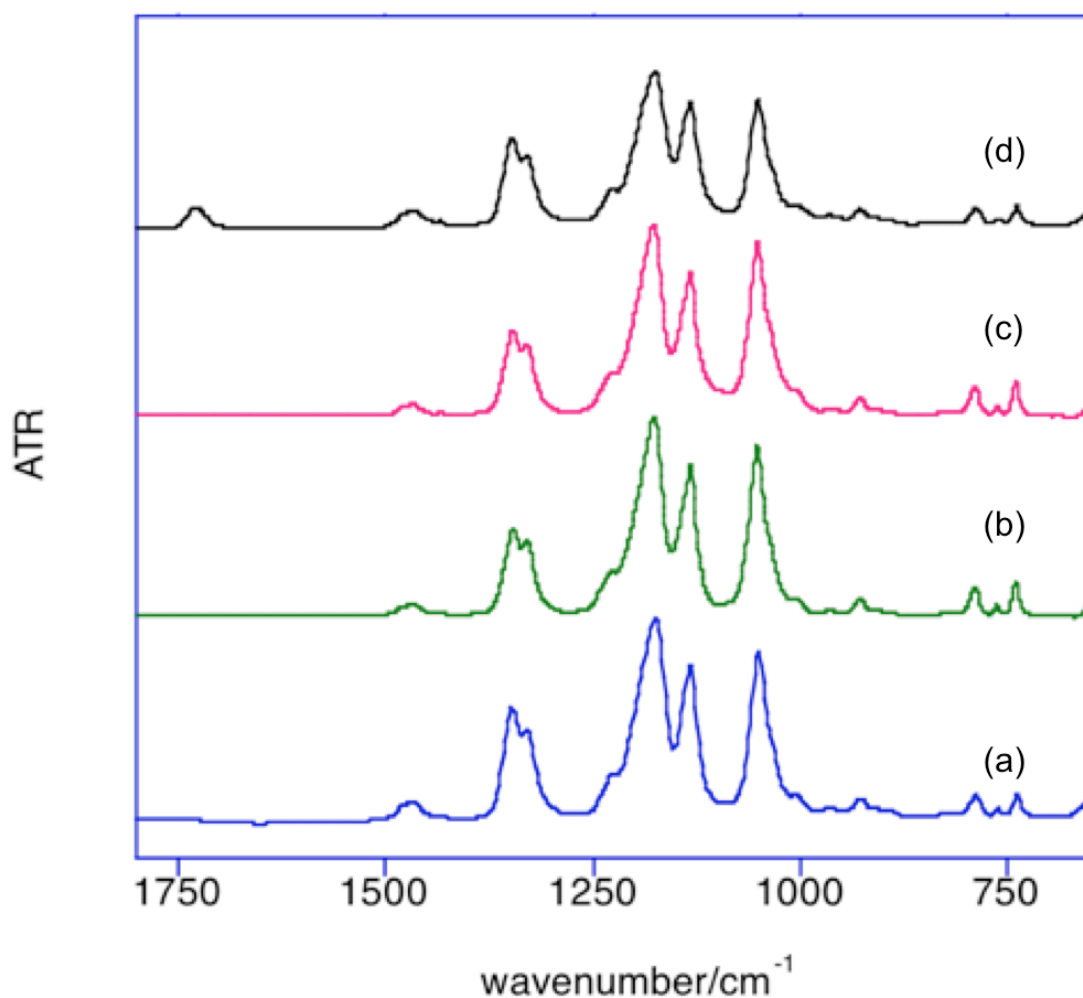


Fig. 1 FTIR spectra of C₄mpyrNTf₂ (a), 0.4M NaNTf₂ C₄mpyrNTf₂ (b), silica gel electrolyte (c) and PMMA gel electrolyte (d).

Voltammetry

Cyclic voltammograms of the 0.4 M NaNTf₂ with 5% SiO₂ gel electrolytes, recorded at room temperature, are shown in Fig. 2. A pair of cathodic and anodic features is observed on the copper-foil working electrode. The cathodic currents correspond to the plating of sodium metal, whilst the anodic currents are the

stripping of the deposited metal. The deposition and dissolution of deposited sodium metal has also been observed in the liquid sodium electrolytes as reported in our previous study²⁵. The deposition of sodium begins at relatively low overpotential, around -0.2V vs. Na/Na⁺. The crossover during cycling that was observed in the liquid electrolyte system, which is usually due to a nucleation over potential and/or charge transfer resistance was not present in the gel system, which suggest that the interfacial process proceeds more easily in the gel system. In another case, Louis et al.³¹, reported that the formation of silica gel suppressed aluminium corrosion and therefore increased the electrochemical stability- another benefit of gelation of the IL electrolyte.

In our previous paper²⁵, we reported the cyclic coulombic efficiency of sodium deposition and stripping in the liquid electrolytes is quite low, around only 30% by CV determination. In this paper, optimization of the negative potential limit to -0.4V produces coulombic efficiency >50%. The same has also been carried out for the liquid based electrolytes and we obtained coulombic efficiency ~ 80% from the fourth to tenth cycle in this manner. This value is closely comparable to lithium electrolytes in an IL based system as reported by Howlett et al.³²

Conversely, in the case of PMMA gel electrolytes, no reversible oxidation and reduction peak can be observed no matter what methodology we attempted. Only one sharp reduction peak occurred in the first cycle (Fig. S3). Since the PMMA gel electrolytes were prepared by radical polymerization, there is a possibility of

unreacted monomer being retained, which may hinder the stripping of sodium metal. The polymer itself should not be a problem as it was previously reported that, in a polymer gel electrolyte system based on PMMA in an organic solvent, the plating and stripping of lithium were observed³³.

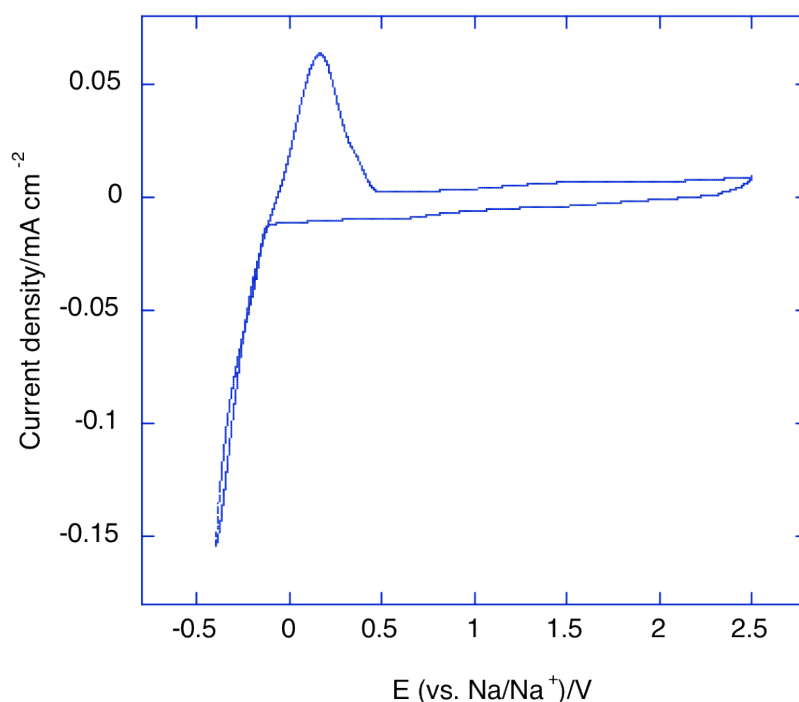


Fig. 2 Cyclic voltammogram of silica gel electrolytes at room temperature (3rd cycle); subsequent cycles shown in the Fig S2.

Differential Scanning Calorimetry (DSC)

In order to observe any phase transitions occurring in the electrolytes, and especially the glass transition temperature (T_g), which is a useful measurement for determining the ultimate practical limit on the electrolyte working temperature, we recorded DSC data for the gel electrolytes. Fig. 3 shows exothermic thermograms

(heating scans) of the sodium gel electrolytes with various composition of sodium salt. Comparing with the DSC thermograms of the corresponding liquid electrolytes²⁵, no significant changes can be seen in the gel electrolytes. However, the T_g values are slightly increased (about 2 to 4 °C), which become -85, -81 and -76 °C for 0.1, 0.3 and 0.5 M NaNTf₂. Similar behavior was observed in other ionogel electrolyte systems^{34, 35}, where the T_g of the ionogel was not affected by the silica content. This situation is a stark contrast to the change in its physical properties observed, from liquid to gel in which form the material does not flow and is stable up to 100 °C. This is a highly desirable decoupling of the mechanical properties from the ion transport that can produce an ideal combination of properties in a gel electrolyte. It also further confirms that the silica nanoparticle acts only as a physical scaffold for the gel. In the case of PMMA gel system, no changes can be seen in its T_g values when its compared with IL electrolytes system, as shown in Table 1. As discussed above, this might be due to residual unreacted monomer retain in the gel electrolytes.

Table 1. Glass transition temperature of sodium gel electrolytes

Sodium gel	T_g (°C)	T_g (°C)	T_g (°C)
electrolytes	0.1 M NaNTf ₂	0.3 M NaNTf ₂	0.5 M NaNTf ₂
Liquid ^a	-87	-84	-80
Silica	-85	-81	-76
PMMA	-86	-84	-80

Looking in more detail at this data, for 0.1 M NaNTf₂ gel electrolytes, a crystallization peak (T_{cry}) is observed at -26 °C, a sign of this material being quenched into the glassy state during the cooling scan. This is subsequently followed by endothermic peaks at -18 and -7 °C (T_{m}). These peaks disappeared in the cooling cycle (Fig. S4). This behavior was also observed in our previous work (liquid electrolytes) as well as in the Na_xEMIm_(1-x)TFSI system described by Monti et al.²⁶ The presence of T_{cry} and T_{m} make this unsuitable candidature for application below -7 °C. On the other hand, for the 0.3 and 0.5M NaNTf₂ gel electrolytes a totally amorphous system is obtained during all heating and cooling treatments. A similar observation was seen in the PMMA gel electrolytes, where T_{m} was observed for the 0.1M NaNTf₂ system but not at higher sodium concentrations, while the T_{g} of all samples do not shift significantly with increasing salt content.

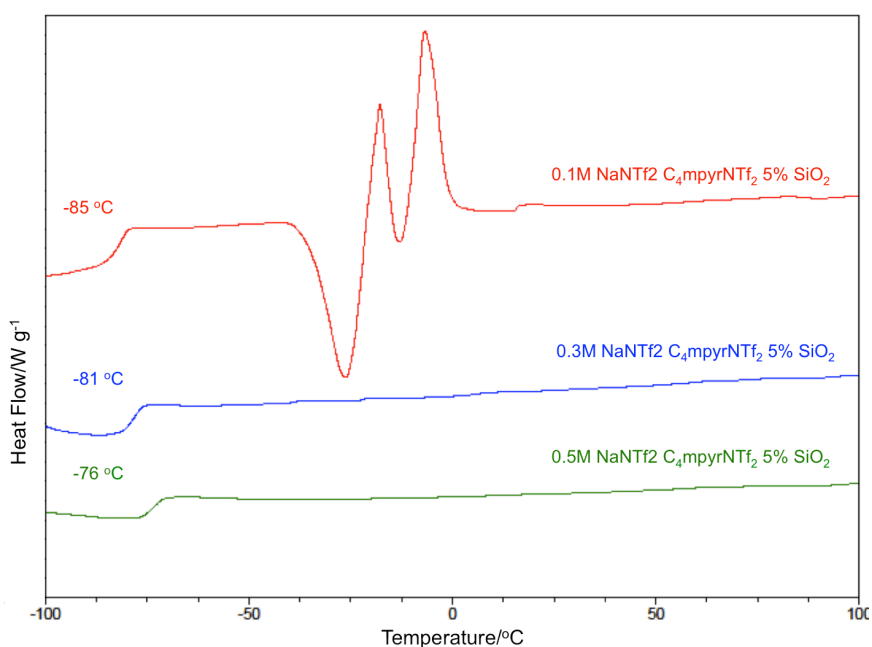


Fig. 3 DSC thermograms of sodium gel electrolytes with different concentrations of NaNTf₂

Ionic conductivity

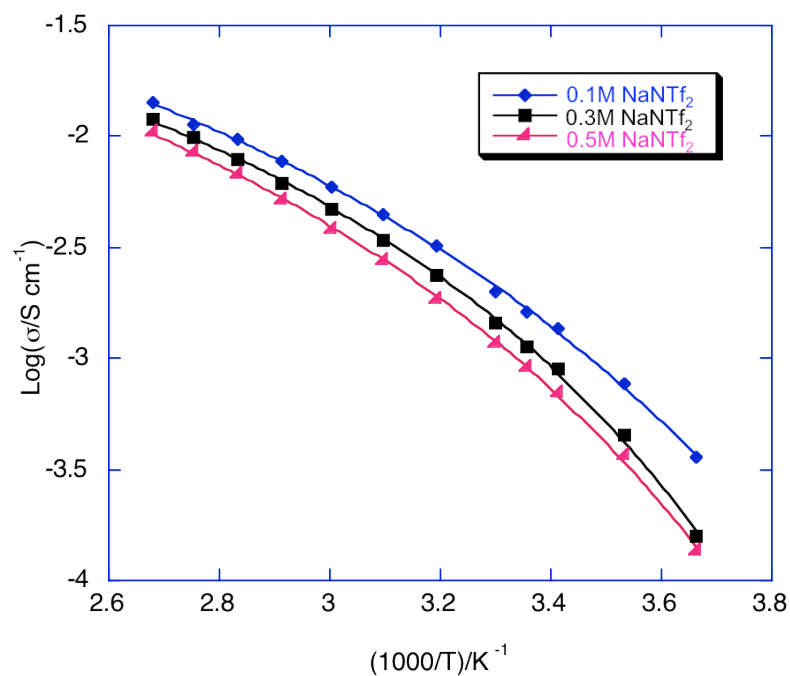
Table 2 shows the room temperature conductivity of the silica and PMMA gel electrolytes with various concentrations of sodium salt compared with the corresponding IL electrolytes²⁵. It can be seen that the ionic conductivity decreased as the sodium concentration increases consistent with formation of ion pairs and/or ion clusters which can lead to reduction in the number of charge carriers and increases the viscosity of the liquid electrolyte before formation of the gel. This has been discussed in our previous paper as well as for other lithium electrolyte systems²⁵. Comparing the liquid systems with silica gel system, the ionic conductivity remains the same for the case of 0.1 M NaNTf₂ and decreased very slightly (between 1.2 to 1.4 times) in the case of 0.3 and 0.5 M NaNTf₂ systems respectively. In these systems, the ionic conductivity also appears to decouple from the mechanical properties of gel electrolytes, which indicates an ideal combination of properties in a gel electrolyte for device application. It also further confirms our observations from the FTIR and DSC results that the silica particle acts only as a structural support (physical gelation) in the gel electrolytes and does not influence the ion dynamics to any great extent.

The ionic conductivity of the silica gel system is slightly higher compared with the PMMA gel system. The primary reason for this is the decreased in concentration of ion, which 8 wt% of MMA monomer needed for PMMA gel electrolytes compared to only 5 wt% of silica for silica content gel electrolytes, as explained in experimental section. Moreover, in PMMA gel electrolytes, the PMMA network

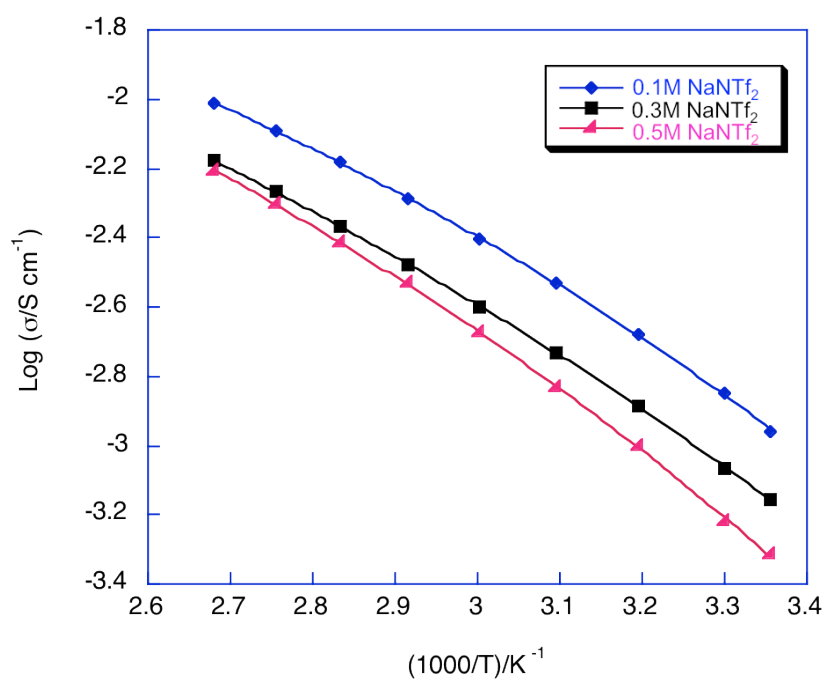
was formed by radical polymerization, while the silica system is formed by dispersing silica nanoparticles in the liquid electrolytes. Although the formation of the PMMA network does not affect the chemical environment of the IL (as discussed in FTIR section), the network does change the physical properties of these gel electrolytes, where the gel becomes elastic. In contrast, silica gel electrolytes are lower elastic modulus, which may account for the slightly higher ionic conductivity of the silica gel system.

The temperature dependence of both gel electrolytes is expressed through an Arrhenius conductivity plot as depicted in Fig. 4, which shows some curvature. Hence, these plots are well described and fitted by the VTF equation (Eq. 1), which suggests that migration of the ions in the gel electrolytes is similar to ionic conduction in a viscous liquid. The VTF parameters are listed in the Table 3. From the table, it can be seen that the T_0 (corresponding to the temperature where ionic conductivity disappears), is near the T_g value measured from the DSC analysis, as expected, and these values almost remain constant as the concentration of salt increased. Interestingly, The T_0 values for the PMMA gelled system is lower compared with the silica content gel electrolytes and almost the same with neat IL electrolytes, especially in high concentration of salt. This is consistent with the T_g values from DSC analysis as discussed above. However, pseudo activation energy (B) appears systematically higher in the case of PMMA gelled system, and which its again silica gel system shown similar behavior to the IL electrolytes system.

$$\sigma = \sigma_0 \exp[-B/(T-T_0)] \quad (\text{Eq. 1})$$



(a)



(b)

Fig. 4 Arrhenius conductivity of silica gel (a) and PMMA gel (b) electrolytes with various concentration of salt

Table 2. Room Temperature ionic conductivity of sodium gel electrolytes

Sodium gel	σ (S.cm ⁻¹)	σ (S.cm ⁻¹)	σ (S.cm ⁻¹)
electrolytes	0.1 M NaNTf ₂	0.3 M NaNTf ₂	0.5 M NaNTf ₂
Liquid ^a	1.7E-3	1.6E-3	1.1E-3
Silica	1.6E-3	1.1E-3	9.1E-4
PMMA	1.1E-3	7.0E-4	4.9E-4

Table 3. VTF parameters for ionic conductivity

Concentration of NaNTf ₂	Log σ_0	B (K)	T ₀ (K)	Log σ_0	B (K)	T ₀ (K)
	(S.cm ⁻¹)	Silica	Silica	(S.cm ⁻¹)	PMMA	PMMA
	Silica			PMMA		
0.1M	-0.5±0.08	-254±20	187±5	-0.3±0.06	-403±22	156±5
0.3M	-0.7±0.07	-205±14	206±3	-0.3±0.10	-398±34	168±7
0.5M	-0.6±0.07	-250±17	197±4	-0.5±0.07	-305±28	175±6

CONCLUSIONS

This study investigates the effect of gelation of ionic liquid based sodium ion electrolytes on their ionic conductivity, thermal properties, chemical interaction and electrochemical stability. A wide liquid temperature range, of more than 100 K around room temperature, is achieved in case of 0.3 and 0.5 M NaNTf₂. The ionic

conductivity was found to slightly decrease as the physical properties changed from liquid to gel. Facile deposition and stripping of sodium are observed around 0 V vs Na/Na⁺ at 298 K. The formation of gel electrolytes does not significantly affect the ion dynamics of the ionic liquid electrolytes. These electrolyte materials are thus promising candidates for secondary sodium batteries, since they may overcome the cost and safety problems associated with conventional electrolytes, while still exhibiting good conductivities and stabilities.

ACKNOWLEDGMENTS

The authors are grateful to the Australian Research Council for funding via DP130101652 and under the Laureate Fellowship schemes (MF and DRM).

REFERENCES

1. Andriola, A.; Singh, K.; Lewis, J.; Yu, L. *J. Phys. Chem. B* **2010**, *114*, 11709-11714.
2. Choi, J. A.; Shim, E. G.; Scrosati, B.; Kim, D. W. *Bull. Korean Chem. Soc.* **2010**, *31*, 3190-3194.
3. Lane, G. H.; Bayley, P. M.; Clare, B. R.; Best, A. S.; MacFarlane, D. R.; Forsyth, M.; Hollenkamp, A. F. *J. Phys. Chem. C* **2010**, *114*, 21775-21785.
4. Lee, J. S.; Quan, N. D.; Hwang, J. M.; Bae, J. Y.; Kim, H.; Cho, B. W.; Kim, H. S.; Lee, H. *Electrochem. Commun.* **2006**, *8*, 460-464.
5. Nguyen, D. Q.; Oh, J. h.; Kim, C. S.; Kim, S. W.; Kim, H.; Lee, H.; Kim, H. S. *bulletin korean chemical society* **2007**, *28*, 2299-2302.
6. MacFarlane, D. R.; Forsyth, M.; Izgorodina, E. I.; Abbott, A. P.; Annat, G.; Fraser, K. *Phys. Chem. Chem. Phys.* **2009**, *11*, 4962-4967.
7. Forsyth, S. A.; Pringle, J. M.; MacFarlane, D. R. *Aust. J. Chem.* **2004**, *57*, 113-119.
8. Forsyth, S. A.; Batten, S. R.; Dai, Q.; MacFarlane, D. R. *Aust. J. Chem.* **2004**, *57*, 121-124.
9. Chowdhury, S. A.; Scott, J. L.; MacFarlane, D. R. *Pure Appl. Chem.* **2008**, *80*, 1325-1335.

10. Earle, M. J.; Seddon, K. R. *Pure Appl. Chem.* **2000**, *72*, 1391-1398.
11. Komaba, S.; Itabashi, T.; Watanabe, M.; Groult, H.; Kumagai, N. *J. Electrochem. Soc.* **2007**, *154*, A322-A330.
12. Afanas'ev, V. N.; Grechin, A. G. *Russ. Chem. Rev.* **2002**, *71*, 775-787.
13. Byrne, N.; Howlett, P. C.; MacFarlane, D. R.; Forsyth, M. *Adv. Mater. (Weinheim, Ger.)* **2005**, *17*, 2497-2501.
14. Dell, R. M. *Solid State Ionics* **2000**, *134*, 139-158.
15. Ellis, B. L.; Nazar, L. F. *Current Opinion in Solid State and Materials Science* **2012**, *16*, 168-177.
16. Risacher, F.; Fritz, B. *Aquatic Geochemistry* **2009**, *15*, 123-157.
17. Yaksic, A.; Tilton, J. E. *Resources Policy* **2009**, *34*, 185-194.
18. Kiran Kumar, K.; Ravi, M.; Pavani, Y.; Bhavani, S.; Sharma, A. K.; Narasimha Rao, V. V. R. *Physica B: Condensed Matter* **2011**, *406*, 1706-1712.
19. Egashira, M.; Asai, T.; Yoshimoto, N.; Morita, M. *Electrochim. Acta* **2011**, *58*, 95-98.
20. Kumar, D.; Hashmi, S. A. *J. Power Sources* **2010**, *195*, 5101-5108.
21. Sudworth, J. L. *J. Power Sources* **1984**, *11*, 143-154.
22. Coetzer, J. *J. Power Sources* **1986**, *18*, 377-380.
23. Fukunaga, A.; Nohira, T.; Kozawa, Y.; Hagiwara, R.; Sakai, S.; Nitta, K.; Inazawa, S. *J. Power Sources* **2012**, *209*, 52-56.
24. Yamamoto, T.; Nohira, T.; Hagiwara, R.; Fukunaga, A.; Sakai, S.; Nitta, K.; Inazawa, S. *J. Power Sources* **2012**, *217*, 479-484.
25. Mohd Noor, S. A.; Howlett, P. C.; Macfarlane, D. R.; Forsyth, M. *Electrochim. Acta* **2013**, *114*, 766-771.
26. Monti, D.; Jónsson, E.; Palacín, M. R.; Johansson, P. *J. Power Sources* **2014**, *245*, 630-636.
27. Wu, X. J.; Wang, Y.; Wang, M.; Yang, W.; Xie, B. H.; Yang, M. B. *Colloid Polym. Sci.* **2012**, *290*, 151-161.
28. Raghavan, P.; Zhao, X.; Manuel, J.; Chauhan, G. S.; Ahn, J.-H.; Ryu, H.-S.; Ahn, H.-J.; Kim, K.-W.; Nah, C. *Electrochim. Acta* **2010**, *55*, 1347-1354.
29. Friedlander, S. K. *Journal of Nanoparticle Research* **1999**, *1*, 9-15.
30. Suh, Y. J.; Ullmann, M.; Friedlander, S. K.; Park, K. Y. *J. Phys. Chem. B* **2001**, *105*, 11796-11799.
31. Louis, H.; Lee, Y. G.; Kim, K. M.; Cho, W. I.; Ko, J. M. *Bull. Korean Chem. Soc.* **2013**, *34*, 1795-1799.
32. Howlett, P. C.; MacFarlane, D. R.; Hollenkamp, A. F. *Electrochem. Solid-State Lett.* **2004**, *7*, A97-A101.
33. Kufian, M. Z.; Aziz, M. F.; Shukur, M. F.; Rahim, A. S.; Ariffin, N. E.; Shuhaimi, N. E. A.; Majid, S. R.; Yahya, R.; Arof, A. K. *Solid State Ionics* **2012**, *208*, 36-42.
34. Gayet, F.; Viau, L.; Leroux, F.; Monge, S.; Robin, J. J.; Vioux, A. *J. Mater. Chem.* **2010**, *20*, 9456-9462.
35. Noor, S. A. M.; Bayley, P. M.; Forsyth, M.; MacFarlane, D. R. *Electrochim. Acta* **2013**, *91*, 219-226.

3.6 Supporting Information

Supplementary Information to accompany:

Gel-Ionic liquid based sodium ion conductors for sodium batteries

Siti Aminah Mohd Noor^{a,b}, Hyungook Yoon^{c,d}, Maria Forsyth^{c,d} and Douglas R
MacFarlane^{a,c}

*^a School of Chemistry, Monash University, Clayton Campus, 3800 Victoria,
Australia*

*^b Chemistry Department, Centre for Defence Foundation Studies, National Defence
University of Malaysia, 57000, Kuala Lumpur, Malaysia*

^c ARC Centre of Excellence for Electromaterials Science (ACES), Australia

^d Institute for Frontier Materials Deakin University, 3125, Victoria, Australia

**Email:* 

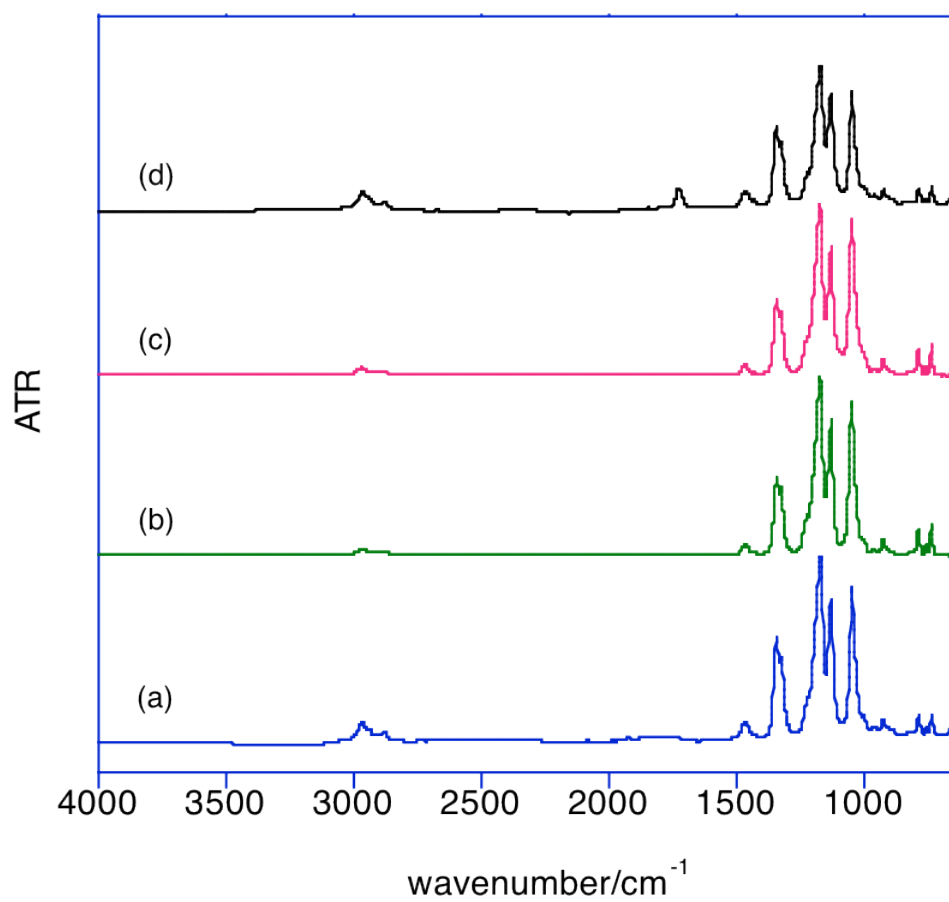


Fig. S1 FTIR spectra of C₄mpyrNTf₂ (a), 0.4M NaNTf₂ C₄mpyrNTf₂ (b), silica gel electrolyte (c) and PMMA gel electrolyte (d).

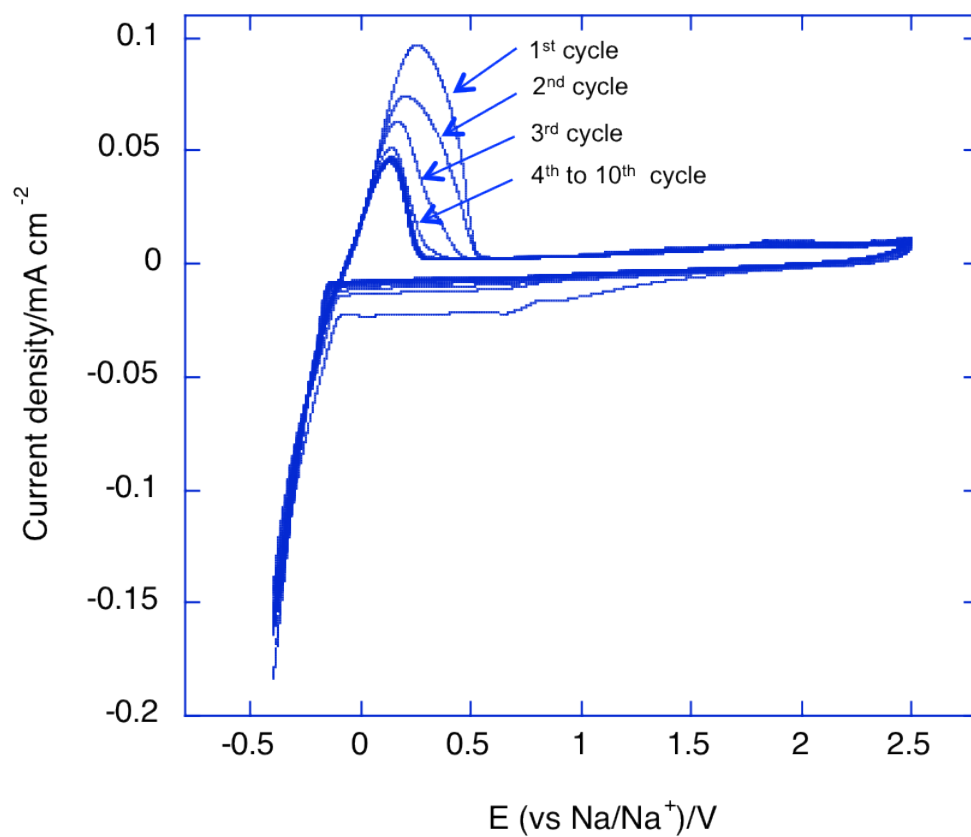


Fig. S2 Cyclic voltammogram of silica gel electrolytes at room temperature (1st to 10th cycle)

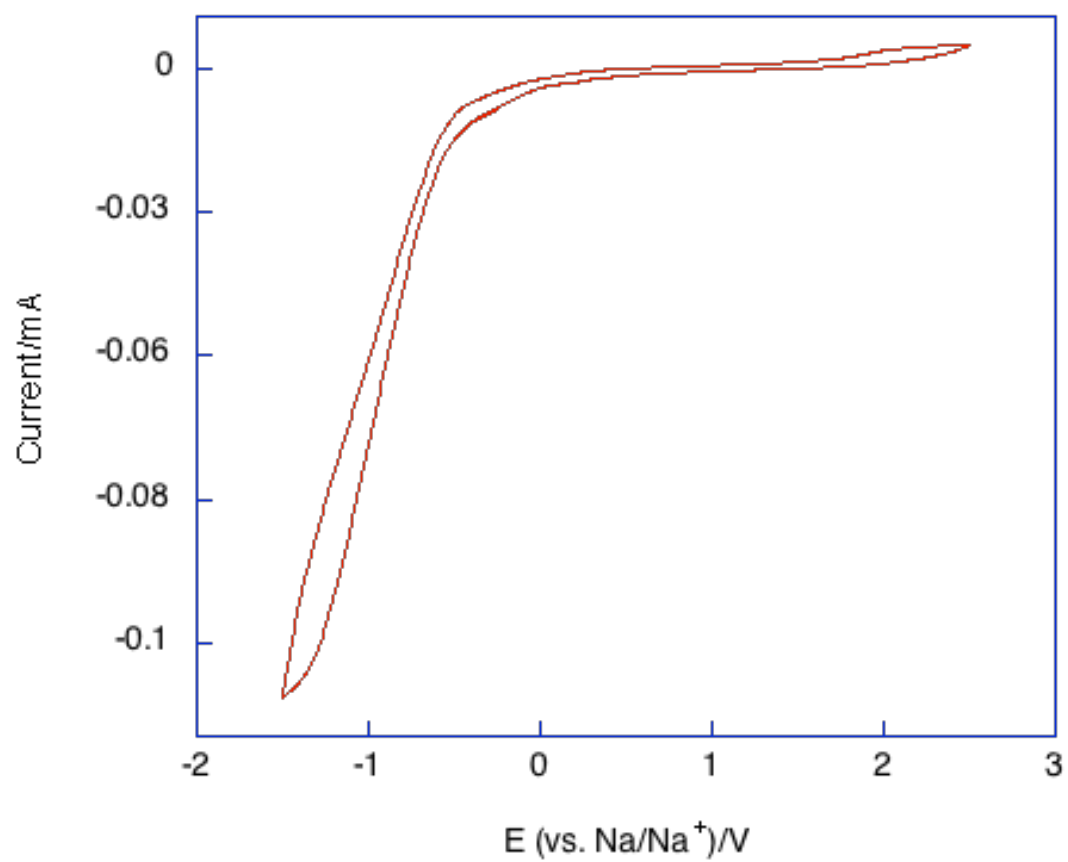


Fig. S3 Cyclic voltammogram of PMMA gel electrolytes at room temperature (1st cycle)

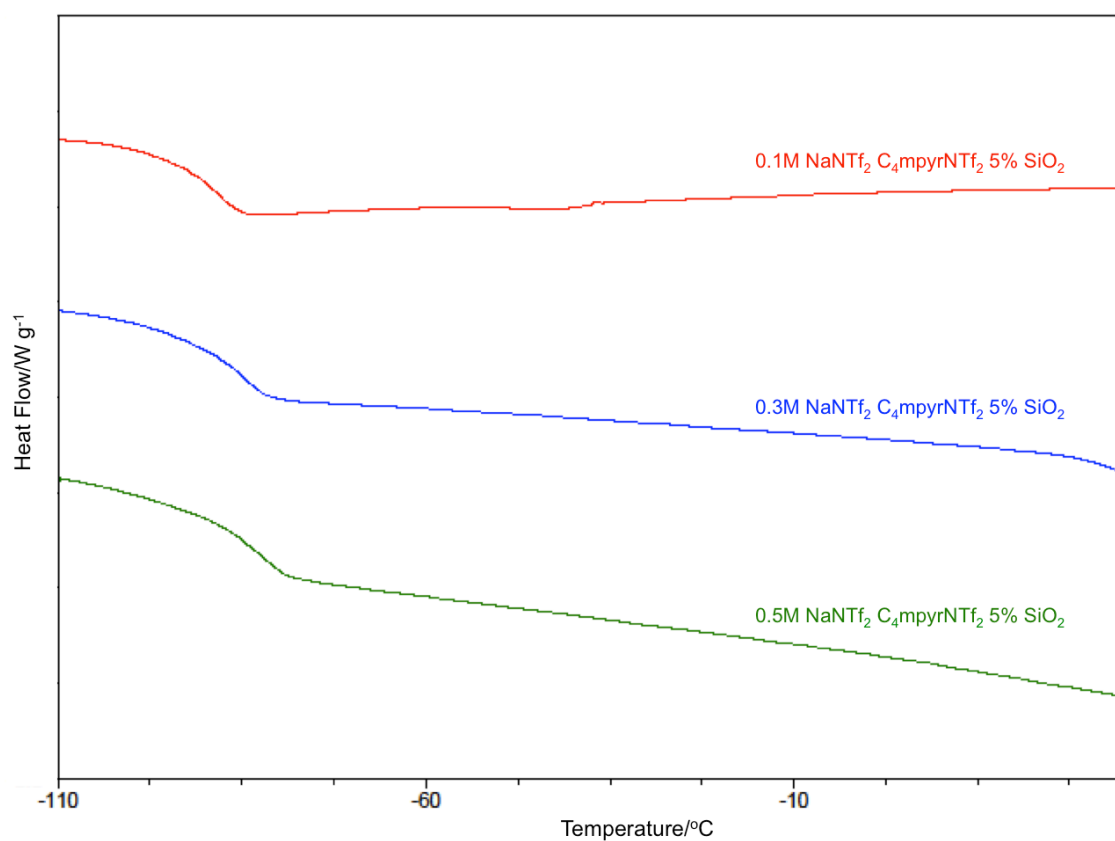


Fig. S4 DSC thermograms of sodium gel electrolytes with different concentrations of NaNTf_2 (cooling scan)

3.7 Bibliography

1. M. Armand, F. Endres, D. R. MacFarlane, H. Ohno and B. Scrosati, *Nat. Mater.*, 2009, **8**, 621-629.
2. R. M. Dell, *Solid State Ionics*, 2000, **134**, 139-158.
3. D. R. Macfarlane, N. Tachikawa, M. Forsyth, J. M. Pringle, P. C. Howlett, G. D. Elliott, J. H. Davis, M. Watanabe, P. Simon and C. A. Angell, *Energy and Environmental Science*, 2014, **7**, 232-250.
4. M. R. Palacín, *Chem. Soc. Rev.*, 2009, **38**, 2565-2575.
5. B. L. Ellis and L. F. Nazar, *Current Opinion in Solid State and Materials Science*, 2012, **16**, 168-177.
6. A. Fukunaga, T. Nohira, Y. Kozawa, R. Hagiwara, S. Sakai, K. Nitta and S. Inazawa, *J. Power Sources*, 2012, **209**, 52-56.
7. T. Yamamoto, T. Nohira, R. Hagiwara, A. Fukunaga, S. Sakai, K. Nitta and S. Inazawa, *J. Power Sources*, 2012, **217**, 479-484.
8. M. Egashira, T. Asai, N. Yoshimoto and M. Morita, *Electrochim. Acta*, 2011, **58**, 95-98.
9. D. Kumar and S. A. Hashmi, *Solid State Ionics*, 2010, **181**, 416-423.
10. D. Monti, E. Jónsson, M. R. Palacín and P. Johansson, *J. Power Sources*, 2014, **245**, 630-636.
11. N. Yoshimoto, S. Yakushiji, M. Ishikawa and M. Morita, *Solid State Ionics*, 2002, **152-153**, 259-266.
12. N. Yoshimoto, T. Shirai and M. Morita, *Electrochim. Acta*, 2005, **50**, 3866 - 3871
13. M. Kar, B. Winther-Jensen, M. Forsyth and D. R. MacFarlane, *Phys. Chem. Chem. Phys.*, 2013, **15**, 7191-7197.
14. S. A. Mohd Noor, P. C. Howlett, D. R. Macfarlane and M. Forsyth, *Electrochim. Acta*, 2013, **114**, 766-771.



Chapter 4

Ionomers as cation only ion conductors

4.1 General Overview

The ionic conductivity of conventional liquid electrolytes, as well as solid polymer electrolyte systems, is the result of contributions from both the cation and anion. In devices utilizing a cation charge carrier, these bi-ion conductors typically exhibit anion buildup at the electrode/electrolyte interface that ultimately lowers the effective field on the cations, thus limiting their performance in batteries and other devices¹⁻⁴. Single ion conductors are needed in order to overcome this “concentration polarization” issue. Single ion conductors can be constructed by covalently attaching the anion to a polymer backbone to make an ionomer or polyelectrolyte^{1, 5, 6}. Therefore, the anion cannot respond to the field on a reasonable time scale and the transference number for the cation will be close to unity.

Various single ion conductor ionomer systems have been developed over the years^{5, 7-9}, yet the ion conductivity in ionomers having metal counterions has been considerably lower than that of, for example, PEO/salt mixtures. A number of methods have been employed in an attempt to increase the ionic conductivity, such as addition of an organic solvent¹⁰ or ionic liquid and exchange of the small cation with more bulky cations^{2, 3, 11} to reduce ion pair association. This method has been shown to assist lithium ion dissociation from the backbone, leading to high ionic conductivities and good performance in Li-ion batteries.^{7, 8}

Here, we report the development of solvent free solid ionomer electrolytes based on the copolymer poly([triethylmethylammonium][2-acrylamido-2-methyl-1-

propane-sulfonic acid]-co-sodium[vinyl sulfonate], poly([N₁₂₂₂][AMPS]-co-Na[VS]), where a fraction of sodium ions were replaced with a bulky, ionic liquid forming, quaternary ammonium cation¹². We found that significant ionic conductivity was measurable below T_g in these systems, indicating an increasingly decoupled ion transport mechanism from the ionomer structural relaxations as the ratio of the sodium to quaternary ammonium cations decreased. More details on this work have been described in Publication 4, which has been published in *Journal of Materials Chemistry A*, as a paper entitled “Ion conduction and phase morphology in sulfonate copolymer ionomers based on ionic liquid-sodium cation mixtures”¹²

The decoupling behavior exhibited in copolymer systems has prompted us to investigate homopolymer ionomer systems. The effect of sodium concentration on the conductivity, thermal stability and phase separation of such systems are explored and discussed here. Moreover, the influence of different types of ammonium counter-cations on the conductivity of ionomers in a homopolymer system has also been studied. In the present systems, the conductivity appears increasingly decoupled from the T_g of the ionomer system, particularly for compositions below 50 mol% Na⁺. An interesting, reproducible observation is that above its T_g the 10% Na⁺ sample has the highest conductivity of all the systems investigated here. Even though the 10% Na samples possess the highest ionic conductivity, it is most likely that the improvement in ionic conductivity originates from the mobility of the quaternary ammonium cation. We also observed a

decreasing T_g with increasing bulkiness of the quaternary ammonium cation, and an increasing degree of decoupling from the glass transition within these systems. More details on these systems are presented in a manuscript entitled “Decoupled ion conduction in poly(2-acrylamido-2-methyl-1-propane-sulfonic acid) (PAMPS) homopolymers” that has been submitted to *Polymer*.

4.2 Specific Declaration

PART B: Suggested Declaration for Thesis Chapter

Monash University

Declaration for Thesis Chapter 4.3

Declaration by candidate

In the case of Chapter 4.3, the nature and extent of my contribution to the work was the following:

Nature of contribution	Extent of contribution (%)
Initiation, key ideas, performed the experiments, synthesis, data analysis and interpretation, manuscript development and writing up	90

The following co-authors contributed to the work. If co-authors are students at Monash University, the extent of their contribution in percentage terms must be stated:

Name	Nature of contribution	Extent of contribution (%) for student co-authors only
Douglas MacFarlane	Key ideas, proof reading and final drafting	-
Maria Forsyth	Key ideas, proof reading and final drafting	-
Daniel Gunzelmann	NMR characterisation and discussions	-
Jiazeng Sun	Synthesis the ionomers	-

The undersigned hereby certify that the above declaration correctly reflects the nature and extent of the candidate's and co-authors' contributions to this work*.

Candidate's Signature		Date 17/7/2014
------------------------------	--	--------------------------

Main Supervisor's Signature		Date 17/7/2014
------------------------------------	--	--------------------------

*Note: Where the responsible author is not the candidate's main supervisor, the main supervisor should consult with the responsible author to agree on the respective contributions of the authors.

4.3 Publication 4

Ion conduction and phase morphology in sulfonate copolymer ionomers based on ionic liquid-sodium cation mixtures

S.A.M.Noor,^{a,b} D.Gunzelmann,^d J. Sun,^a D.R. MacFarlane,^{a,c} M. Forsyth,^{c,d*}

^a *School of Chemistry, Monash University, Clayton Campus, Victoria, Australia*

^b *Chemistry Department, Centre for Defence Foundation Studies, National Defence University of Malaysia, 57000, Kuala Lumpur, Malaysia*

^c *ARC Centre of Excellence for Electromaterials Science (ACES) Australia*

^d *Institute for Frontier Materials Deakin University, Victoria, Australia*

* *Corresponding Author:*

[REDACTED]

[REDACTED]

Journal of Materials Chemistry A

2 (2014) 365-374

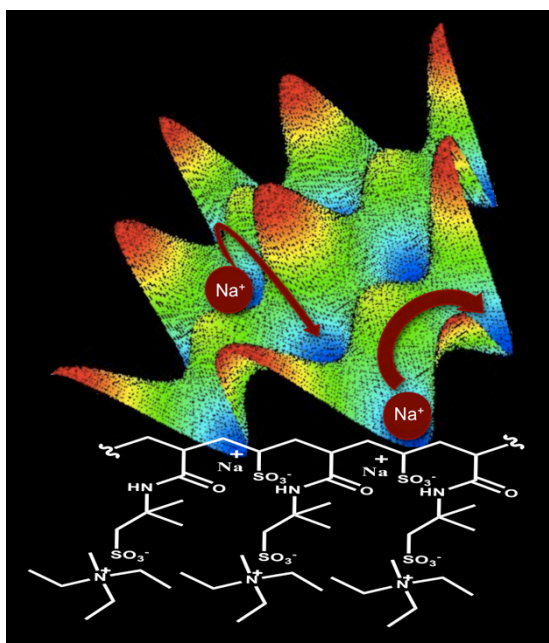
DOI: 10.1039/c3ta13835f

Graphical Abstract

Ion conduction and phase morphology in sulfonate copolymer ionomers based on ionic liquid-sodium cation mixtures

S.A.M.Noor,^{a,b} D.Gunzelmann,^d J. Sun,^a D.R. MacFarlane,^{a,c} M. Forsyth,^{c,d*}

A series of sulfonate based copolymers have been prepared by partially replacing sodium cations with bulky ionic liquid cations, thereby providing more conduction sites for the sodium ion to ‘hop’ to in the ionomers and improving the ionic conductivity of the material.



Ion conduction and phase morphology in sulfonate copolymer ionomers based on ionic liquid–sodium cation mixtures†

Cite this: *J. Mater. Chem. A*, 2014, 2, 365Siti Aminah Mohd Noor,^{ab} Daniel Gunzelmann,^d Jiazeng Sun,^a
Douglas R. MacFarlane^{ac} and Maria Forsyth^{*cd}

A series of sulfonate based copolymer ionomers based on a combination of ionic liquid and sodium cations have been prepared in different ratios. This system was designed to improve the ionic conductivity of ionomers by partially replacing sodium cations with bulky cations that are less associated with anion centres on the polymer backbone. This provides more conduction sites for sodium to 'hop' to in the ionomers. Characterization showed the glass transition and ¹⁵N chemical shift of the ionomers did not vary significantly as the amount of Na⁺ varied, while the ionic conductivity increased with decreasing Na⁺ content, indicating conductivity is increasingly decoupled from *T*_g. Optical microscope images showed phase separation in all compositions, which indicated the samples were inhomogeneous. The introduction of low molecular weight plasticizer (PEG) reduced the *T*_g and increased the ionic conductivity significantly. The inclusion of PEG also led to a more homogeneous material.

Received 24th September 2013
Accepted 7th November 2013

DOI: 10.1039/c3ta13835f

www.rsc.org/MaterialsA

Introduction

Polymer electrolytes are of immense interest due to their applicability in energy conversion and storage devices such as fuel cells and batteries. They present significant advantages over liquid electrolytes and ceramic electrolytes, on one hand due to the removal of volatile, liquid components and on the other hand their potential flexibility and moldability. Polymer electrolytes have been under investigation since the late 1970s when Wright *et al.*¹ discovered that polyether complexes of alkali salts were ionically conductive and later Armand *et al.*^{2,3} suggested these could potentially be useful in solid state batteries.

Over the past three decades there has been intense research in trying to improve the ionic conductivity in solid polymer electrolytes.⁴ Amorphous polyethylene oxide (PEO) based systems have generally shown the highest conductivity, with some significant improvement in properties and conductivity obtained by using nanofillers in PEO based solid polymer electrolytes (SPEs).^{5–9} One desirable property in any given electrolyte is a high transport number for the target ion of interest;

for example lithium ion for a lithium battery, protons in the case of proton membrane fuel cells and sodium if we consider a sodium device. In devices utilizing a cation charge carrier, anion mobility is undesirable, as the device would then suffer from undesirable concentration polarization, in which anion build up occurs at the electrode/electrolyte interface due to its high mobility in the electrolyte, and this concentration polarization diminishes battery performance.¹⁰

One method of achieving only cation conductivity in a polymer system is to tether the anion to the polymer backbone, as in a polyelectrolyte or an ionomer system. Numerous single-ion conductor ionomer systems have been developed over the years; for example those based on poly(2-acrylamido-2-methyl-1-propane-sulfonic acid) (PAMPS)^{11,12} and copolymers of sulfonate polyester, sulfonated ethylene/styrene and styrene-ethylene/butylene-styrene.^{13–17} In general, however, the anion on the polymer backbone is somewhat basic, from which the cation does not readily dissociate, resulting in low ionic conductivity. A number of methods have been employed in an attempt to increase the ionic conductivity; for example the AMPS monomer has been copolymerized with *N,N'*-dimethylacrylamide (DMAA) to separate the ionic moieties along the backbone and thereby avoid multiple anion association to the cation.¹⁸ The addition of an organic solvent or ionic liquid has been shown to assist lithium ion dissociation from the backbone leading to high ionic conductivities and good performance in Li-ion batteries.^{11,19–22} Whilst these materials retain good elastomeric, solid-state properties, they nevertheless still contain a low molecular weight solvent that could either leak or

^aSchool of Chemistry, Monash University, Clayton Campus, Victoria, Australia^bChemistry Department, Centre for Defence Foundation Studies, National Defence University of Malaysia, 57000, Kuala Lumpur, Malaysia^cARC Centre of Excellence for Electromaterials Science (ACES), Australia^dInstitute for Frontier Materials Deakin University, Victoria, Australia. E-mail: [redacted]

† Electronic supplementary information (ESI) available. See DOI: 10.1039/c3ta13835f

be volatile. Therefore it is still desirable to prepare solvent free, or very low solvent content, polymer electrolytes.

Recently, Colby *et al.* have investigated cation dynamics in polyester based ionomers and sulfonated polystyrene, with a variety of cations ranging from the inorganic Na^+ , Li^+ and Cs^+ , to organic cations which are typically used to prepare ionic liquid salts.²³ It was very interesting to observe that the glass transition temperatures of these ionomers were significantly reduced when the organic cations were used as the ionomer charge carriers, with the ionic conductivity increasing by as much as 10^4 times when a tetrabutylammonium ion was used instead of a sodium cation.²⁴ This was attributed primarily to a lowering in the glass transition temperature, T_g , due to the weaker electrostatic interactions between the cation and the backbone-tethered sulfonate anion. Interestingly, when the conductivities were scaled with T_g , it was apparent that the ionic transport was still intimately coupled to the polymer backbone mobility, just as is observed in PEO based polymer electrolytes where a lithium salt is dissolved in the polymer. Under such circumstances, the conductivity can only be improved by further reducing T_g . On the other hand, rigid ceramic materials such as lithium aluminium titanium phosphates (LATP)^{25,26} or β -alumina^{27,28} have extraordinarily high single ion conduction, completely decoupled from the rigid nature of the host ceramic. It was postulated that the mechanism for such high single ion transport lies in multiple equi-energy sites available to charge carriers, such that ions can 'hop' from site to site relatively unencumbered.

Our hypothesis is that a similar mechanism can be designed to achieve high ionic conductivity in an ionomer system, by creating anion centres on the polymer that are less associated with the corresponding counterions and therefore the cation

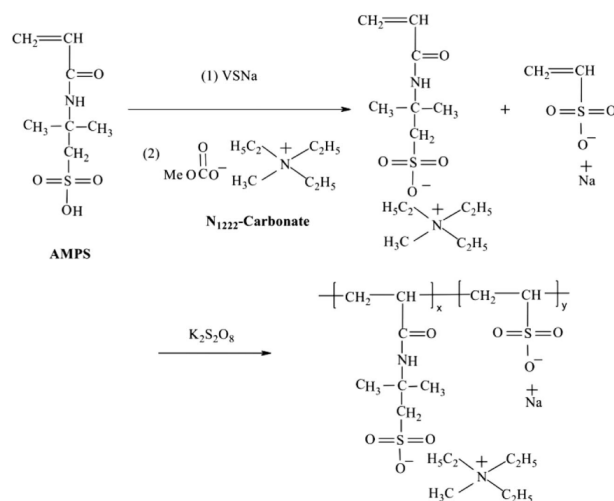
motion is less coupled to the bulk dynamics of the material. Essentially, by replacing a fraction of the sodium ions with a bulky ionic liquid cation, more anion sites become available to the sodium and therefore its diffusive motion more facile. The variable cation composition in such systems allows us to explore a spectrum of degrees of decoupling over quite a wide range from strongly coupled to significantly decoupled. Furthermore, the use of the flexible organic counterions should serve to decrease the T_g , as was shown by Colby *et al.*,²⁴ which could lead to still higher ionic conductivities and improved mechanical properties of the ionomer electrolytes.

In this paper, we prepare a series of ionomers by copolymerizing a sodium vinyl sulfonate (NaVS) monomer, and AMPS-triethylmethylammonium monomer in different ratios. These materials are characterized using a.c. impedance to measure ionic conductivity, optical microscopy to observe the morphology and variable temperature, multi-nuclear solid-state NMR spectroscopy to study the dynamic behaviour of the ionomers.

Materials and experimental

Sample preparation

Preparation of copolymers of 2-acrylamido-2-methyl-1-propane-sulfonate (AMPS) (as the alkyl-ammonium/sodium salts) and the sodium salt of vinyl sulfonate (NaVS) was carried out based on Scheme 1. Typical procedures for synthesis were as follows: 5.017 g of AMPS (0.0241 mol, Aldrich) was dissolved in 10 ml of distilled water; NaVS was added drop-wise at room temperature with magnetic stirring; N_{1222} -carbonate solution (Aldrich) was added until the pH of the solution reached 7; $\sim 0.2\%$ of $\text{K}_2\text{S}_2\text{O}_8$ was then added into the solution and stirred at $\sim 85^\circ\text{C}$ for



Scheme 1 Schematic preparation of poly([N_{1222}][AMPS]-co-[NaVS]) ionomers.

2 days. After removing the solvents from the reaction mixture the samples were dried under vacuum at $\sim 70^\circ\text{C}$ for at least 2 days prior to any characterisation. Mole ratio of $[\text{N}_{1222}][\text{AMPS}]$ and NaVS was varied from 90 : 10 to 50 : 50.

Ionic conductivity

The ionic conductivity of the ionomers was measured by ac impedance spectroscopy using a high frequency response analyzer (HFRA; Solartron 1296). Handled in the dry box, the dried powder samples were first pressed into pellets (1 mm thick and 13 mm in diameter) using a KBr die and a hydraulic press at 10 tonne for 30 min; pellets were aged in the oven at 393 K overnight and then sandwiched between two stainless steel blocking electrodes. The sample was also further heated up to 120°C in the conductivity barrel cell before conductivity measurement started. Data was collected over a frequency range of 0.1 Hz to 10 MHz (ten points per decade) with a 30 mV amplitude over a temperature range of 298 to 423 K in 10 K intervals. The temperature was controlled to within 1 K using a Eurotherm 2204e temperature controller and a band heater with a cavity for the cell using a thermocouple type T, which was embedded in the cell. The sample was held for a short equilibration time, up to 2 min, to stabilize the temperature prior to impedance measurement. The conductance was determined from the impedance data using the touch down of the semi-circle fit in Z-view (Version 2.3).

Differential scanning calorimetry (DSC)

DSC measurements were carried out on the as prepared samples, using a DSC Q100 series instrument (TA Instruments), and the data was evaluated with Universal Analysis 2000 software. Approximately 8 to 10 mg of the ionomer sample was tested over a temperature range of 273 to 423 K at a scanning rate of 10 K min^{-1} . The glass transition temperature was determined from the onset of the heat capacity change on heating ramp.

Solid-state nuclear magnetic resonance (NMR)

Solid-state NMR spectra were recorded with a BRUKER Avance III 300WB spectrometer operating at 300.13, 79.39, 75.46 and 30.42 MHz for ^1H , ^{23}Na , ^{13}C and ^{15}N , respectively. All ^1H and ^{13}C spectra are given relative to tetramethylsilane, ^{15}N spectra with respect to nitromethane and ^{23}Na spectra were referenced to 1 M $\text{NaCl}_{(\text{aq})}$. Samples were packed in standard 4 mm MAS rotors, loaded and measured in a 4 mm double-resonance MAS probe (BRUKER) spinning at 10 kHz. Cross-polarization from ^1H was used to excite ^{13}C and ^{15}N nuclei applying a ramped (50 to 100% power) shape pulse on the proton frequency with a contact time of 2–10 ms and a SPINAL64 proton decoupling with an nutation frequency of 114 kHz was applied during acquisition. Recycle delays were set between 3 and 5 times the proton T_1 relaxation constants, which were determined from earlier spectra. Static ^1H and ^{23}Na spectra were measured with a solid-echo sequence using a $2.5\text{ }\mu\text{s}$ 90 degree pulse and an echo delay of $20\text{ }\mu\text{s}$.

Optical microscopy

Optical micrographs were recorded through a microscope equipped with a digital camera (Nikon D200). Images were taken directly from the surface of aged pellet samples at room temperature after conductivity measurements.

Results and discussion

Thermal properties

Fig. 1 shows the DSC thermogram of ionomers for the first scan (top) and second scan (bottom). It can be seen that there is endothermic peak (T_g overshoot) in the first thermal cycle, which is more obvious at lower concentration of Na^+ . According to Berens and Hodge^{29,30} an enthalpy overshoot at T_g is often observed in polymers when structural relaxation takes place near T_g . However, during the subsequent scans, the enthalpy overshoot no longer appeared, and only a broad T_g can be reproducibly observed. This broad T_g suggests that the sample

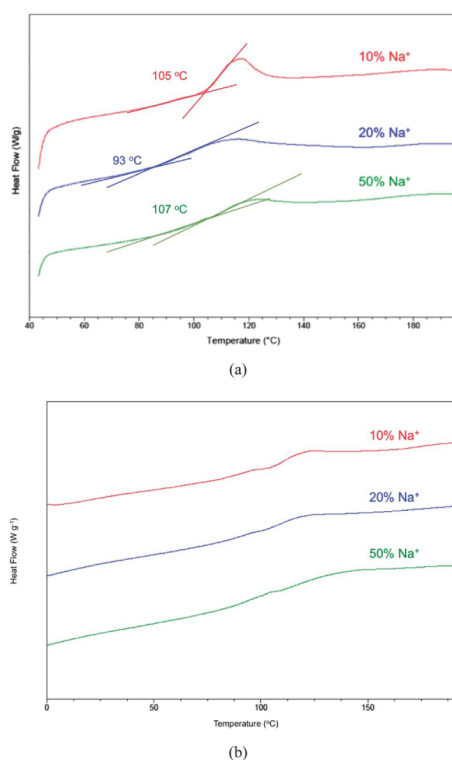


Fig. 1 DSC thermograms of poly($[\text{N}_{1222}][\text{AMPS}]$ -co- $\text{Na}[\text{VS}]$) ionomers with different mol% of NaVS (a) first thermal cycle and (b) second and subsequent cycles.

is not completely homogeneous at the molecular level. This behavior will be further discussed below. Overall, these thermograms suggest that T_g does not vary significantly as the amount of sodium changes from 10–50 mol%. This is in contrast to expectations, given that Colby *et al.*^{10,23,24} reported that the T_g of ionomers was reduced significantly when the ionic liquid cation was used instead of Na^+ . However, in those systems, 100% of the ions were exchanged and therefore the residual Na^+ ions in the present ionomers may influence T_g significantly. The composition dependence of T_g is discussed in more detail with respect to conductivity below.

Ionic conductivity

The ionic conductivity of the ionomers was measured both during one full cycle of heating (40 °C to 150 °C) and then on subsequent cooling (150 °C to 40 °C) to observe the reproducibility and any hysteresis that might be present. Fig. 2 presents the Nyquist plots for the ionomer containing 10% Na^+ at 60, 70, 80 and 100 °C. We observed that, during the heating cycle, a second semicircle appeared in the impedance diagrams for temperatures below 100 °C. This suggests two conduction processes are present and, as with the DSC data, may reflect an inhomogeneous material in which two different transport mechanisms exist. The change in impedance of the lower frequency arc is more rapid with temperature than the high frequency arc and, above T_g , the semicircles merge leading to a single apparent conduction process. On cooling, only this single process is observed, even below T_g . Subsequent heating/cooling

cycles showed reproducible behaviour with two processes always appearing at temperatures below T_g upon heating. The implications of this for the phase behaviour will be discussed further below.

Fig. 3a inset shows similar behavior for the sample containing 50% Na^+ , whereby two semicircles can be observed during the heating cycle for temperatures below T_g . Fig. 3 shows the Arrhenius plot for this sample, which appears to follow Arrhenius behaviour over this temperature range above and below T_g . The blue square data points show the ionic conductivity for the second process at lower frequency. In this case, the conductivity determined from the second process at 100 °C is actually higher than the process that dominates above T_g and the higher activation energy (160 compared with 212 kJ mol^{-1}) for the low frequency process is evident in Fig. 3a. Once again, a single impedance arc is seen at all temperatures upon cooling (Fig. 3b), as was the case for the 10% Na^+ sample shown in Fig. 2.

Fig. 4 presents the Arrhenius plots for each of the ionomers with various compositions, from 0 to 100% NaVS. The 100% Na^+ ionomer shows very low conductivity, probably due to strong association of Na^+ to the sulfonate anion from the backbone, as has previously been reported for Na^+ based ionomers.²³ On the other hand, below 50% of Na^+ , the ionic conductivity follows an Arrhenius behaviour, indicating a thermally activated conduction process that persists even below T_g . Indeed there is no apparent rapid decrease as T_g is approached, in contrast to the data trends observed in polyester sulfonate ionomers with ionic

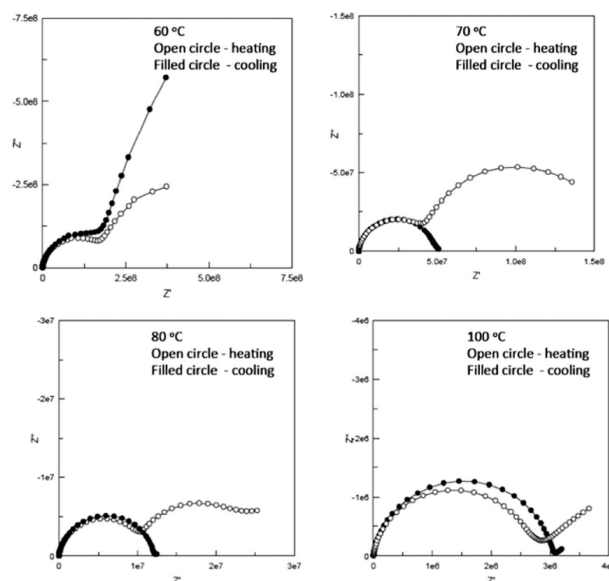


Fig. 2 Impedance plane plots of poly([N₁₂₂₂][AMPS]-co-Na[VS]) ionomers with 10% NaVS.

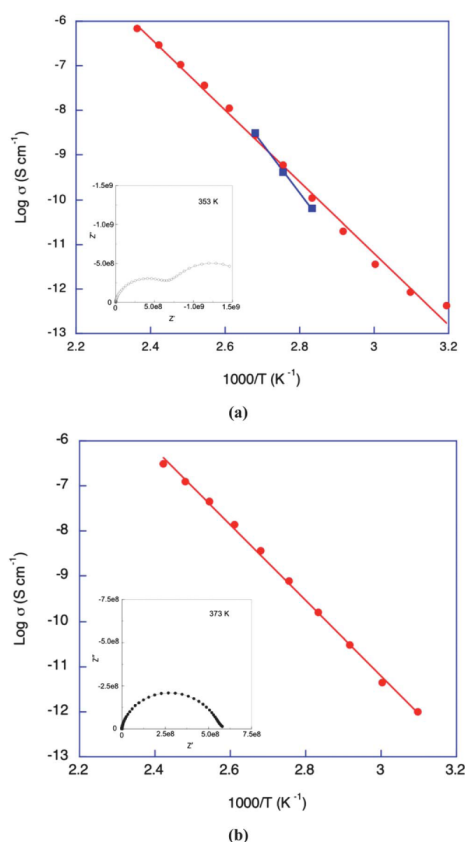


Fig. 3 Impedance plane plots and the conductivity of poly([N₁₂₂₂][AMPS]-co-Na[VS]) ionomer with 50% NaVS (a) heating (b) cooling cycle. The squares are the conductivity values from the low frequency process.

liquid counterion systems,^{10,24} where conductivity approached 10^{-12} S cm⁻¹ at T_g . In the work by Colby *et al.*,²⁴ despite the T_g decreasing as the counterion was fully replaced by an ionic liquid cation, the conductivity still remained coupled to T_g . In the present systems, the conductivity appears increasingly decoupled from the T_g of the ionomer system, particularly for compositions below 50% Na⁺. An interesting, reproducible observation is that above its T_g , the 10% Na⁺ sample has the highest conductivity of all the systems investigated here. Therefore it appears that mixing the two cations leads to favorable properties for conductivity in these materials. The activation energy also seems to be composition dependent, decreasing with increasing ammonium cation content as represented in Table 1.

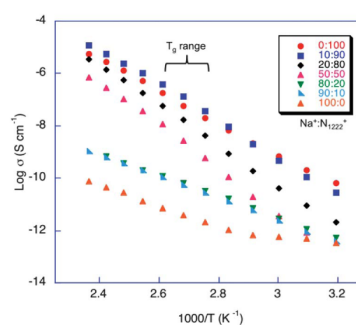


Fig. 4 Ionic conductivity of poly([N₁₂₂₂][AMPS]-co-Na[VS]) ionomers with various mol% of NaVS.

Table 1 Arrhenius parameters of poly([N₁₂₂₂][AMPS]-co-Na[VS]) ionomers with various mol% of NaVS

Na ⁺ (mol%)	E_a (kJ mol ⁻¹)	Log (σ_0 / S cm ⁻¹)	r^2
0	117 ± 2	9.2 ± 0.2	0.999
10	133 ± 2	11.6 ± 0.3	0.999
20	147 ± 1	12.8 ± 0.2	0.999
50	160 ± 2	13.7 ± 0.3	0.999
80	77 ± 1	0.6 ± 0.1	0.999
90	80 ± 1	0.9 ± 0.1	0.999
100	57 ± 1	-3.3 ± 0.6	0.973

The composition dependence of conductivity and its relationship to T_g is more clearly shown in Fig. 5, which presents the measured conductivity at 373 K together with the T_g for each of the compositions. From this data it can be seen that with addition of 10 mol% of Na⁺, the ionic conductivity of the ionomer increases by a factor of two relative to the 100% poly([N₁₂₂₂][AMPS]) sample. However, as sodium concentration is further increased, the ionic conductivity decreases dramatically, especially at 90 mol% of Na⁺. The primary reason for this

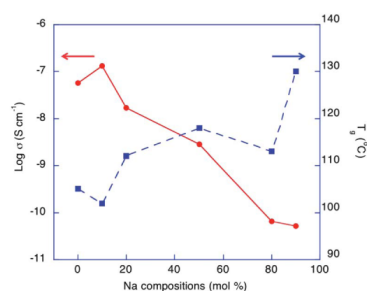


Fig. 5 Ionic conductivity at 373 K and glass transition temperature (T_g) of poly([N₁₂₂₂][AMPS]-co-Na[VS]) ionomers (90 : 10) as a function of Na⁺ concentration.

appears to be the increase in glass transition temperature for the ionomer with increasing Na^+ content. Even though there appears to be decoupling of conductivity from T_g , (*i.e.* there is significant measurable conductivity even below T_g) the higher the Na content the lower the extent of decoupling. In other words, as we approach 100% Na the conductivity (and hence ion mobility) at T_g is very low, indicating that the ion motion (both organic cation and Na^+) is more strongly linked to local polymer motions. The extent to which the conductivity is due to the N_{1222}^+ cation or the Na^+ cation motion cannot be determined at this stage.

Morphology

As discussed in the DSC and conductivity sections, the broad T_g that is observed and also the two semicircles seen in the Nyquist plot may be due to the sample being inhomogeneous. Fig. 6 depicts the optical microscope images for ionomers with different compositions of Na^+ . Here we can clearly see that phase separation does indeed occur for all compositions, as evidenced by the differences in the colour contrast in the optical images. This phase separation is more obvious and appears coarser as the amount of Na^+ increased, and is especially evident at 50% Na^+ composition. This observation is also consistent with the possibility of two conduction processes

occurring in these ionomers. If these materials are truly random copolymers, then this phase separation is challenging to understand, unless the Mw distribution is bimodal, which could lead to phase separation.³¹ Alternatively, these copolymers could be more block-like which has been shown to result in phase separation.³² The presence of two different cation counterions may also play a role in the observed phase separation, for example if the cations appeared in 'blocks' rather than randomly along the polymer chain.

To understand whether the phase separation is likely due to the presence of large homopolymer blocks within the copolymer or a polymer blend of two different materials we can consider the polymerisation chemistry, however, the reactivity ratios of this combination of monomers are not known. McCormick *et al.*^{33,34} reported that polymerisation of sodium AMPS (m1) monomer with [2-(acrylamido)-2-methylpropyl]trimethylammonium chloride (AMPTAC) (m2) formed a water-soluble copolymer with reactivity ratios of $r_1 = 0.52$ and $r_2 = 0.62$ and this copolymer was strongly alternating. The percentage of homo-blocks was, however, dependent on the monomer feed ratio, while monomer alternation was found to increase with less AMPS monomer in the feed. In addition, the Mw of the homopolymer presented in McCormick's work was lower than the Mw of the copolymer. Other work by Tong *et al.*³⁵ reported the copolymerisation of AMPS (m1) with 2-hydroxypropyl methacrylate (HPM) (m2). They discovered that the reactivity ratios for this copolymer are $r_1 = 0.04$ and $r_2 = 6.30$, and mean sequence length of m1 is shorter than m2. In this case HPM is insoluble in water while AMPS is water soluble. High resolution liquid NMR carried in the present work was unable to distinguish between the various carbons in the copolymer and hence we were not able to characterise the polymer further. However, it appears from the literature discussed above that the reactivity ratios of the monomers are similar and therefore the final ionomer will most likely be a semi-random copolymer of the two monomers.

Solid-state nuclear magnetic resonance (NMR)

Solid-state NMR spectroscopy was used to check the structure and composition of the polymer materials as well as study the dynamic behaviour *via* variable temperature (VT) wide-line experiments. The ^{13}C CPMAS spectra (Fig. 7 top) show broad and narrow signals, which can be easily assigned. The narrow signals with chemical shifts of 55.5, 46.7 and 7.2 ppm were assigned to the $\text{N}-\text{CH}_2$ -, the $\text{N}-\text{CH}_3$ and the $\text{C}-\text{CH}_3$ groups of the N_{1222} cation, respectively. Line widths between 70 Hz for the methyl signal and 120 Hz for the CH_2 signal are reduced by a factor of 2–3 compared to the matching 220 Hz for the side group methyl signal and 240 Hz and 300 Hz for the side group and backbone CH_2 signals, respectively. This indicates the higher mobility of the ammonium cation in the polymer matrix (mainly rotational but also translational motion). The broad signals are caused by the shorter T_2 of the polymer nuclei due to the inherent lower mobility of the polymer backbone and side groups. Thus the signals from 176, 61, 52.5, 42, 38 to 26 ppm are assigned to the amide carbon, the side group $-\text{CH}_2$ -, the

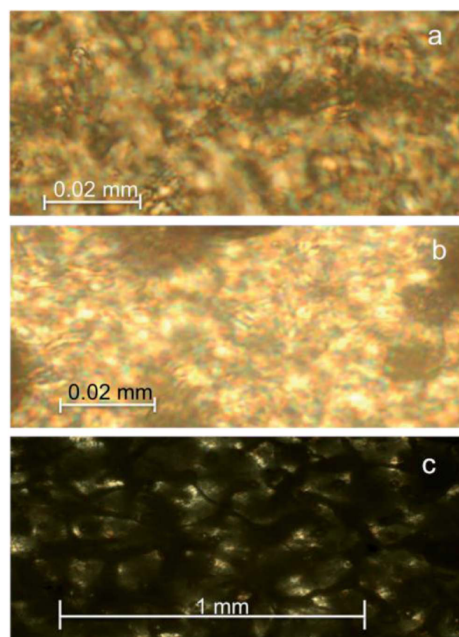


Fig. 6 Optical microscope images of poly($[\text{N}_{1222}][\text{AMPS}]\text{-co-Na[VS]}$) ionomers with various mol% of NaVS (a) 10% (b) 20% (c) 50%.

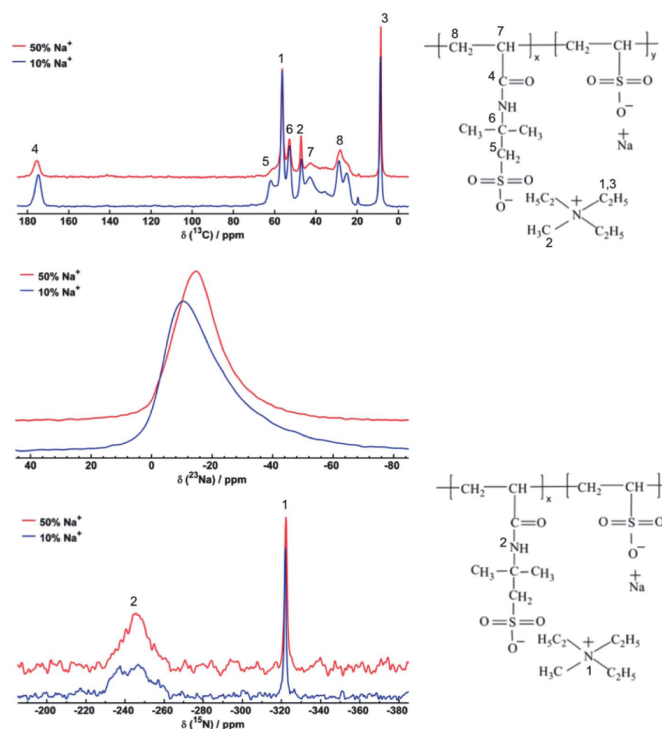


Fig. 7 MAS NMR spectra for ^{13}C , ^{23}Na and ^{15}N (top to bottom) for 10% and 50% Na^+ content.

quaternary carbon, the backbone $-\text{CH}-$, the backbone $-\text{CH}_2-$ and the side chain $-\text{CH}_3$ group, respectively. The assignment was checked with a CPPI experiment as well as *via* diffusion filtered solution NMR experiments and is in accordance with reported literature shifts of PAMPS polymers.³⁶

The ^{23}Na spectra (Fig. 7 middle) both show an asymmetric quadrupolar lineshape which is strongly Gaussian broadened, probably mainly caused by a broad, inhomogeneous distribution of the ^{23}Na chemical environment. It is interesting to note a small shift to lower frequencies for the chemical shift from -5 to -10 ppm with increasing Na^+ content, indicating a small change in the chemical environment (or distribution of environments) of the Na^+ ions. In addition, the ^{15}N CPMAS spectra (Fig. 7 bottom) give two signals that can be assigned to the amide nitrogen (broad due to low mobility and inhomogeneous environment) at -230 to -250 ppm and the quaternary ammonium nitrogen (narrow due to high mobility) at -322 ppm and support the carbon signal assignment. No significant change can be observed in the ^{15}N shifts with increasing Na^+ content.

To study ion dynamics, static wideline ^1H and ^{23}Na spectra at different temperatures were recorded. Assuming a thermally

driven motion process is the main cause for nuclear relaxation, a uniform line narrowing of the static NMR signals with increasing temperature would be expected. By measuring static ^{23}Na spectra the $^{23}\text{Na}^+$ cation dynamic behaviour is probed. It is important to point out that static ^1H spectra include both components, the signals of the more mobile quaternary ammonium cation and the less mobile polymer, thus the ^1H variable temperature experiments are probing a dynamic behaviour consisting of at least two differing components contributing to the relaxation process.

The ^1H wideline spectra (Fig. 8 top) for the 10% Na^+ containing sample show an inhomogeneous line narrowing, with some narrow components already detectable above 303 K. When approaching T_g (~ 373 K) an overall line narrowing can be observed, but when keeping the sample slightly below T_g the signals converge into a more homogeneous shape. The differing line widths indicate the presence of inhomogeneous dynamic behaviour in the sample due to partial phase separation. Such inhomogeneity can be removed by annealing the material slightly below T_g . This is consistent with the single impedance arc observed in the conductivity measurement at higher temperatures. The ^{23}Na wideline spectra (Fig. 8 bottom) show

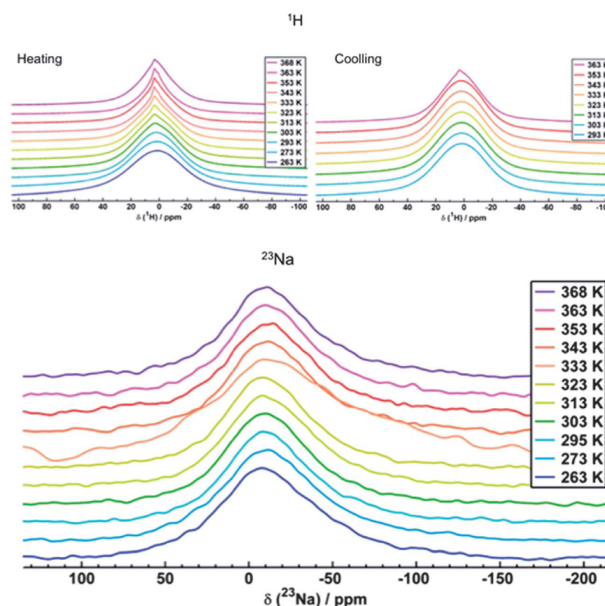


Fig. 8 ^1H (top) and ^{23}Na (bottom) VT Wideline NMR spectra of poly([N_{1222}][AMPS]-co-Na[VS]) (90 : 10) in the temperature range from 263 to 368 K.

no significant line narrowing but suffer from bad S/N due to the low Na^+ content. The ^{23}Na lines here are already relatively narrow for a quadrupolar nucleus and thus suggest some degree of mobility is present. The lack of narrowing with increasing temperature may reflect that the linewidth is dominated by an inhomogeneous and distributed environment for the ^{23}Na nucleus, which is highly probable for a quadrupolar nucleus in a changing asymmetric environment.

The effect of 10% PEG additions into the poly([N_{1222}][AMPS]-co-Na[VS]) (90 : 10) ionomer

Even though the conductivity measured in these materials appears to be decoupled from the T_g of the ionomer itself, the values are still too low for application in practical devices. Furthermore, we are unable to confirm the role of Na^+ in this conduction process. In order to increase the ionic conductivity and possibly decouple the Na^+ still further from the ionomer backbone, a small amount (10 wt%) of low molecular weight plasticizer, polyethylene glycol (PEG 400) was introduced into the ionomer. Fig. S1† represents the DSC thermogram of poly([N_{1222}][AMPS]-co-Na[VS]) (90 : 10) ionomer with 10% PEG. In this sample, a T_g overshoot was not observed in contrast to the sample without PEG. The T_g still appears broad and has decreased by 40 °C to a value of ~50 °C (onset). This indicates that even 10% PEG significantly plasticizes the ionomer,

possibly by interacting with the Na^+ ions as we hypothesized, thereby reducing the coulombic interactions between the cation and the polymer backbone.

The conductivity of the PEG plasticized ionomer was also measured upon both heating and cooling cycles. As can be seen from the Nyquist plot Fig. S2,† only one semicircle can be observed in both cycles. This is consistent with only one conduction process in this system, which suggests that the phase separation may no longer be present. The optical microscopy of these plasticized ionomers (as shown in the insert picture in Fig. 9) further confirms that the addition of PEG leads to a more homogeneous material. Significantly, the conductivity was found to increase by four orders of magnitude at room temperature as shown in Fig. 9 and reaches $10^{-5} \text{ S cm}^{-1}$ at T_g . Therefore this system also shows strong decoupling of the ionic conductivity from the T_g . This increase in conductivity may arise for either higher mobility of the N_{1222}^+ cation, or from the additional contribution of the Na^+ ion. ^{23}Na NMR was used to try to provide further insights into the mobility in these systems as discussed below.

The addition of plasticizer had an observable effect on the ^{23}Na static NMR spectra (see Fig. 10a). Compared to the 10% Na^+ sample the half width increased by nearly a factor 2 from 5 kHz to 8.5 kHz for the 10% PEG sample. Whereas the linewidth for both materials only changes slightly with increasing temperature. Fig. 10b shows the effect of temperature on the

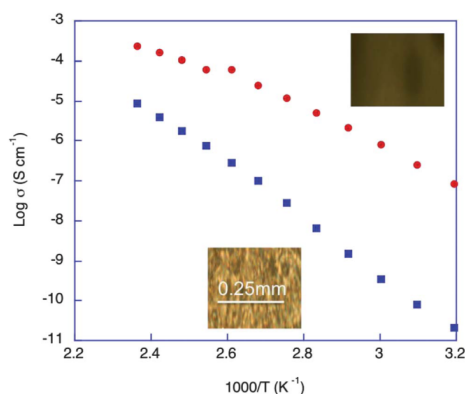


Fig. 9 The ionic conductivity along with the optical images of the poly([N₁₂₂₂][AMPS]-co-Na[VS]) (90 : 10) (blue data) with 10% PEG (red data).

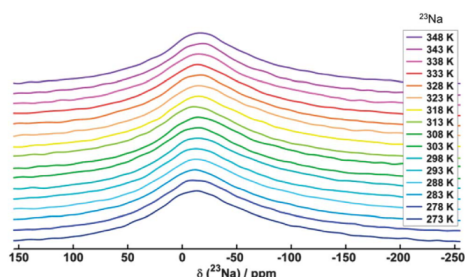


Fig. 10 NMR spectra of ²³Na poly ([N₁₂₂₂][AMPS]-co-Na[VS]) (90 : 10) with 10% PEG.

²³Na chemical shift for the pure and PEG containing ionomer and it is apparent that the addition of PEG changes the overall environment of the Na⁺ ion. The more negative chemical shift could reflect a decreasing interaction with the sulfonate anion and a stronger interaction with the PEG oxygens in the plasticized sample. Furthermore, whilst there is a significant degree of scatter in the data, the overall trend does seem to favour a shift to more negative chemical shifts in both systems, which again may reflect less association with the ionomer backbone. The broader lines for the plasticizer added sample show either a higher distribution of frequencies and thus a broader distribution of chemical environments for the sodium ions, or an even lower T_2 value, which could arise from a rapid exchange between very different environments. This provides evidence that the presence of the PEG plasticizer as well as a competing counter ion in the ionomer, means that the sodium ions are less strongly coordinated to the ionomer backbone and are likely distributed (and possibly exchanging) amongst varying

environments. The minor change in linewidth and shift relative to varying temperature indicates that the plasticizer does not significantly influence the dynamic behavior of the sodium ions but only the distribution width of sodium coordination. This NMR data correlate well with the observations from DSC and conductivity measurements.

Conclusions

The preparation and characterization of a series of sulfonate based copolymer ionomers with mixtures of ionic liquid and sodium cations have been reported. The T_g , ¹⁵N and ²³Na chemical shift of ionomers do not vary significantly as the amount of Na⁺ changes, while the ionic conductivity increased with decreasing Na⁺ composition. The data show that the conductivity is increasingly decoupled from the T_g of the ionomer systems as Na⁺ concentration is decreased. The presence of a broad T_g , asymmetric quadrupolar lineshape of ²³Na in NMR spectra and two semicircles observed in the impedance diagrams suggests two conduction processes are present in these ionomer systems, and indicates inhomogeneity or phase separation in these materials. The optical microscope images confirm the presence of phase separation in all compositions. An ether based plasticizer, PEG, has been introduced into the ionomer to further improve the ionic conductivity and possibly decouple the Na⁺ further from the ionomer backbone. The reduction in T_g and increasing of ionic conductivity shows that even 10% of PEG significantly plasticized the ionomer and increased the conductivity by several orders of magnitude. Furthermore, the impedance and optical microscopy data suggests that the addition of PEG, also leads to a more homogeneous material.

Acknowledgements

The authors are grateful to the Australian Research Council for funding via DP130101652 and under the Laureate Fellowship scheme (MF and DRM). We also acknowledge the ARC for support of the NMR facility through the grant LE110100141.

References

- 1 D. E. Fenton, J. M. Parker and P. V. Wright, *Polymer*, 1973, **14**, 589.
- 2 S. Lascaud, M. Perrier, M. Armand, J. Prud'homme, B. Kapfer, A. Vallée and M. Gauthier, *Electrochim. Acta*, 1998, **43**, 1407–1414.
- 3 D. Benrabah, S. Sylla, F. Alloin, J. Y. Sanchez and M. Armand, *Electrochim. Acta*, 1995, **40**, 2259–2264.
- 4 F. M. Gray, *Solid polymer electrolytes: fundamentals and technological applications*, New York, NY, VCH, New York, NY, 1991.
- 5 S. H. Chung, Y. Wang, L. Persi, F. Croce, S. G. Greenbaum, B. Scrosati and E. Plichta, *J. Power Sources*, 2001, **97–98**, 644–648.
- 6 B. Scrosati, F. Croce and S. Panero, *J. Power Sources*, 2001, **100**, 93–100.

- 7 M. Marcinek, A. Bac, P. Lipka, A. Zalewska, G. Zukowska, R. Borkowska and W. Wieczorek, *J. Phys. Chem. B*, 2000, **104**, 11088–11093.
- 8 W. Wieczorek, D. Raducha, A. Zalewska and J. R. Stevens, *J. Phys. Chem. B*, 1998, **102**, 8725–8731.
- 9 S. R. Mohapatra, A. K. Thakur and R. N. P. Choudhary, *Ionics*, 2008, **14**, 255–262.
- 10 W. Wang, W. Liu, G. J. Tudryn, R. H. Colby and K. I. Winey, *Macromolecules*, 2010, **43**, 4223–4229.
- 11 C. Tiyaipoonchaiya, J. M. Pringle, D. R. MacFarlane, M. Forsyth and J. Z. Sun, *Macromol. Chem. Phys.*, 2003, **204**, 2147–2154.
- 12 H. I. Ünal and H. Yilmaz, *J. Appl. Polym. Sci.*, 2002, **86**, 1106–1112.
- 13 M. Annala, S. Lipponen, T. Kallio and J. Seppälä, *J. Appl. Polym. Sci.*, 2012, **124**, 1511–1519.
- 14 H. Hu, W. Liu, L. Yang, M. Xiao, S. Wang, D. Han and Y. Meng, *Int. J. Hydrogen Energy*, 2012, **37**, 4553–4562.
- 15 A. A. Santiago, J. Vargas, J. Cruz-Gómez, M. A. Tlenkopatchev, R. Gaviño, M. López-González and E. Riande, *Polymer*, 2011, **52**, 4208–4220.
- 16 L. Sun, J. Guo, J. Zhou, Q. Xu, D. Chu and R. Chen, *J. Power Sources*, 2012, **202**, 70–77.
- 17 G. J. Tudryn, M. V. O'Reilly, S. Dou, D. R. King, K. I. Winey, J. Runt and R. H. Colby, *Macromolecules*, 2012, **45**, 3962–3973.
- 18 C. Tiyaipoonchaiya, D. R. MacFarlane, J. Sun and M. Forsyth, *Macromol. Chem. Phys.*, 2002, **203**, 1906–1911.
- 19 N. Byrne, P. C. Howlett, D. R. MacFarlane and M. Forsyth, *Adv. Mater.*, 2005, **17**, 2497–2501.
- 20 J. Travas-Sejdic, R. Steiner, J. Desilvestro and P. Pickering, *Electrochim. Acta*, 2001, **46**, 1461–1466.
- 21 M. J. Park and S. Y. Kim, *J. Polym. Sci., Part B: Polym. Phys.*, 2013, **51**, 481–493.
- 22 P. G. Bekiarian, M. Doyle, W. B. Farnham, A. E. Feiring, P. A. Morken, M. G. Roelofs and W. J. Marshall, *J. Fluorine Chem.*, 2004, **125**, 1187–1204.
- 23 W. Wang, G. J. Tudryn, R. H. Colby and K. I. Winey, *J. Am. Chem. Soc.*, 2011, **133**, 10826–10831.
- 24 G. J. Tudryn, W. Liu, S. W. Wang and R. H. Colby, *Macromolecules*, 2011, **44**, 3572–3582.
- 25 A. S. Best, P. J. Newman, D. R. MacFarlane, K. M. Nairn, S. Wong and M. Forsyth, *Solid State Ionics*, 1999, **126**, 191–196.
- 26 H. Morimoto, H. Awano, J. Terashima, Y. Shindo, S. Nakanishi, N. Ito, K. Ishikawa and S. I. Tobishima, *J. Power Sources*, 2013, **240**, 636–643.
- 27 J. L. Sudworth, *J. Power Sources*, 1984, **11**, 143–154.
- 28 J. Coetzer, *J. Power Sources*, 1986, **18**, 377–380.
- 29 A. R. Berens and I. M. Hodge, *Macromolecules*, 1982, **15**, 756–761.
- 30 I. M. Hodge and A. R. Berens, *Macromolecules*, 1982, **15**, 762–770.
- 31 Z. J. Zhang, Z. Y. Lu and Z. S. Li, *Chin. J. Polym. Sci.*, 2009, **27**, 493–500.
- 32 L. Leibler, *Macromolecules*, 1980, **13**, 1602–1617.
- 33 C. L. McCormick and C. B. Johnson, *Macromolecules*, 1988, **21**, 694–699.
- 34 C. L. McCormick and L. C. Salazar, *Macromolecules*, 1992, **25**, 1896–1900.
- 35 Z. Tong, Y. Yi and X. Liu, *Polym. Bull.*, 1995, **35**, 591–597.
- 36 P. Shestakova, R. Willem and E. Vassileva, *Chem.-Eur. J.*, 2011, **17**, 14867–14877.

4.4 Supporting Information

Supporting Information to accompany:

**Ion conduction and phase morphology in sulfonate
copolymer ionomers based on ionic liquid-sodium cation
mixtures**

S.A.M.Noor,^{a,b} D.Gunzelmann,^d J. Sun,^a D.R. MacFarlane,^{a,c} M. Forsyth,^{c,d*}

^a *School of Chemistry, Monash University, Clayton Campus, Victoria, Australia*

^b *Chemistry Department, Centre for Defence Foundation Studies, National Defence*

University of Malaysia, 57000, Kuala Lumpur, Malaysia

^c *ARC Centre of Excellence for Electromaterials Science (ACES) Australia*

^d *Institute for Frontier Materials Deakin University, Victoria, Australia*

^{*} *Corresponding Author:*

[REDACTED]

[REDACTED]

Supporting Information

Ion Conduction and phase morphology in sulfonate copolymer ionomers based on ionic liquid - sodium cation mixtures.

Siti Aminah Mohd Noor,^{a,b} Daniel Gunzelmann,^d Jiazeng Sun,^a Douglas R MacFarlane^{a,c} and Maria Forsyth,^{c,d*}

^a School of Chemistry, Monash University, Clayton Campus, Victoria, Australia

^b Chemistry Department, Centre for Defence Foundation Studies, National Defence University of Malaysia, 57000, Kuala Lumpur, Malaysia

^c ARC Centre of Excellence for Electromaterials Science (ACES)

^d Institute for Frontier Materials Deakin University, Victoria, Australia

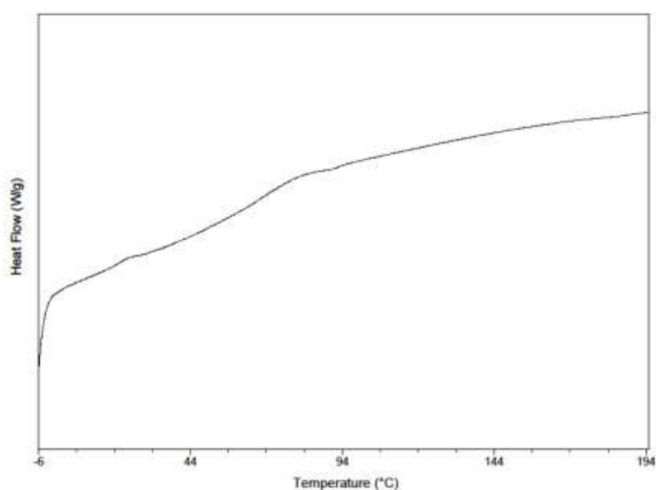


Fig. S1 DSC thermogram of poly ([N₁₂₂₂][AMPS]-co-Na[VS]) (90:10) ionomer with 10% PEG

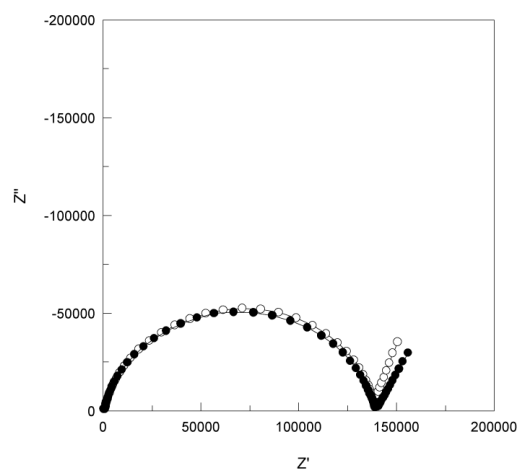


Fig. S2 Impedance plane plot of poly ([N₁₂₂₂][AMPS]-co-Na[VS]) (90:10) ionomer with 10% PEG

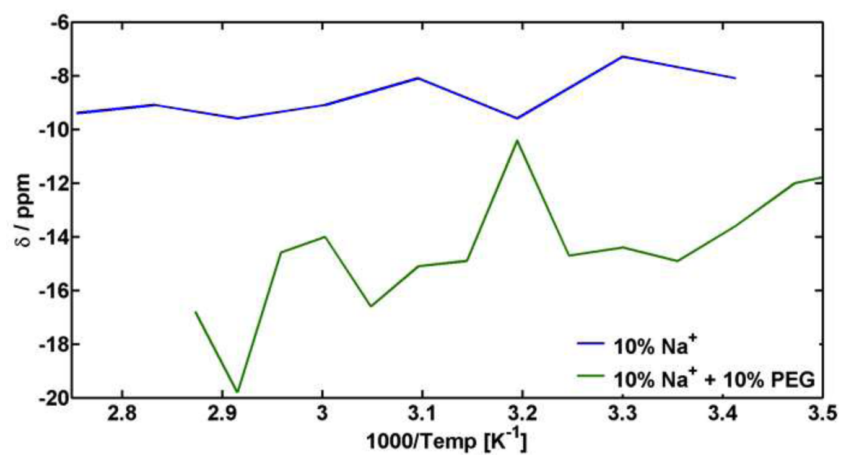


Fig. S3 Comparison of the position of the intensity maximum for 10% Na⁺ and 10% PEG addition

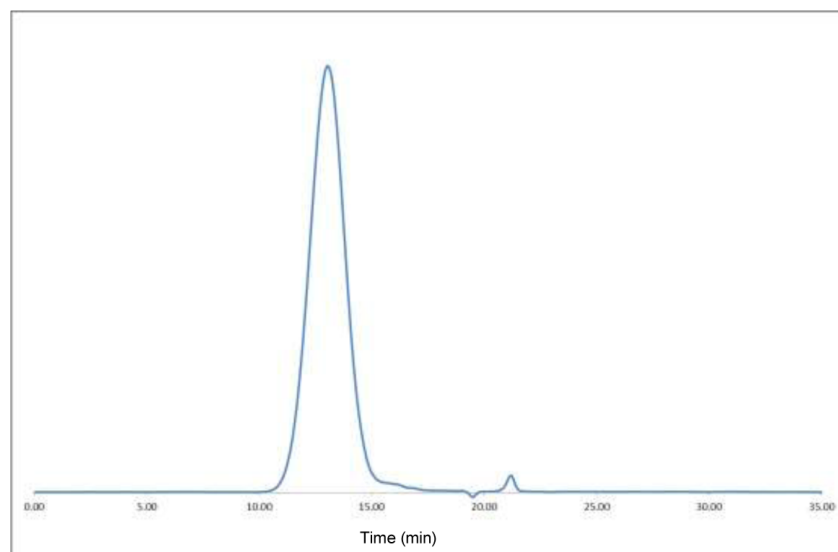


Fig. S4 Gel Permeation Chromatography of poly ([N₁₂₂₂][AMPS]-co-Na[VS]) (50:50). Note that the small peak is solvent peak.

Table S1 Molecular weight and polydispersity index of poly ([N₁₂₂₂][AMPS]-co-Na[VS]) with various composition of Na⁺

Sample (%Na ⁺)	Mn (g/mol)	PDI
50	19905	2.599
20	24928	2.559
10	24750	2.589

4.5 Specific Declaration

PART B: Suggested Declaration for Thesis Chapter

Monash University

Declaration for Thesis Chapter 4.6

Declaration by candidate

In the case of Chapter 4.6, the nature and extent of my contribution to the work was the following:

Nature of contribution	Extent of contribution (%)
Initiation, key ideas, performed the experiments, synthesis, data analysis and interpretation, manuscript development and writing up	90

The following co-authors contributed to the work. If co-authors are students at Monash University, the extent of their contribution in percentage terms must be stated:

Name	Nature of contribution	Extent of contribution (%) for student co-authors only
Douglas MacFarlane	Key ideas, proof reading and final drafting	-
Maria Forsyth	Key ideas, proof reading and final drafting	-
Daniel Gunzelmann	NMR characterisation and discussions	-
Jiazeng Sun	Synthesis the ionomers	-
Michel Armand	Synthesis the ionic liquid	-

The undersigned hereby certify that the above declaration correctly reflects the nature and extent of the candidate's and co-authors' contributions to this work*.

**Candidate's
Signature**

	Date 17/7/2014
--	--------------------------

**Main
Supervisor's
Signature**

	Date 17/7/2014
---	--------------------------

*Note: Where the responsible author is not the candidate's main supervisor, the main supervisor should consult with the responsible author to agree on the respective contributions of the authors.

4.6 Publication 5

Decoupled ion conduction in poly(2-acrylamido 2methyl-1-propane-sulfonic acid) (PAMPS) homopolymers

Siti Aminah Mohd Noor,^{a,b} Jiazeng Sun,^a Douglas R MacFarlane^{a,c}, M. Armand^d, D. Gunzelmann^e and Maria Forsyth,^{c,e}

^a *School of Chemistry, Monash University, Clayton Campus, Victoria, Australia*

^b *Chemistry Department, Centre for Defence Foundation Studies, National Defence University of Malaysia, 57000, Kuala Lumpur, Malaysia*

^c *ARC Centre of Excellence for Electromaterials Science (ACES)*

^d *CIC Energigune, Vitoria, Spain*

^e *Institute for Frontier Materials Deakin University, Victoria, Australia*

* Corresponding Author: * Email: [REDACTED]
[REDACTED]
[REDACTED]

Submitted to *Polymer*

June, 2014

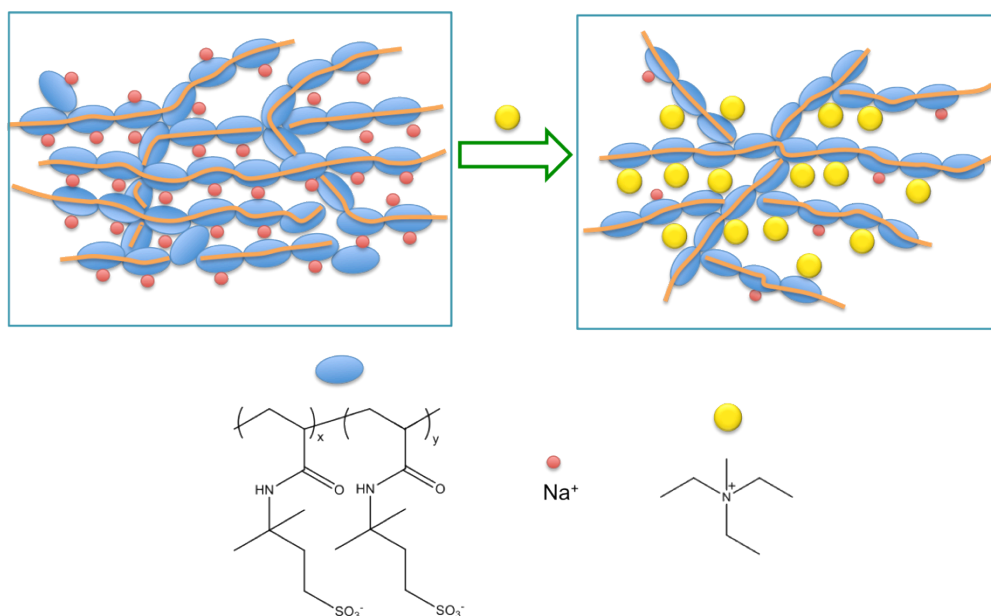
Graphical Abstract

Decoupled ion conduction in poly(2-acrylamido 2methyl-1-propane-sulfonic acid) (PAMPS) homopolymers

Siti Aminah Mohd Noor,^{a,b} Jiazeng Sun,^a Douglas R MacFarlane^{a,c}, M.

Armand^d, D. Gunzelmann^e and Maria Forsyth,^{c,e}

A family of novel sulfonate based homopolymers has been prepared by partially replacing sodium cations with different types of ionic liquid ammonium counter-cations, which are hypothesized to increase the degree of decoupling from local segmental motions of the ionomers and thereby improve ionic conductivity.



Decoupled ion conduction in poly(2-acrylamido 2methyl-1-propane-sulfonic acid) (PAMPS) homopolymers

Siti Aminah Mohd Noor,^{a,b} Jiazeng Sun,^a Douglas R MacFarlane^{a,c}, M. Armand^d, D. Gunzelmann^e and Maria Forsyth,^{c,e}

^a School of Chemistry, Monash University, Clayton Campus, Victoria, Australia

^b Chemistry Department, Centre for Defence Foundation Studies, National Defence University of Malaysia, 57000, Kuala Lumpur, Malaysia

^c ARC Centre of Excellence for Electromaterials Science (ACES)

^d CIC Energigune, Vitoria, Spain

^e Institute for Frontier Materials Deakin University, Victoria, Australia

* Corresponding Author: *Email: [REDACTED]
[REDACTED]

ABSTRACT

As the focus on developing new polymer electrolytes continues to intensify in the area of alternative energy conversion and storage devices, the rational design of polyelectrolytes with high single ion transport rates has emerged as a primary strategy for enhancing device performance. Previously, we reported a series of sulfonate based copolymer ionomers based on combining quaternary ammonium ionic liquid cations and sodium cations. By mixing the two cations in a copolymer based ionomer system, improvements in the conductivity were observed and the conductivity appeared increasingly decoupled from the T_g of the ionomer. In this article, we study the effect of different types of ammonium counter-cations on the

conductivity of ionomers in a homopolymer system. We observe a decreasing T_g with increasing the bulkiness of the quaternary ammonium cation, and an increasing degree of decoupling from T_g within these systems. Somewhat surprisingly, phase separation is observed, as evidenced from multiple impedance arcs, raman mapping and SEM. The thermal properties, morphology and the effect of plasticizer on the transport properties in these ionomers are also presented. The addition of 10 wt.% plasticizer increased the ionic conductivity between two and three orders of magnitudes

Keywords: single ion conductor, ionomer, conductivity, sodium ion, decoupling

INTRODUCTION

The electrolyte is a key component of an electrochemical device, since it serves as the medium for ionic transport, and thus much research has been expended on improving the performance, safety and cost of electrolytes¹⁻⁵. One way to improve the safety of a device, such as a battery, is to develop a solid state electrolyte with appropriate target ion transport properties. In this respect, solid polymer electrolytes (SPEs) have been investigated since the late 1970s⁶. The use of a SPE in a power source leads to improvements in performance by providing mechanical stability (flexibility and moldability), reduced weight, and operational safety (no leakage of corrosive materials and zero volatility/flammability)^{4, 7-9}.

SPEs based on polyethers have been extensively studied for applications in Lithium batteries¹⁰⁻¹², however, their performance is limited by the fact that the cation transport number (eg. Li^+) is significantly less than 0.5 and thus anion aggregation occurs at the electrode interface; this eventually leads to concentration polarization of the electrode¹³⁻¹⁶. To overcome this polarization, one needs to ensure that the cation transport number is as close to unity as possible. One way to do this is to tether the anionic species covalently to the polymer backbone or an attached pendant group^{10, 17-19}. This allows the counter-cation to be the sole charge carrier. Such polyelectrolyte systems are often referred to as ionomers.

Numerous single-ion conducting ionomer systems have been developed^{10, 20-22}; yet these systems display ionic conductivities far lower than their polymer/salt mixture counterparts. Various techniques have been employed to increase the ionic conductivity of these materials, such as incorporation of an organic solvent or ionic liquid^{10, 12, 23, 24} to assist the cation dissociation from the polymer backbone. Even though these materials provide high ionic conductivity as well as good elastomeric properties, the existence of a low molecular weight solvent leaves the possibility that the electrolytes may leak or be volatile.

Very recently, we reported the development of solvent free solid ionomer electrolytes based on the copolymer poly([triethylmethylammonium][2-acrylamido-2-methyl-1-propane-sulfonic acid]-co-sodium[vinyl sulfonate], poly([N₁₂₂₂][AMPS]-co-Na[VS]), where a fraction of sodium ions were replaced

with a bulky, ionic liquid forming, quaternary ammonium cation¹⁹. This is designed to create anion centers on the polymer that are less associated with a cation and therefore that the metal cation motion may be less coupled to the bulk dynamics of the ionomer. We found that significant ionic conductivity was measurable below T_g in these systems, indicating an increasingly decoupled ion transport mechanism from the ionomer's backbone motions and structural relaxations (which are responsible for the glass transition temperature, T_g) as the ratio of the sodium to quaternary ammonium cation decreased.

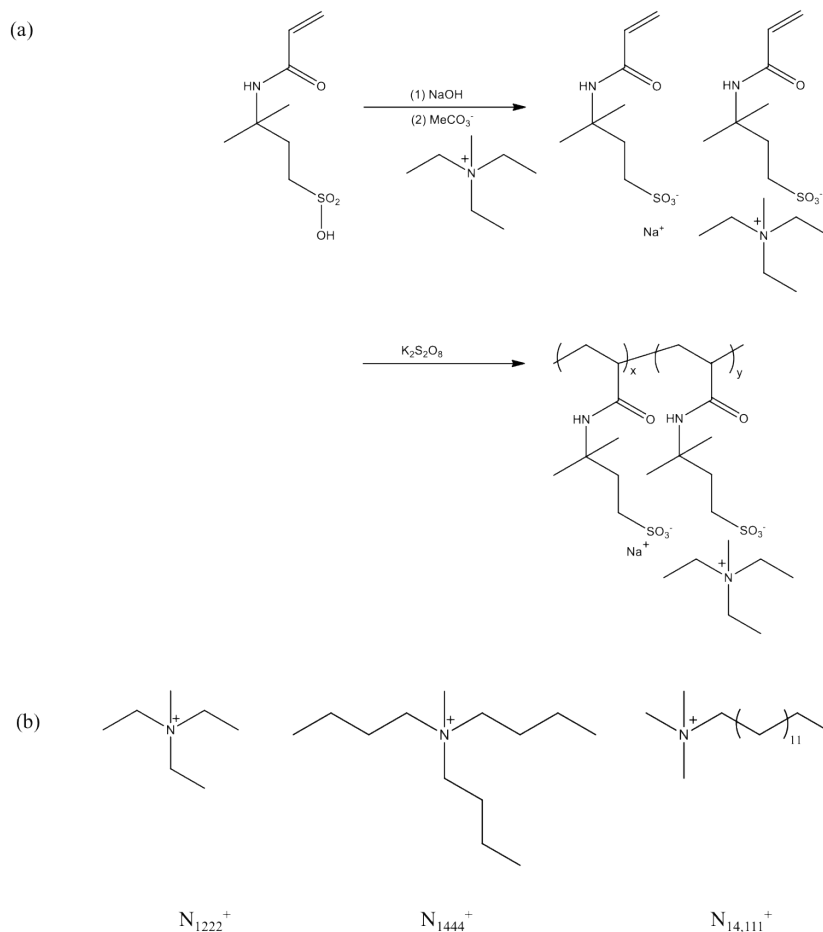
This remarkable finding has prompted us to study the effect of different types of ammonium cation on the conductivity of ionomers and also the differences between homopolymer and copolymer ionomer systems. In this paper, we prepare three different ammonium-based homopolymer ionomers (where the alkyl chain length on the counterion is modified) and also a series of ionomers containing the triethylmethyammonium (N_{1222}) cation and different amounts of Na^+ ($poly(N_{xyyy})_zNa_{1-z}[AMPS]$). This system can be compared with the copolymer ionomer system previously reported by us. These samples are characterized using DSC to determine the glass transition and a.c. impedance spectroscopy to measure ionic conductivity, while solid state NMR was performed to study the dynamic behavior of the ionomers. Raman Spectroscopy and SEM have also been used to observe the ionomer morphology.

EXPERIMENTAL

Sample preparation

Preparation of poly(2-acrylamido-2-methyl-1-propane-sulfonic acid) (PAMPS) (alkyl-ammonium/sodium salts) was carried out based on Scheme 1.

1. Typical procedures for synthesis of a PAMPS sample are as follows: 5.017 g of AMPS (0.0241 mol, Aldrich) was dissolved in 10ml of distilled water; to form the sodium salt, NaOH-water solution containing 0.01205 mol of NaOH was added drop-wise at room temperature with magnetic stirring until the pH value of the solution reached ~ 7 . In the same way a certain amount of the tetraalkyl ammonium-carbonate solution (Aldrich) was added to the AMPS solution to form the tetraalkyl ammonium salt. $\sim 0.2\%$ (w/w) $K_2S_2O_8$ was then added and the solution was stirred at $\sim 85^\circ C$ for 2 days. After removing the solvents from the polymer/co-polymer solutions all the prepared samples were dried under vacuum at $\sim 70^\circ C$ for at least 2 days before any characterisation was undertaken. Two types of plasticizer have been used in this system; these are tetraglyme (tetraethylene glycol dimethyl ether (purum, $\geq 99.0\%$ (GC), Fluka)) and N,N-dimethyl-3-methoxypropylammonium bis(fluorosulfonyl)imide ($N_{22}(3O)_2FSI$) which was prepared as reported elsewhere²⁵⁻²⁷.



Scheme 1 (a) Schematic preparation of $(\text{poly}(N_{1222})_z\text{Na}_{1-z}[\text{AMPS}])$. ionomers (b) cationic counterion structures: triethylmethylammonium (N_{1222}^{+}), tributylmethylammonium (N_{1444}^{+}) and trimethyltetradecylammonium ($N_{14,111}^{+}$)

Ionic Conductivity

The ionic conductivity of the ionomers was measured by ac impedance spectroscopy using a high frequency response analyzer (HFRA; Solartron 1296). The powder samples were first pressed into pellets (1 mm thick and 13 mm in diameter) using a KBr die and a hydraulic press at 10 tonne for 30 min; pellets were pressed and aged in the oven at 443 K overnight; pressed pellets were coated

with gold using a gold sputter coater (SPI-Module Sputter Coater - Division of Structure Probe Inc. with plasma uses argon gas) at plasma current of about 20 mA (DC) for 2 minutes and then sandwiched between two stainless steel blocking electrodes. Data was collected over a frequency range of 0.1 Hz to 10 MHz (ten points per decade) with a 30 mV amplitude over a temperature range of 298 to 443 K in 10 K intervals. The temperature was controlled to within 1 K using a Eurotherm 2204e temperature controller and a band heater with a cavity for the cell using a thermocouple type T, which was embedded in the cell. The sample was held for a short equilibration time, up to 2 minutes, to stabilize the temperature prior to impedance measurement. The conductance was determined from the impedance data using the series circuit in Z-view (Version 2.3).

Differential Scanning Calorimetry (DSC)

DSC measurements were carried out on the as-prepared samples, using a DSC Q100 series instrument (TA Instruments), and the data was evaluated with Universal Analysis 2000 software. Approximately 8 to 10 mg of the ionomer sample was hermetically sealed in Aluminium pans and measured over a temperature range of 273 to 423 K at a scanning rate of 10 K.min⁻¹. The glass transition temperature was determined from the onset of the heat-capacity change during the heating ramp.

Solid-state nuclear magnetic resonance (NMR)

Solid-State NMR spectra were recorded with a BRUKER Avance III 300WB

spectrometer operating at 300.13, 79.39, 125.76 and 30.42 MHz for ^1H , ^{23}Na , ^{13}C and ^{15}N , respectively. All ^1H and ^{13}C spectra are given relative to tetramethylsilane, ^{15}N spectra with respect to nitromethane and ^{23}Na spectra were referenced to 1M $\text{NaCl}_{(\text{aq})}$. Samples were packed in standard 4mm MAS rotors, loaded and measured in a 4 mm double-resonance MAS probe (BRUKER) spinning at 10 kHz. Cross-Polarization from ^1H was used to excite ^{13}C and ^{15}N nuclei applying a ramped (50 to 100% power) shape pulse on the proton frequency with a contact time of 2 and 10 ms, respectively. A SPINAL64 high power proton decoupling with a nutation frequency of 114 kHz was applied during acquisition. Recycle delays were set between 3-5 times the proton T_1 relaxation constants, which were determined earlier. Static ^1H and ^{23}Na spectra were measured with a solid-echo sequence using a 2.5 μs , 90 degree pulse and an echo delay of 20 μs .

Raman Spectroscopy

For Raman mapping measurements, a confocal Raman system, Witec 300R, based on an integral Olympus BX40 microscope with a 50x objective (8 mm) was used. The spatial resolution was about 2 μm . The calibration was undertaken referring to the 520.5 cm^{-1} line of silicon. A 785 nm laser source was used for excitation. The collection time for each spectrum was 1 s with one accumulation. The spectrometer grating had 80 points/line. An automatic motorized translator X – Y stage was used to perform Raman mapping.

Raman images were recorded by first positioning the ionomer sample in the laser focus using a video camera and white-light illumination, followed by scanning over the mapping region (selected as $250 \times 250 \mu\text{m}^2$ in step sizes of $3 \mu\text{m}$) and accumulating a full spectrum at each pixel. A total of 6400 Raman spectra (250×250 probe spots) were measured for each sample. Witec Project processing software was used to operate the mapping system, record the spectra and process the data.

Scanning Electron Microscopy (SEM)

SEM images were collected using a Phillips XL20 SEM with an Oxford X-Max 50 mm^2 silicon drift detector. The accelerating voltage used was 5kV

RESULTS AND DISCUSSION

1. Effect of ammonium cation alkyl chain length in the homopolymer of (poly(N_{xyyy}) $_{0.5}$ Na $_{0.5}$ [AMPS])

Thermal properties

Fig. 1 shows the DSC thermograms of the sodium homopolymer systems at a cation ratio of 50:50 (poly(N_{xyyy}) $_{0.5}$ Na $_{0.5}$ [AMPS]) , with three different quaternary ammonium cations. It can be seen that N_{1444}^+ containing system has a lower T_g compared to the N_{1222}^+ system. This is expected since the aliphatic chains in N_{1444}^+ are bigger and bulkier than the ethyl groups on the N_{1222}^+ cation, which lead to lower inter- and intra-chain ionic interactions. Although it is well known that T_g increases with ion content due to the presence of physical cross-links, this effect is

notably reduced with larger counterions^{28,29, 30}. Tudyryn et al. reported that²⁹, with constant ion content, their polyester-sulfonate ionomers showed T_g decreasing as counterion size increases. They suggest that this is caused by two factors^{30, 31} (i) larger counterions associate less with the backbone anions, forming fewer and weaker physical cross-links that then leads to a decrease in T_g for ionomers (ii) larger counterions act as plasticizers, further lowering T_g .

However, $N_{14,111}^+$ possesses the highest T_g , among the ionomers prepared in this work, despite having the longest aliphatic chain. This may be due to there only being one long aliphatic chain on the nitrogen atom along with the three methyl groups, which makes the cation effectively less bulky compared to N_{1444} and thus the charge on the nitrogen in the $N_{14,111}^+$ cation may be less sterically shielded, leading to stronger ionic interaction with the polymer anionic groups. This finding is similar to the behavior reported by Weiss et al.³² where they investigated ionic interactions in sulfonated polystyrene ionomers by use of alkyl-substituted ammonium counterions. They found that the relative degree of ionic interaction in their materials can be summarized as follows: $NH_4^+ > BuNH_3^+ > Me_3NH^+ > Bu_2NH_2^+ \sim Bu_4N^+ > Bu_3NH^+ \sim PS$, where $Bu = C_4H_9$ and $Me = CH_3$. The ionic interaction of $BuNH_3$ is stronger than Me_3NH even though the alkyl chain in $BuNH_3$ is larger. They also suggested that more significant decreases in the interactions are achieved by substituting alkyl groups for hydrogen atoms on the ammonium ion.

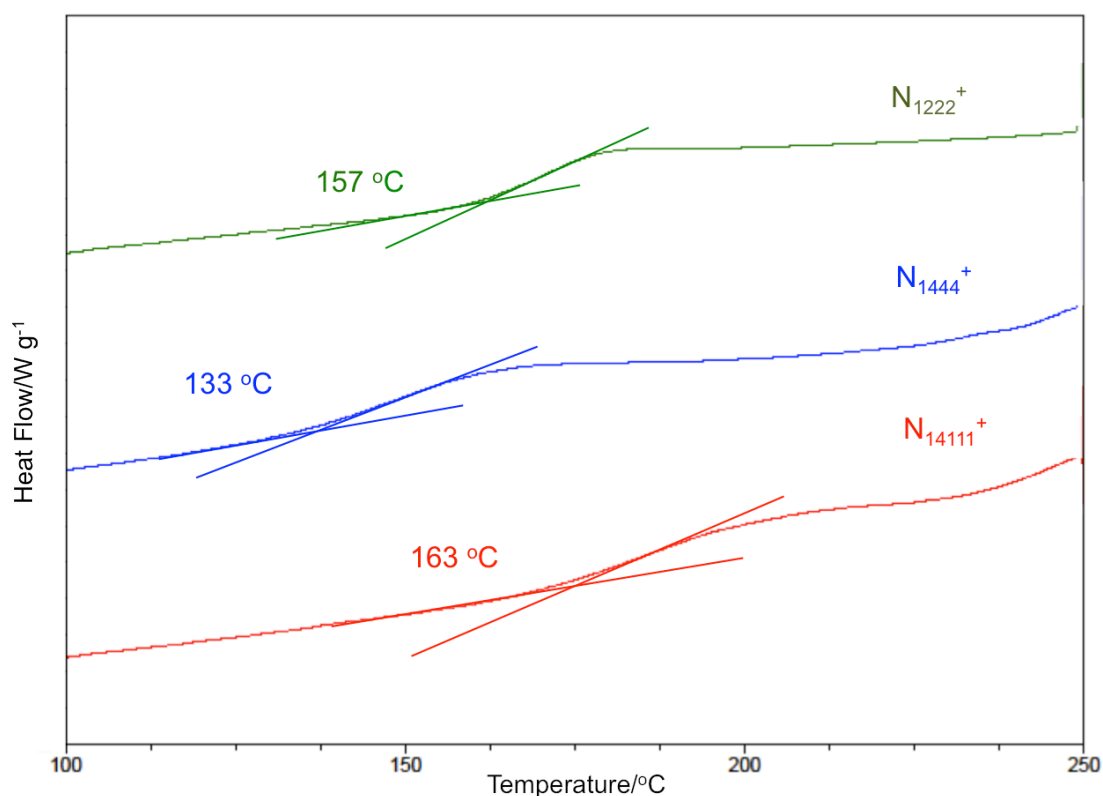


Fig. 1 DSC thermograms of (Poly(N_{xyyy}) $_{0.5}$ Na $_{0.5}$ [AMPS]) ionomers with different types of quaternary cation where x and y reflect different length alkyl chains on the Nitrogen atom.

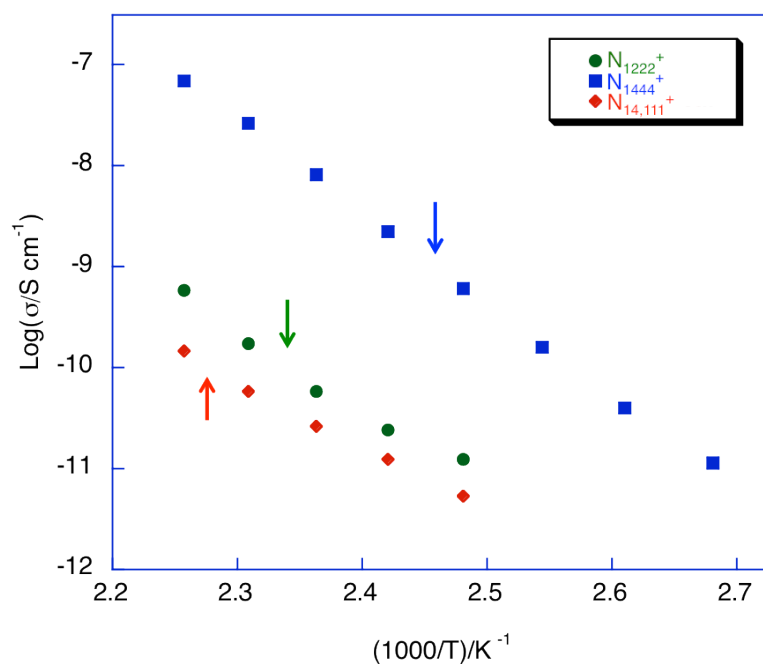
Ionic Conductivity

Fig. 2(a) presents the Arrhenius Plot of ionic conductivity for the (poly(N_{xyyy}) $_{0.5}$ Na $_{0.5}$ [AMPS]) with three different tetraalkyl ammonium cations; the arrow indicates the T_g region of each ionomer. As noted in the trends in T_g discussed above, the polymer chain dynamics (ie. local segmental motions) are more facile in the N_{1444}^+ ionomer, and this seems to result in the highest conductivity amongst the ionomers investigated. In all cases the ionic conductivity follows an Arrhenius behavior, indicating a thermally activated conduction process that persists even below T_g . There is a significant measurable conductivity

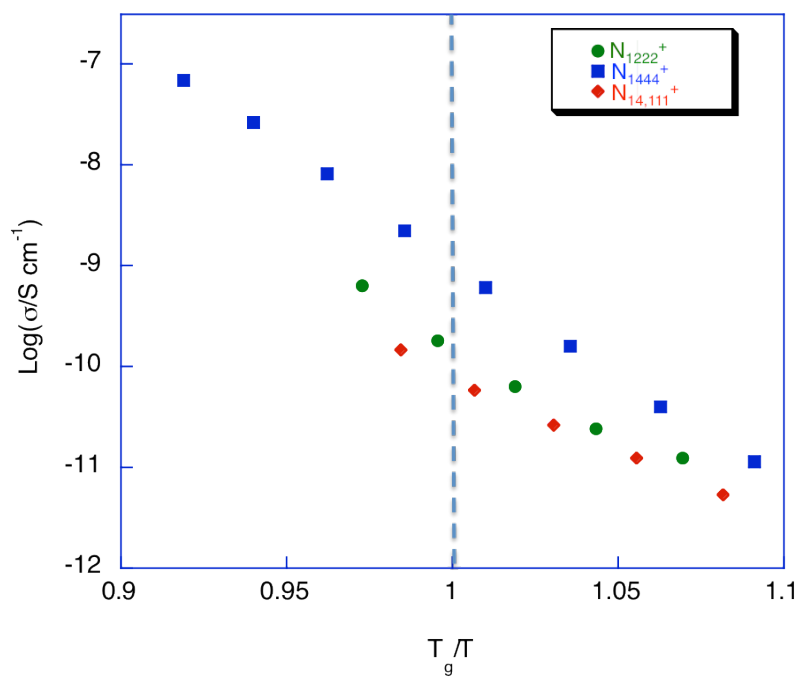
below T_g in all ionomers, indicating decoupling of ionic conductivity from the local segmental motions that govern the T_g of the ionomers. In order to confirm this, we plot Log conductivity versus the reduced temperature T_g/T in Fig. 2(b). Sokolov et al. investigated the decoupling of ion transport from polymer segmental motion. In their work, they showed that as temperature approached T_g , the ionic conductivity is shows a higher and more flexible backbone approached $<10^{-12} \text{ S.cm}^{-1}$. This is typically, which is expected when conductivity ia coupled to the glass transition temperature of the polymer. In our case, the conductivity is up to three orders magnitude higher than this at T_g , therefore indicating an increasing decpouling of ion transport for the N_{1444}^+ mixed cation system. From this representation of the data, we can directly observe that the ionic conduction does not solely rely on the segmental motion of the ionomer backbone, but is increasingly decoupled (higher conductivity at any reduced temperature) as the alkyl chains in the ammonium cation become more bulky. The idea of decoupling will be discussed in more detail when the ratio of cations is varies in the PAMPS homopolymer system.

This finding correlates well with our previous work¹⁹ in a sulfonate copolymer ionomer system, which showed that the ionic conduction was increasingly decoupled from T_g , particularly for compositions containing less than 50% Na. Thus it is again apparent that mixing two cations (ie. Na^+ and a quaternary ammonium cation) in an ionomer system leads to favorable properties for conductivity in terms of decoupling of the conductivity from the segmental

motions, in contrast to the findings when a single counterion is present (e.g. either only Na or only a bulky organic cation), as reported elsewhere^{18, 29, 33}. The dependences of both conductivity and T_g on the chemical structure of the quaternary ammonium cation are shown in Fig. 3, which presents the measured conductivity at 423K together with the T_g for each ionomer.



(a)



(b)

Fig. 2 (a) Arrhenius conductivity plot of $(\text{Poly}(\text{N}_{\text{xyyy}})_{0.5}\text{Na}_{0.5}[\text{AMPS}])$ ionomers with different types of quaternary ammonium cation. The arrows represent T_g in each system (b) ionic conductivity of the ionomers as a function of quaternary ammonium cation with the inverse temperature normalized by T_g for each polymer (bottom).

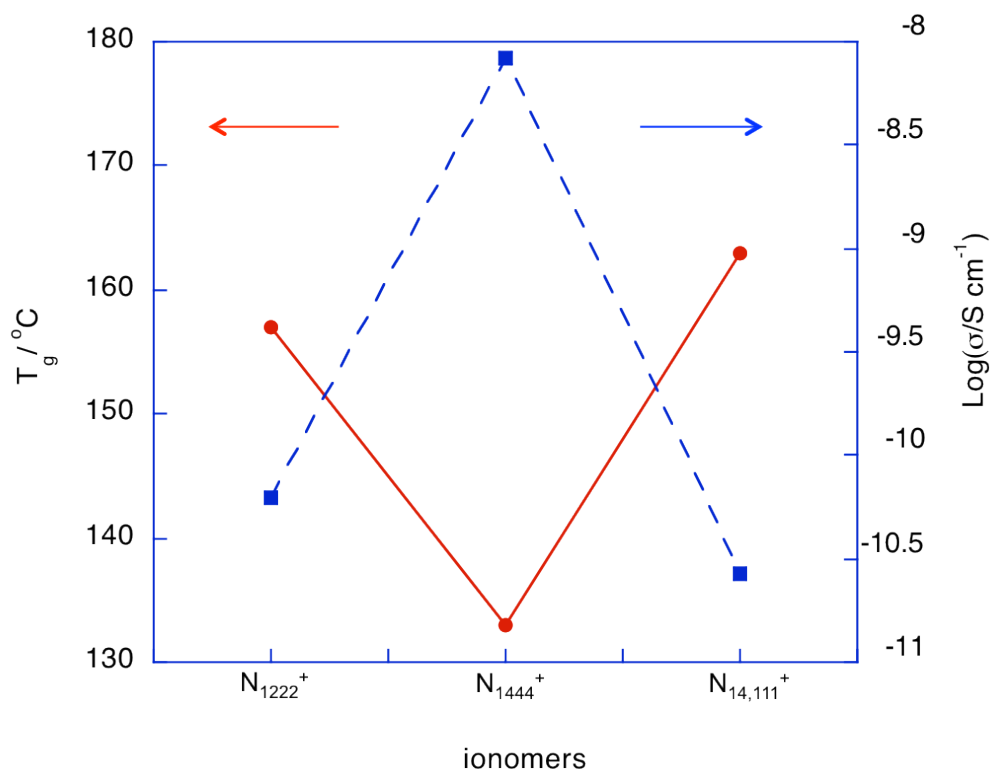


Fig. 3 Ionic conductivity at 423K and the glass transition temperature (T_g) of (Poly(N_{xyyy}) $_{0.5}\text{Na}_{0.5}[\text{AMPS}]$) ionomers as a function of tetraalkylammonium cation

NMR Characterisation

Solid-state NMR was used to characterize the ionomers and further study the dynamic behavior of the materials on a molecular level. The carbon spectra (Fig 4a) show the broad signals of the polymer backbone and narrow signals of the alkyl ammonium cations, indicating a higher mobility of the cations relative to the polymer chains. The signal assignment is as reported previously^{19, 34}. The higher mobility of these species can also be seen in the narrow ^{15}N signals (Fig 4b) of the ammonium cations. The line width of the N_{1444} signal at -321 ppm of 47 Hz is slightly larger than the line width of N_{1222} (37 Hz) and $\text{N}_{14,111}$ (36 Hz). This indicates a slightly lower mobility of the more bulky N_{1444} compared to the other

ammonium ions used and may be due to the larger, bulkier cation size in this case. The position of the ^{15}N chemical shift is also indicative of the changing electron density around the nitrogen center in these quaternary ammonium cations, which is dependent on the nature of the attached alkyl chains. As with the copolymer systems we recently reported, the sodium spectra (Fig 4c) of all samples are all quite similar and show a featureless, broad lineshape. Somewhat counter-intuitive to the Tg and conductivity data presented in Figure 3, the N1444 sample has a slightly broader lineshape.

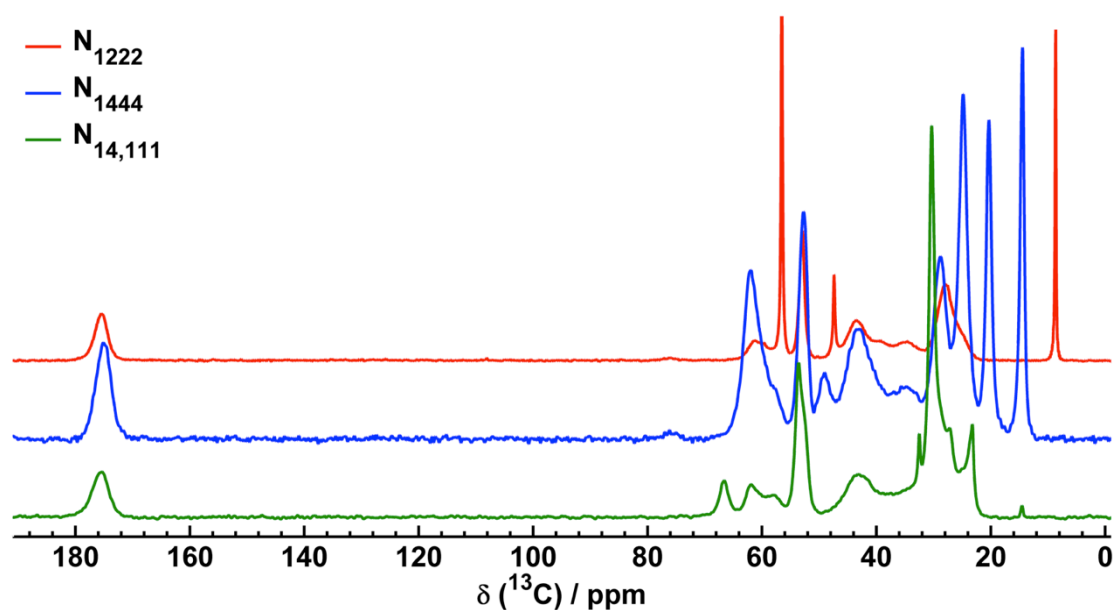


Fig. 4a ^{13}C CPMAS spectra of the ionomers containing different ammonium ions. Spectra were recorded at room temperature and 10 kHz magic angle spinning (MAS).

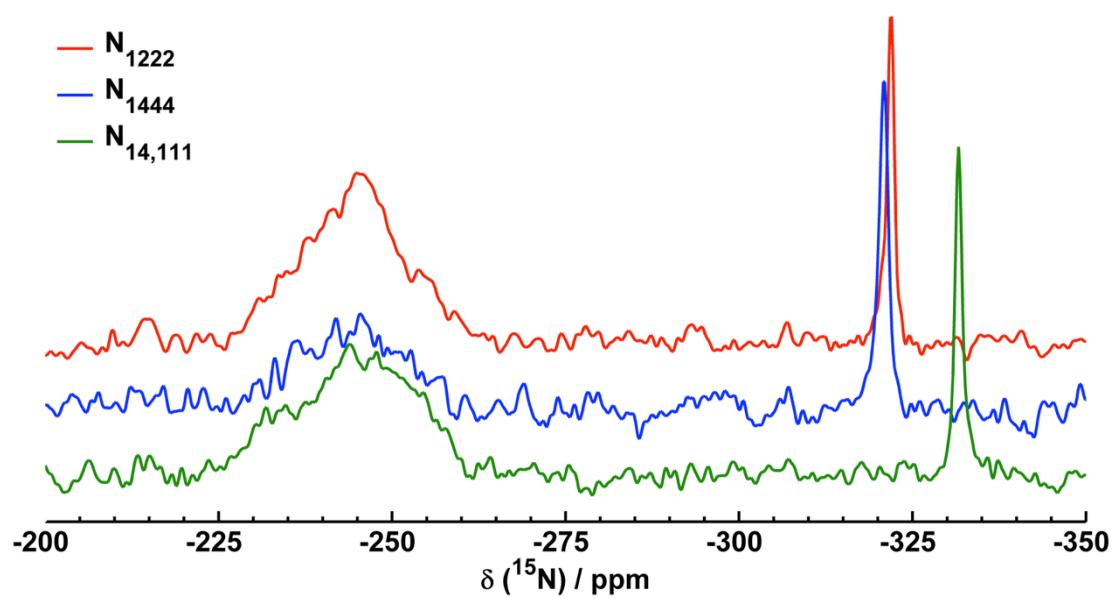


Fig 4b ^{15}N CPMAS spectra of ionomers with varying ammonium ions.

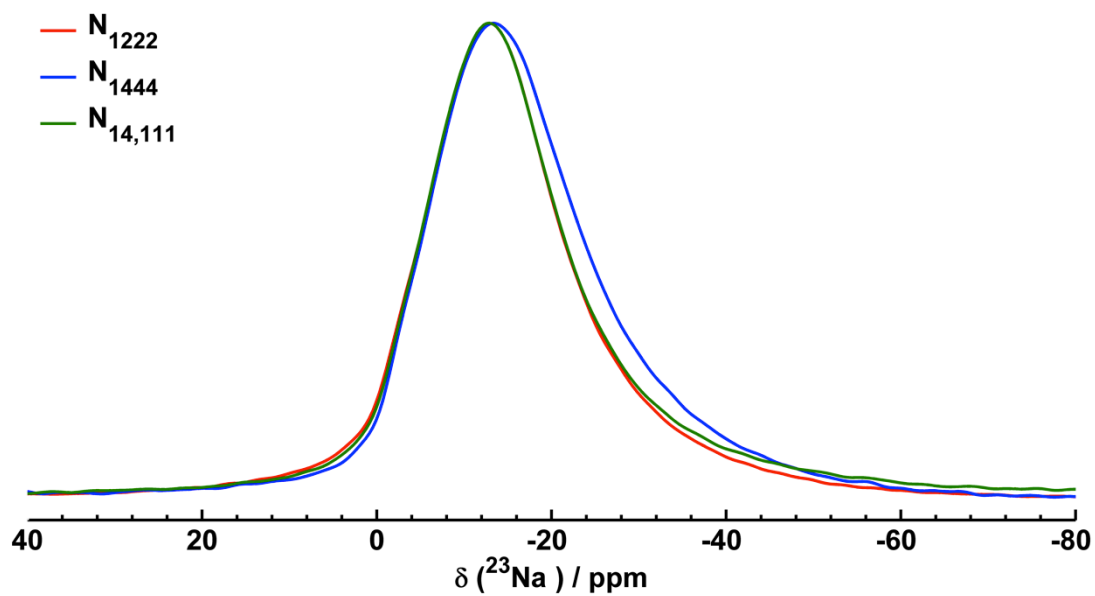


Fig 4c ^{23}Na MAS spectra of ionomers with varying ammonium counterions.

2. Effect of sodium content in the homopolymer of (Poly(N₁₂₂₂)_zNa_{1-z}[AMPS])

In our previous work, we reported the effect of Na content in a copolymer of poly([N₁₂₂₂][AMPS]-co-Na[VS]) ionomers. The data show that the conductivity is increasingly decoupled from the T_g of the ionomer systems as the Na⁺ concentration decreased. In this section we discuss the effect of Na content in a PAMPS homopolymer with different ratios of N₁₂₂₂ and Na⁺ counterions (Poly(N₁₂₂₂)_zNa_{1-z}[AMPS]) to compare the differences between homopolymer and copolymer ionomer systems.

Thermal Properties

Fig. 5 shows the DSC thermograms of ionomers with different Na contents. As expected, the T_g increases (indicating segmental motion within the ionomers is reduced) with a decreasing fraction of the bulky cation, since the interchain interactions become stronger with higher Na⁺ content. This is in contrast with copolymer ionomers system, in which the T_g does not vary significantly as the Na content changes from 10 to 50%. The glass transition of the homopolymer systems presented here is also not as broad as in the case of the copolymer materials¹⁹. The broadness of the glass transition has been calculated from the difference between onset and endpoint of each DSC thermogram. For example, the width of 20% Na copolymer system is 28 °C while in the homopolymer system, with the same Na content, it is only 13 °C. This is less than half the value for the copolymer systems,

which may reflect a more homogenous material in this case. This behavior will be further discussed in the ionic conductivity and morphology section below.

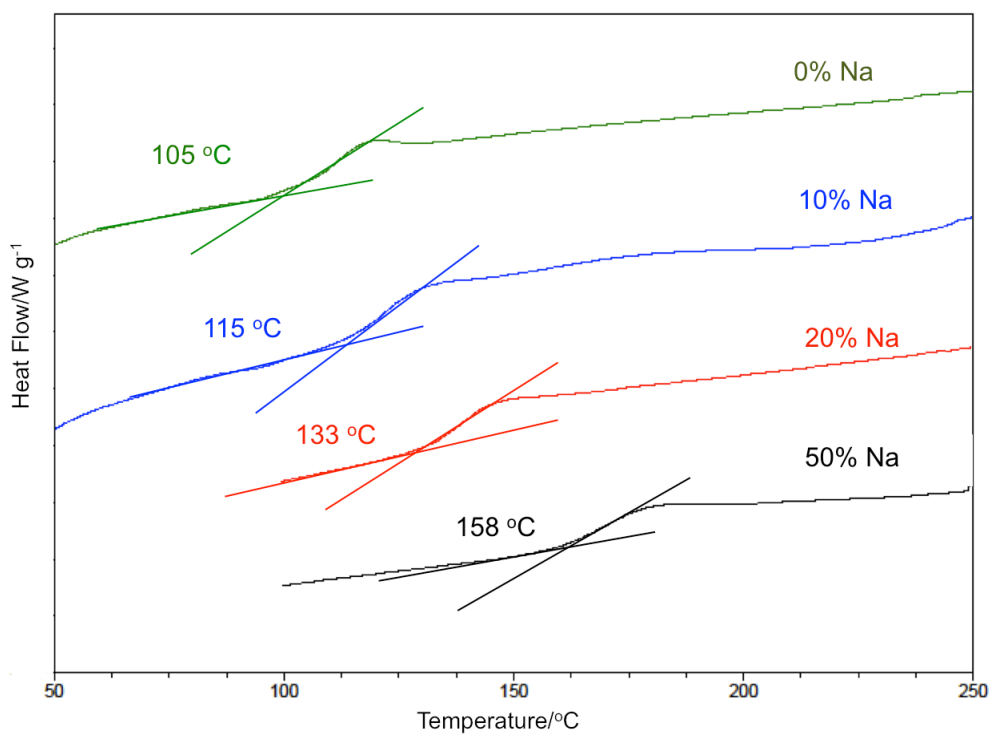


Fig. 5 DSC thermograms of (Poly(N_{1222}) $_z$ Na $_{1-z}$ [AMPS]) ionomers with different mol% of Na

Ionic Conductivity

The Nyquist plot for the ionomer containing 10% Na⁺ (Poly(N_{1222}) $_{0.9}$ Na $_{0.1}$ [AMPS]) at 373 K (below T_g) and at 403 K (above T_g) are presented in Fig. S1. Below T_g , two semicircles can be observed, indicating two conduction processes might be present. In order to calculate the total conductivity of the ionomers, the conductivity data has been fitted with a series circuit as depicted in Fig. S2. Similar observations were encountered in the copolymer

system discussed in our previous work¹⁹, where two distinguishable semicircles appeared in the Nyquist plot below the T_g of the samples. However, in the homopolymer system, the two semicircles are not as clearly separated, which might again reflect greater homogeneity. However, some degree of inhomogeneity can still be detected at the microscopic level as will be discussed further below. Fig. 6 presents the Arrhenius plots of each of the ionomers with various compositions, from 0 to 100% Na, with arrows showing the T_g region in each case. From this data, it can be seen that the 50% and 100% Na samples show very low conductivity, consistent with a high T_g , and probably due to strong associations of Na^+ to the sulfonate anion on the ionomer backbone, that leads to a reduction of the segmental motion of the ionomers as previously reported elsewhere.^{19, 29, 33}

On the other hand, below 20% Na^+ , the ionic conductivity shows curvature consistent with Vogel-Tamman-Fulcher (VTF) behavior^{7, 35}. VTF behaviour suggests that migration of the ions in the ionomer systems is similar to ionic conduction observed in the case of a liquid. If the ionic conductivity follows VTF behaviour, the plot of log conductivity versus $1000/(T-T_0)$ should present a straight line. In order to confirm this, we show log conductivity versus inverse temperature of $(T-T_0)$, where T_0 was taken from the fitted VTF parameter value as depicted in Fig. S3. A straight line (with a regression coefficient of 0.999) can be observed from this plot, indicating the ionomers containing less than 20% Na^+

indeed follow VTF behaviour over this temperature range. The values of the fitted VTF parameters are summarized in Table 1.

Table 1 VTF ionic conductivity parameters for (Poly(N₁₂₂₂)_zNa_{1-z}[AMPS])

Na ⁺ (mol%)	Log σ_0 /S cm ⁻¹	B/K	T ₀ /K	R
0	-5.2±0.1	-140±22	311±6	0.999
10	-5.2±0.1	-132±9	324±2	0.999
20	-2.4±0.9	-912±317	245±27	0.999

Furthermore, a measureable conductivity can be observed below T_g for all samples, which indicates the ionic conductivity is again increasingly decoupled from the segmental motion of the polymers. Fig. 7 normalizes the temperature by the DSC T_g, showing that the segmental motion of the ionomer backbone is not the sole source of improvement in ionic conductivity. A remarkable finding is that the conductivity at fixed T_g/T shows 10% Na⁺ possesses the highest ionic conductivity among all the systems studied here. This is consistent with the behavior we previously observed in the copolymer ionomers where 10% Na⁺ shows the highest conductivity of all the samples investigated¹⁹. Hence it appears that incorporation of two cations leads to favorable properties for conductivity in these materials (both copolymer and homopolymer ionomer systems), especially for lower Na⁺ concentrations.

As shown earlier, the conductivity at T_g is significantly greater than 10-12 S.cm⁻¹ commonly observed when conductivity is coupled to T_g. The low Na

concentration appears to be extensively decoupled in the case where N_{1222} cation replace the Na cation. Interestingly, previous work by Sokolov et al., has shown that, which the ionic conductivity can be coupled to T_g , there is still extensive decoupling of ion transport in some polymer electrolyte, as evidence from a comparison of structural relaxation due to local segmental motion and the ionic conductivity. In that work, Sokolov et al. correlated with the ionomer's fragility^{36, 37}. They postulated that in polymers that possesses high fragility, ions can freely move throughout the loose structure resulting from frustrated packing, even if the structure has overall very slow segmental relaxation. Conversely, greater flexibility produces a more dense structure (i.e. well packed polymer chains), hence less fragile and mobility of ions only occurs when polymer segments are able to move. They also suggested that condensed structures (i.e least fragile) can form from well-packed, flexible chains and will show almost Arrhenius temperature dependence of the segmental dynamics, while strongly non-Arrhenius temperature variations can be exhibited by the frustrated packing of rigid chains from forming a loose structure (i.e very fragile systems). Thus it appears that the incorporation of a larger quaternary ammonium cation such as N_{1222} in the present ionomers leads to a looser packing of the polymer chains and hence higher fragility.

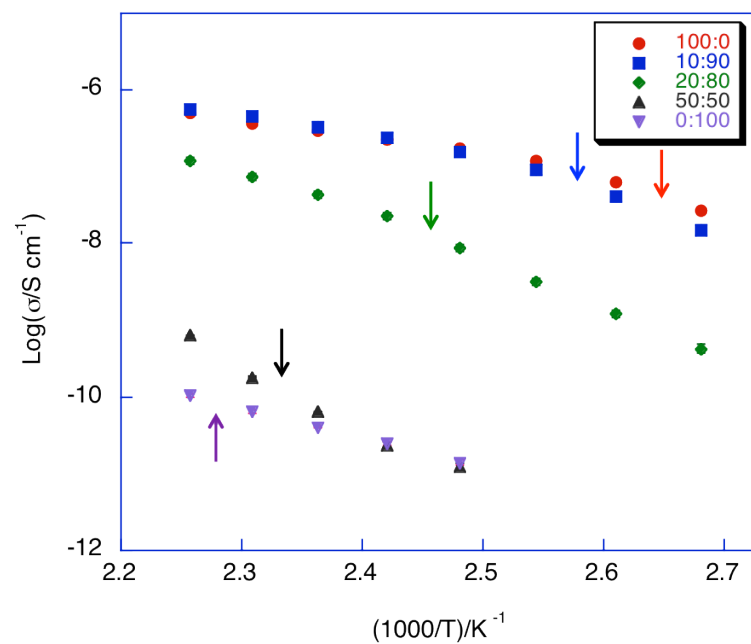


Fig. 6 Arrhenius conductivity plot of $(\text{Poly}(\text{N}_{1222})_z\text{Na}_{1-z}[\text{AMPS}])$ ionomers with various mol% of Na. The arrows indicate the T_g for each system.

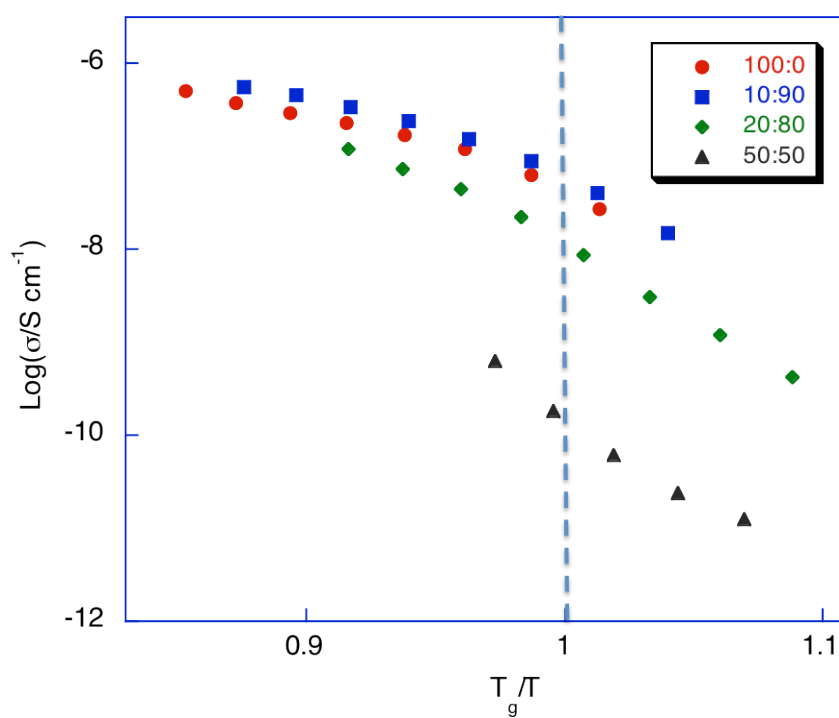


Fig. 7 Ionic conductivity of the ionomers as a function of Na^+ concentrations and temperature normalized by T_g

3. The effect of plasticizer into the poly($[\text{N}_{1222}][\text{AMPS}]\text{-Na}$) ionomers

The ionic conductivity of the 50% Na^+ ionomer system (Poly(N_{1222}) $_{0.5}\text{Na}_{0.5}[\text{AMPS}]$) is very low, consistent with a high glass transition temperature as discussed above. However, when the conductivity is scaled by the T_g , this system also shows some decoupling from the backbone structural relaxation. An addition of 10 wt.% of plasticizer to the copolymer ionomer system showed that the ionic conductivity improved by three orders or magnitude¹⁹. We therefore also investigated the incorporation of plasticizer for the homopolymer system to observe if higher ionic conductivities can be obtained in this system. Fig. 8 (a) and (b) present the conductivity of plasticized ionomers in Arrhenius format and scaled with respect to T_g respectively. The T_g of the plasticized ionomers (arrows in the Arrhenius plot) does not change significantly compared to the unplasticized material, however, the ionic conductivity increased dramatically, up to three orders of magnitude, when the IL is incorporated as a plasticizer, and by one and a half orders when tetraglyme (G4) is added. Furthermore it appears that the ionic conductivity in these plasticized systems is even more strongly decoupled from the T_g of the materials. The effect of IL plasticizer on the 10% Na^+ ionomer system was also investigated and in this case the ionic conductivity increased by nearly a factor of 100, as can be seen in Fig. 8.

This additional increase may be at least in part due to the presence of additional ions from the IL.

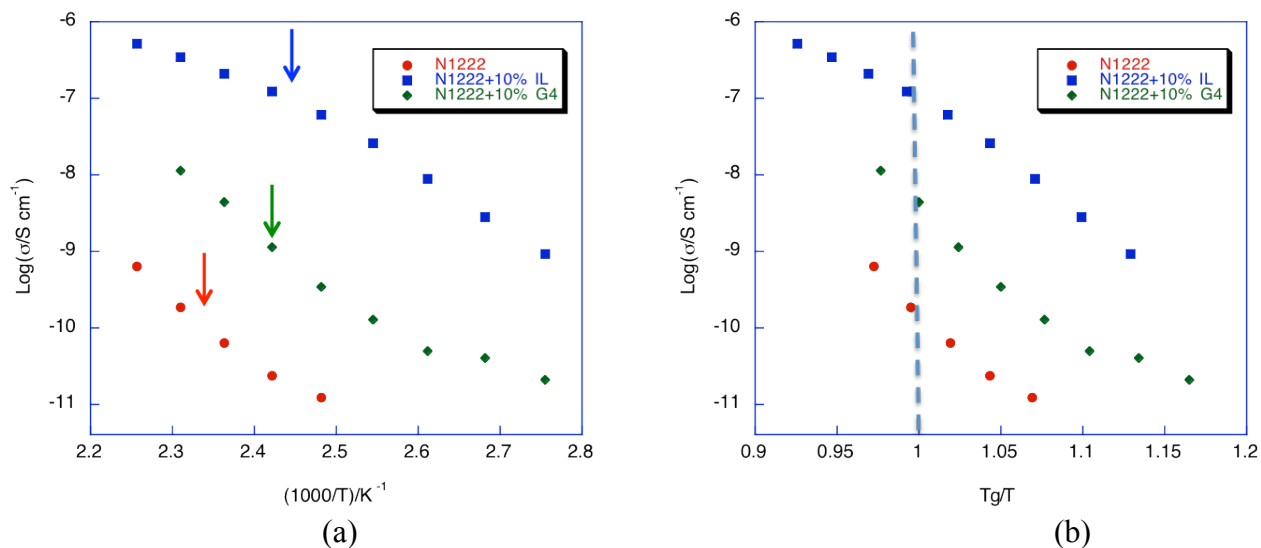


Fig. 8 (a) Arrhenius conductivity plot of $(\text{Poly}(\text{N}_{1222})_{0.5}\text{Na}_{0.5}[\text{AMPS}])$ ionomers with 10 wt.% IL and tetraglyme (b) Ionic conductivity of the ionomers as a function of plasticizer and temperature normalized by T_g

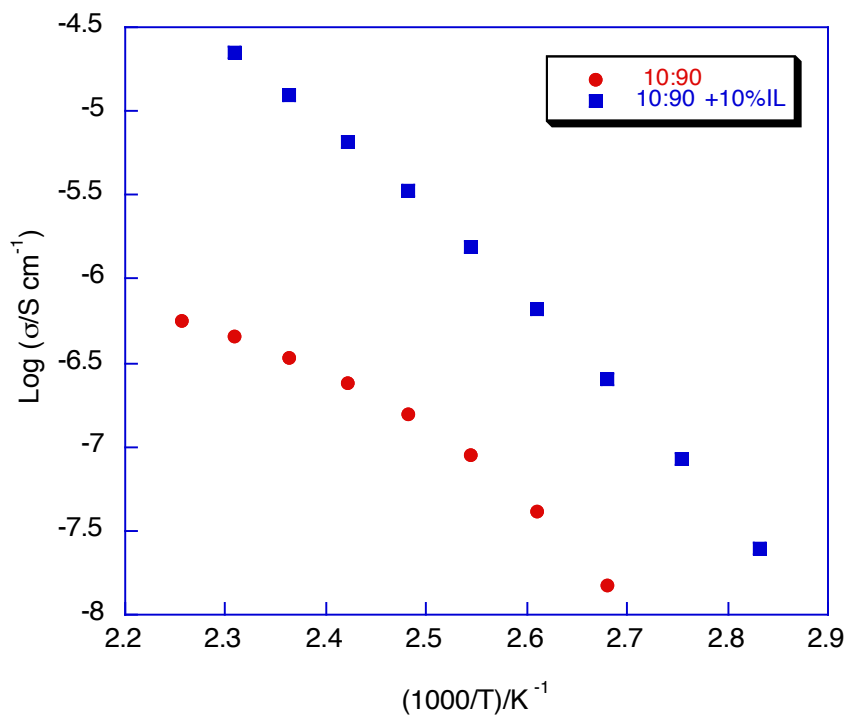


Fig. 9 Arrhenius conductivity plot of (Poly(N₁₂₂₂)_{0.9}Na_{0.1}[AMPS]) ionomers with 10 wt.% IL

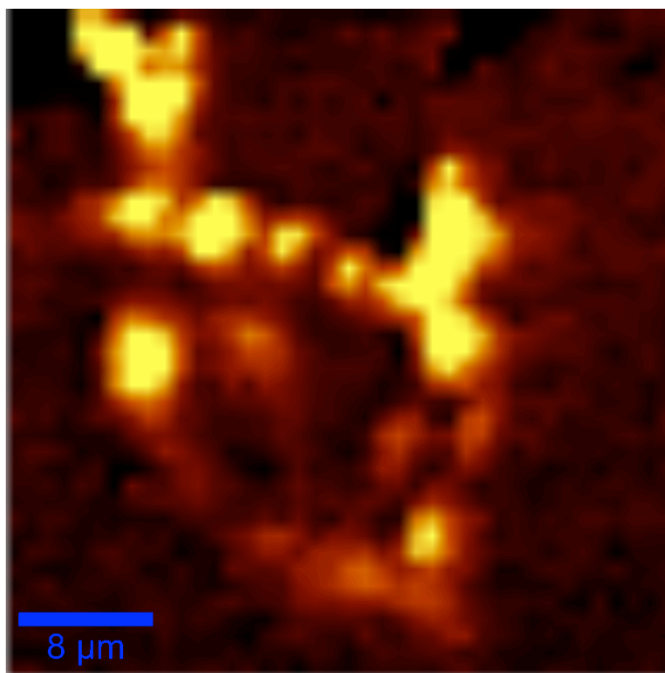
Morphology

As discussed in the thermal properties and ionic conductivity sections, the broad glass transition observed and the presence of two semicircles in the Nyquist plot may reflect heterogeneity or phase separation within these ionomers. In contrast to the copolymer systems, the T_g is not as broad and the two semicircle also are not as clearly separated. Interestingly, whereas phase separation was clearly visible in the copolymer systems using optical microscopy, this is not the case for the homopolymer systems discussed in the present work; thus the phase separation cannot be detected by optical microscopy, as seen in Fig. S4. However, to investigate whether phase separation might have occurred at a smaller length scale, or even at a nano level (given that we do observed two semicircle in the Nyquist plot), we performed micro- Raman Spectroscopy. This provides sub-micron spatial resolution to precisely choose the area of interest in which to carry out chemical analysis. The chemical mapping of polymer blends or composites, based on their characteristic Raman peaks, can be used to probe the domains of phase separated polymer blends with phase domain sizes as small as $\sim 200\text{nm}$ ³⁸.

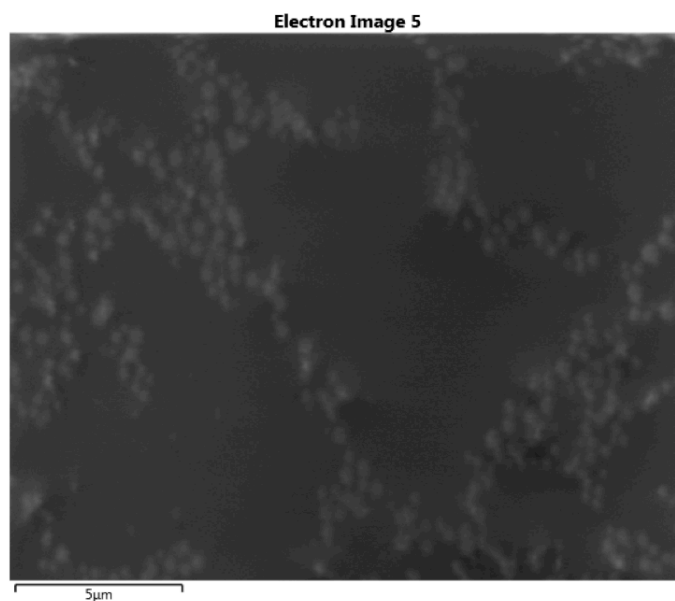
Before mapping, the ionomer samples were positioned in the laser focus using a video camera and white-light illumination. A suitable region was chosen that appeared relatively flat. Preliminary studies on the spectra of the three ionomers

(0%, 50% and 100% Na⁺) showed that there was very useful information in the 1500 – 300 cm⁻¹ spectral regions (Fig. S5); therefore, spectra were only collected in this region to reduce the measurement time. Fig. 10 (a) presents the fine raman map of ionomers from 1100 – 600 cm⁻¹. The presence of bright and dark regions can clearly be seen, indicating phase separation might have occurred in this ionomer.

The phase separation observed in Raman imaging results was also verified by SEM observation of the (Poly(N₁₂₂₂)_{0.5}Na_{0.5}[AMPS]) sample, as shown in Fig. 10 (b). In this case we observe the presence of dark and bright areas, and the bright areas represent a ‘network’ that correlates well with the bright regions from the Raman imaging results.



(a)



(b)

Fig. 10 (a) fine map of ionomers from 1100 – 600 cm^{-1} (b) SEM images of the 50% Na^+ ionomers

CONCLUSIONS

Notwithstanding the strong decoupling behavior, the ionic conductivity of the ionomers investigated in this work is still too low for them to be considered for practical devices. In part this is due to the relatively high T_g values and also to the strong ionic interactions between the sodium and the conduction sites available for the sodium ions to ‘hop’ between. Introduction of plasticizer into the ionomers significantly increased the ionic conductivity, by up to three orders magnitude. In this paper, we also showed that a bulky ionic liquid cation is necessary in order to reduce the electrostatic interchain interactions. It is therefore possible to synthesize copolymer ionomers with a bulky ionic liquid counterion, while preserving the decoupling properties. If these two factors are adequately

addressed, copolymer ionomers should be promising candidates for realizing single ion conduction with high ionic conductivity in solid-state electrolytes.

ACKNOWLEDGEMENTS

The authors are grateful to the Australian Research Council for funding via DP130101652 and under the Laureate Fellowship schemes (MF and DRM). We also acknowledge the ARC for support of the NMR facility through the grant LE110100141

REFERENCES

1. Noor, S. A. M.; Ahmad, A.; Talib, I. A.; Rahman, M. Y. A. *Ionics* **2010**, *16*, 161-170.
2. Morita, M.; Shirai, T.; Yoshimoto, N.; Ishikawa, M. *J. Power Sources* **2005**, *139*, 351-355.
3. Mohd Noor, S. A.; Howlett, P. C.; Macfarlane, D. R.; Forsyth, M. *Electrochim. Acta* **2013**, *114*, 766-771.
4. Kumar, D.; Hashmi, S. A. *Solid State Ionics* **2010**, *181*, 416-423.
5. Gayet, F.; Viau, L.; Leroux, F.; Monge, S.; Robin, J. J.; Vioux, A. *J. Mater. Chem.* **2010**, *20*, 9456-9462.
6. Fenton, D. E.; Parker, J. M.; Wright, P. V. *Polymer* **1973**, *14*, 589.
7. Gray, F. M., *Solid polymer electrolytes : fundamentals and technological applications*. New York, NY : VCH: New York, NY, 1991.
8. Noor, S. A. M.; Ahmad, A.; Rahman, M. Y. A.; Talib, I. A. *J. Appl. Polym. Sci.* **2009**, *113*, 855-859.
9. Ueno, K.; Hata, K.; Katakabe, T.; Kondoh, M.; Watanabe, M. *J. Phys. Chem. B* **2008**, *112*, 9013-9019.
10. Tiyyapiboonchaiya, C.; Pringle, J. M.; MacFarlane, D. R.; Forsyth, M.; Sun, J. *Macromol. Chem. Phys.* **2003**, *204*, 2147-2154.
11. Roach, D. J.; Dou, S.; Colby, R. H.; Mueller, K. T. *J. Chem. Phys.* **2012**, *136*.
12. Travas-Sejdic, J.; Steiner, R.; Desilvestro, J.; Pickering, P. *Electrochim. Acta* **2001**, *46*, 1461-1466.
13. Capuano, F.; Croce, F.; Scrosati, B. *J. Electrochem. Soc.* **1991**, *138*, 1918-1922.
14. Appetecchi, G. B.; Zane, D.; Scrosati, B. *J. Electrochem. Soc.* **2004**, *151*, A1369-A1374.

15. Evans, J.; Vincent, C. A.; Bruce, P. G. *Polymer* **1987**, *28*, 2324-2328.
16. Watanabe, M.; Nishimoto, A. *Solid State Ionics* **1995**, *79*, 306-312.
17. Tudryn, G. J.; O'Reilly, M. V.; Dou, S.; King, D. R.; Winey, K. I.; Runt, J.; Colby, R. H. *Macromolecules* **2012**, *45*, 3962-3973.
18. Wang, W.; Tudryn, G. J.; Colby, R. H.; Winey, K. I. *J. Am. Chem. Soc.* **2011**, *133*, 10826-10831.
19. Mohd Noor, S. A.; Gunzelmann, D.; Sun, J.; MacFarlane, D. R.; Forsyth, M. *J. Mater. Chem. A* **2014**, *2*, 365-374.
20. Ünal, H. I.; Yilmaz, H. *J. Appl. Polym. Sci.* **2002**, *86*, 1106-1112.
21. Annala, M.; Lipponen, S.; Kallio, T.; Seppälä, J. *J. Appl. Polym. Sci.* **2012**, *124*, 1511-1519.
22. Santiago, A. A.; Vargas, J.; Cruz-Gómez, J.; Tlenkopatchev, M. A.; Gaviño, R.; López-González, M.; Riande, E. *Polymer (United Kingdom)* **2011**, *52*, 4208-4220.
23. Byrne, N.; Howlett, P. C.; MacFarlane, D. R.; Forsyth, M. *Adv. Mater. (Weinheim, Ger.)* **2005**, *17*, 2497-2501.
24. Park, M. J.; Kim, S. Y. *J. Polym. Sci., Part B: Polym. Phys.* **2013**, *51*, 481-493.
25. Kar, M.; Winther-Jensen, B.; Forsyth, M.; MacFarlane, D. R. *Phys. Chem. Chem. Phys.* **2013**, *15*, 7191-7197.
26. Tang, S.; Baker, G. A.; Zhao, H. *Chem. Soc. Rev.* **2012**, *41*, 4030-4066.
27. Tamura, T.; Yoshida, K.; Hachida, T.; Tsuchiya, M.; Nakamura, M.; Kazue, Y.; Tachikawa, N.; Dokko, K.; Watanabe, M. *Chem. Lett.* **2010**, *39*, 753-755.
28. Eisenberg, A.; Kim, J.-S., *Introduction to ionomers*. Wiley Inter-Science: New York, 1998.
29. Tudryn, G. J.; Liu, W.; Wang, S. W.; Colby, R. H. *Macromolecules* **2011**, *44*, 3572-3582.
30. Lefelar, J. A.; Weiss, R. A. *Macromolecules* **1984**, *17*, 1145-1148.
31. Grady, B. P.; Moore, R. B. *Macromolecules* **1996**, *29*, 1685-1690.
32. Weiss, R. A.; Agarwal, P. K.; Lundberg, R. D. *J. Appl. Polym. Sci.* **1984**, *29*, 2719-2734.
33. Wang, Y.; Agapov, A. L.; Fan, F.; Hong, K.; Yu, X.; Mays, J.; Sokolov, A. P. *Phys. Rev. Lett.* **2012**, *108*.
34. Shestakova, P.; Willem, R.; Vassileva, E. *Chem.-Eur. J.* **2011**, *17*, 14867-14877.
35. Smedley, S. I., *The interpretation of ionic conductivity in liquids*. New York : Plenum Press Wellington, New Zealand, 1980; p 195.
36. Agapov, A. L.; Sokolov, A. P. *Macromolecules* **2011**, *44*, 4410-4414.
37. Ediger, M. D.; Harrowell, P.; Yu, L. *J. Chem. Phys.* **2008**, *128*.
38. Kumar, C. S. S. R., *Raman spectroscopy for nanomaterials characterization*. Berlin ; New York : Springer: Baton Rouge, LA, USA, 2012.

4.7 Supporting Information

Supporting Information to accompany:

Decoupled ion conduction in poly(2-acrylamido 2methyl-1-propane-sulfonic acid) (PAMPS) homopolymers

Siti Aminah Mohd Noor,^{a,b} Jiazeng Sun,^a Douglas R MacFarlane^{a,c}, M. Armand^d, D. Gunzelmann^e and Maria Forsyth,^{c,e}

^a *School of Chemistry, Monash University, Clayton Campus, Victoria, Australia*

^b *Chemistry Department, Centre for Defence Foundation Studies, National Defence University of Malaysia, 57000, Kuala Lumpur, Malaysia*

^c *ARC Centre of Excellence for Electromaterials Science (ACES), Australia*

^d *CIC Energigune, Vitoria, Spain*

^e *Institute for Frontier Materials Deakin University, Victoria, Australia*

* Corresponding Author: * Email:

[REDACTED]

[REDACTED]

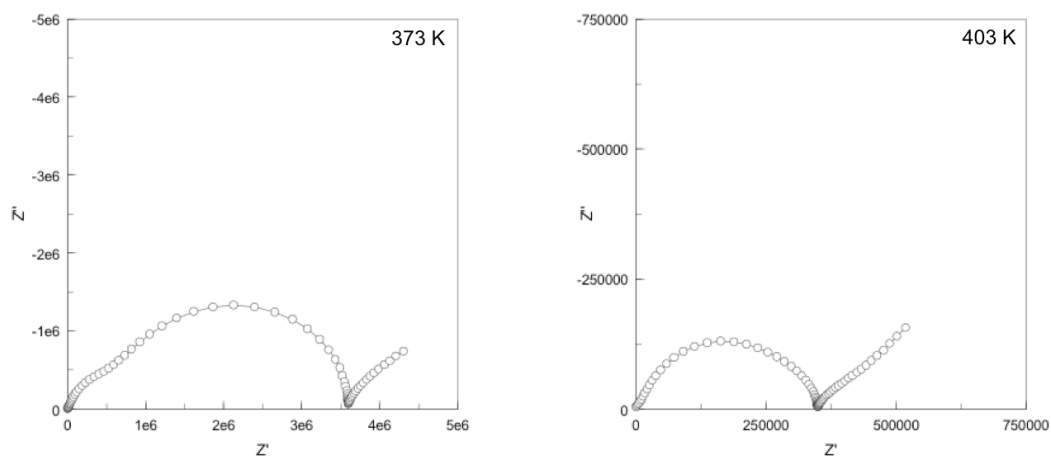


Fig S1 Nyquist plots of (poly(N₁₂₂₂)_{0.9}Na_{0.1}[AMPS]). Na at 303 K and 403 K

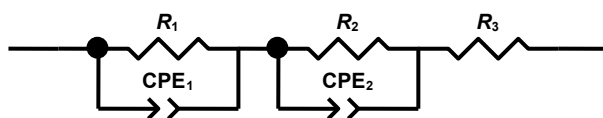


Fig S2 Series circuit for fitting two semi-circles of impedance data

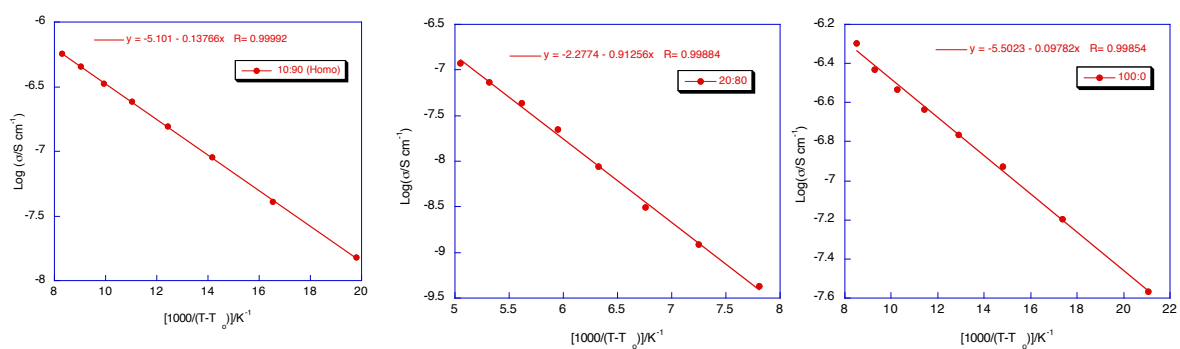


Fig S3 Plot of log conductivity versus $1000/(T-T_0)$ of poly((N₁₂₂₂)_{0.9}Na_{0.1}[AMPS])

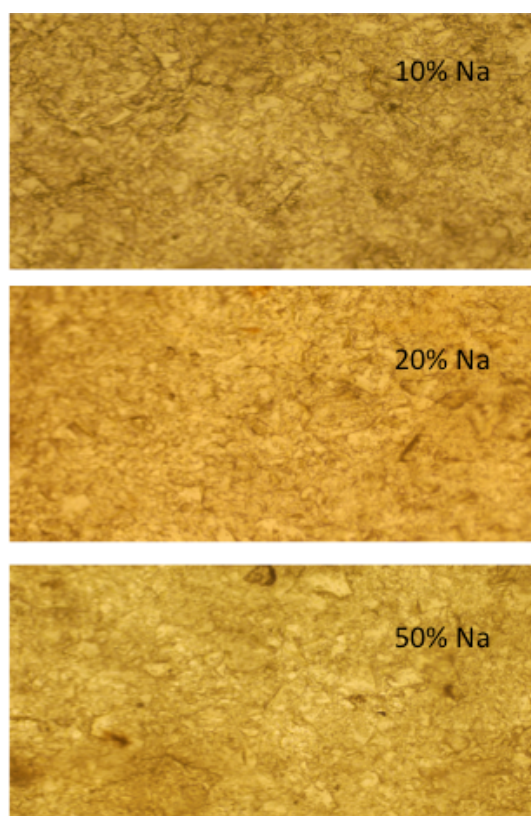


Fig S4 Optical microscope images of $(\text{Poly}(\text{N}_{1222})_z\text{Na}_{1-z}[\text{AMPS}])$ ionomers with various mol% of Na (a) 10% (b) 20% (c) 50%.

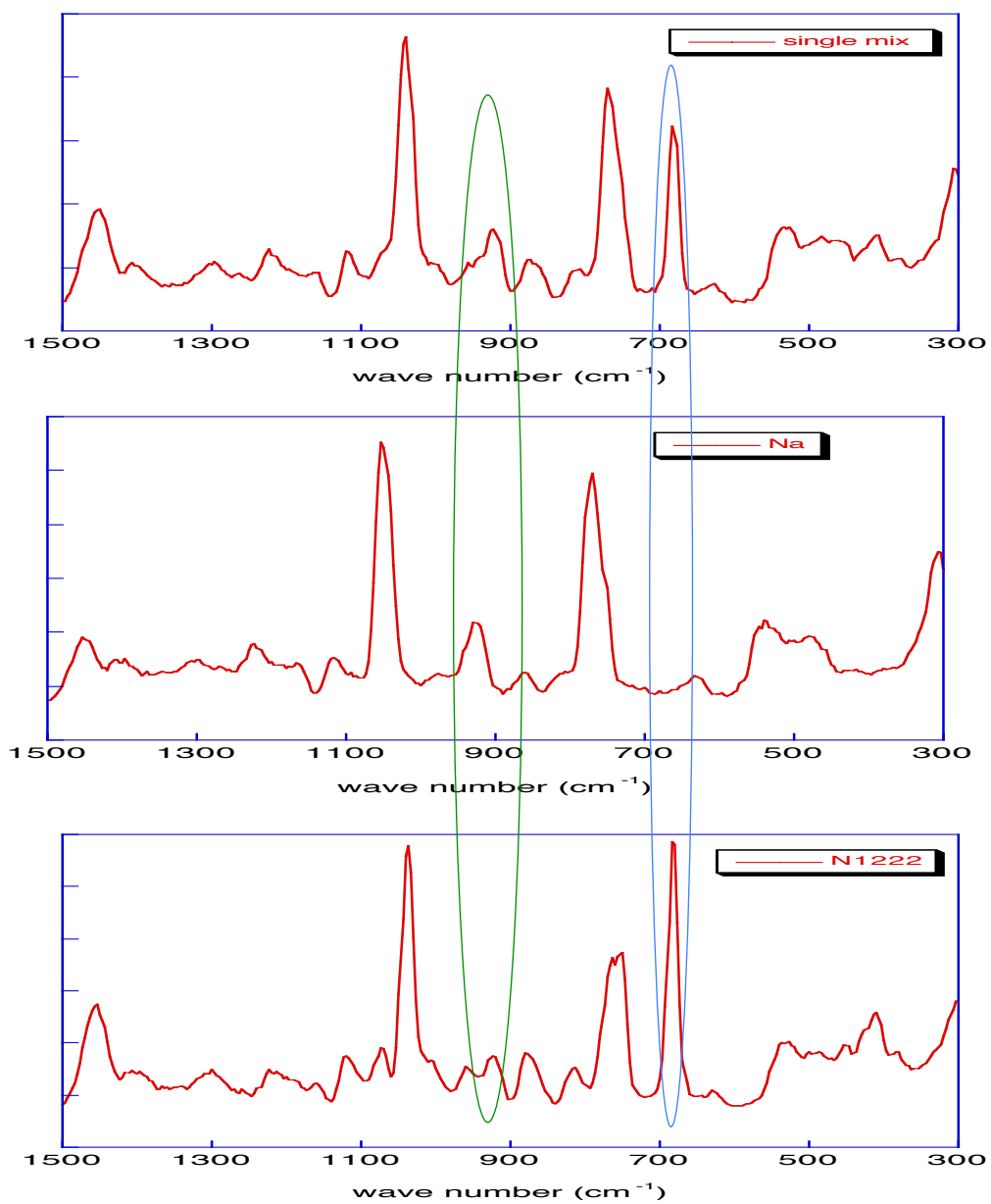


Fig S5 Raman spectra of (Poly(N₁₂₂₂)_zNa_{1-z}[AMPS]), $z=1.0$, 0.5 , and 0.0

4.8 Bibliography

1. Gray, F. M., *Polymer electrolytes*. Cambridge : Royal Society of Chemistry: Cambridge, 1997.
2. Roach, D. J.; Dou, S.; Colby, R. H.; Mueller, K. T. *J. Chem. Phys.* **2012**, *136*.
3. Tudryn, G. J.; Liu, W.; Wang, S. W.; Colby, R. H. *Macromolecules* **2011**, *44*, 3572-3582.
4. Eisenberg, A.; Kim, J.-S., *Introduction to ionomers*. Wiley Inter-Science: New York, 1998.
5. Wang, Y.; Agapov, A. L.; Fan, F.; Hong, K.; Yu, X.; Mays, J.; Sokolov, A. *P. Phys. Rev. Lett.* **2012**, *108*.
6. Wang, W.; Liu, W.; Tudryn, G. J.; Colby, R. H.; Winey, K. I. *Macromolecules* **2010**, *43*, 4223-4229.
7. Tiyaipiboonchaiya, C.; Pringle, J. M.; MacFarlane, D. R.; Forsyth, M.; Sun, J. *Macromol. Chem. Phys.* **2003**, *204*, 2147-2154.
8. Travas-Sejdic, J.; Steiner, R.; Desilvestro, J.; Pickering, P. *Electrochim. Acta* **2001**, *46*, 1461-1466.
9. Roach, D. J.; Dou, S.; Colby, R. H.; Mueller, K. T. *J. Chem. Phys.* **2013**, *138*.
10. Tiyaipiboonchaiya, C.; MacFarlane, D. R.; Sun, J.; Forsyth, M. *Macromol. Chem. Phys.* **2002**, *203*, 1906-1911.
11. Wang, W.; Tudryn, G. J.; Colby, R. H.; Winey, K. I. *J. Am. Chem. Soc.* **2011**, *133*, 10826-10831.
12. Mohd Noor, S. A.; Gunzelmann, D.; Sun, J.; MacFarlane, D. R.; Forsyth, M. *J. Mater. Chem. A* **2014**, *2*, 365-374.



Chapter 5

Conclusions and future work

5.1 Conclusions

Solid - state, sodium ion containing, ionic liquid based electrolytes were successfully prepared and characterized in this work. This study has shown that these sodium-based materials have the potential to make conductive, safe and low-cost solid-state electrolytes that are promising candidates for secondary sodium battery applications.

The main outcomes of this study are as follows:

- i. The formation of a silica network by a sol-gel process in an ionogel does not affect the dynamic properties of the entrained IL, particularly at low content of silica. This has been confirmed by several observations: the ionic conductivity of 3 wt.% silica is close to that of the pure IL, and the glass transition temperature does not significantly change as silica content increases. ATR-FTIR and solid state NMR analysis also indicate the formation of the silica network does not change the chemical environment of the IL. The high thermal stability of the IL is maintained, even at high loading of silica in the ionogel.
- ii. The ionic conductivity of sodium containing ionic liquid electrolytes was shown to be marginally lower compared with analogous lithium-ionic liquid electrolytes. The deposition and dissolution of both sodium and lithium has been observed through cyclic voltammetry analysis of these electrolytes. We conclude that sodium-ionic liquid electrolytes can potentially be good

electrolytes for secondary sodium battery applications since they may overcome the safety problems associated with conventional solvent based electrolytes.

- iii. Gelled sodium-ionic liquid electrolytes were successfully obtained by (i) dispersion of nano-particle fumed silica, or (ii) radical polymerization of MMA monomer in the IL. The formation of the gel does not significantly affect the ion dynamics in the gelled ionic liquid; the ionic conductivity was found to only slightly decrease as the physical properties changed from liquid to gel. Plating and stripping of sodium metal was observed in the case of the silica gel electrolyte.
- iv. For single ion/mixed sodium-ionic liquid cation conductor systems, we found that both copolymer and homopolymer ionomer systems show the conductivity is increasingly decoupled from the T_g of the ionomer systems as Na^+ concentration decreased. In these systems, the 10% Na^+ sample shows the highest conductivity of all systems (even 0% Na^+), thus it appears that mixing two cations leads to favorable properties in terms of conductivity. Moreover, we also showed that a bulky ionic liquid cation is necessary in order to reduce the electrostatic interchain interactions

In conclusion, in this study we are successfully develop various promising electrolytes for sodium energy storage applications, which can be an alternative system to the high demand of lithium batteries.

5.2 Future Work

In order to develop the potential of these promising results of sodium-ionic liquids electrolytes for sodium energy storage applications, these are some directions for future work:

- i. To further study sodium ion mobility in gel electrolytes, Na^+ transport should be studied by NMR diffusion techniques. Also, the transference number of Na^+ also can be calculated from a combination of a.c. impedance and d.c. polarization techniques.
- ii. Battery testing on both liquid and gel sodium-ionic liquid electrolytes can be done to evaluate their performance in practical application.
- iii. The effect of diluents on the properties of gel electrolytes would make an interesting study, especially to determine their effect on the ionic conductivity and to potentially increase sodium mobility in the electrolytes. Propylene carbonate or ethylene carbonate would be promising diluents to use since they have been shown to increase the ionic conductivity in conventional gel electrolytes.
- iv. From our study in only cation ion conductors section, we proved that mixing two cations increases the ionic conductivity of the ionomer system and it was found that the copolymer system possesses higher conductivity than homopolymer system. Moreover, a bulky ionic liquid cation is necessary to reduce the electrostatic interchain interactions. It is therefore possible to synthesize copolymer ionomers with a bulky ionic liquid counterion, while preserving the decoupling properties. If these two factors

are adequately addressed, copolymer ionomers should be promising candidates for realizing only cation ion conductors with high ionic conductivity in solid-state electrolytes.